THERMODYNAMIC PROPERTIES OF A 5 MOLE PERCENT PROPANE IN METHANE MIXTURE

V. L. Bhirud and J. E. Powers

August 1969

Tulsa, Oklahoma

Department of Chemical and Metallurgical Engineering

TABLE OF CONTENTS

INTRODUCTION 1

Composition 1

Sources of Data 2

Calorimetric Data 2
Volumetric Data 2

Calculation Procedures 4

Enthalpy $\underline{H}$, Isobaric heat capacity, C_p, and Isothermal Throttling coefficient, $\emptyset$ 4
Entropy, $\underline{S}$, Fugacity, f, and Specific Volume, $\underline{V}$ . . . 7

Skeleton Tables of Thermodynamic Values 10

Thermodynamic Diagrams 12

Acknowledgments 12

NOTATION 23

BIBLIOGRAPHY 27

APPENDICES

I. REVIEW OF LITERATURE 32

Calorimetric Data 32
Volumetric Data 38

II. BASIC INTERPRETATION OF CALORIMETRIC DATA 43

Isobaric Determinations 44

Single Phase 44
General Procedure 44
Interpretation of Data at 1000 psia 48
Interpretation of data at 500 psia 52
Extrapolation with respect to temperature . . . 58

Two-Phase (Enthalpy Traverse) 61

Isothermal Determinations (Single Phase) 64

III. THERMODYNAMIC CONSISTENCY CHECKS AND FINAL ADJUSTMENT OF VALUES OF C_p AND $\emptyset$ 67

Thermodynamic Consistency Checks 67

Adjustment of Values of $\Delta\underline{H}_i$ 70

Adjustment of Values of C_p and $\emptyset$ 71

IV. PREPARATION OF PTH TABLES AND DIAGRAMS 72

Selection of Arbitrary Reference States 73

Determination of $\underline{H}_i$ for Pure Components as Ideal Gases at +200°F 74

Propane 74
Impurities 74
Methane 75

Calculation of $\underline{H}_m$ for the Mixture as Ideal Gas at +200°F 82

Incorporation of Isobaric and Isothermal Enthalpy Differences at Elevated Pressures 82

Corrections to Obtain Complete Agreement at -280°F . 83

Interpolate to Intermediate Values of Temperature and Pressure 84

V. EQUATIONS USED IN CALCULATING VALUES OF ENTROPY AND FUGACITY 85

The Basic Property Relation 85

Isobaric Change in Entropy 86

Isothermal Change in Entropy 87

Absolute Entropy Values 88

Fugacity Function 92

VI. PRIMARY INTERPRETATION OF DATA FROM THE LITERATURE TO ESTIMATE THE VOLUMETRIC BEHAVIOR OF THE 5% MIXTURE . . 94

Isotherms at 91.6 and 200°F 94

Isotherms at -147.4 and -27°F 96

VII. CALCULATIONS OF ENTROPY DIFFERENCES 101

Isobaric Differences in Entropy 101

Isothermal Entropy Differences 103

VIII. THERMODYNAMIC CONSISTENCY CHECKS FOR ENTROPY AND ADJUSTMENT OF VALUES OF ENTROPY, COMPRESSIBILITY FACTOR, Z, AND SPECIFIC VOLUME, $\underline{V}$, CALCULATION OF FUGACITY 109

Thermodynamic Consistency Checks 109

Corrections to Obtain Thermodynamic Consistency . . 110

Calculation of Fugacity 111

IX. PREPARATION OF MOLLIER DIAGRAM AND SKELETON TABLE OF THERMODYNAMIC PROPERTIES FOR THE MIXTURE 112

Absolute Entropy of the Mixture at One Atmosphere and 91.6°F 112

Tables and Diagram of Thermodynamic Properties for the Mixture 113

X. SIMPSON'S RULE 115

Area Under Given Curve 115

Numerical Integration to Obtain Area Under a Curve 117

Proofs and Comments on Simpson's Rule 118

Procedure for Curve Fitting Using Simpson's Rule 120

LIST OF TABLES

1. Composition of Nominal 5% Propane in Methane Mixture 2

2a. Tables of Thermodynamic Data Values at the Temperatures of Isothermal and Isenthalpic Determinations (T = 200°F) 13

2b. Tables of Thermodynamic Data Values at the Temperatures of Isothermal and Isenthalpic Determinations (T = 91.6°F) 14

2c. Tables of Thermodynamic Data Values at the Temperatures of Isothermal and Isenthalpic Determinations (T = -27°F) 15

2d. Tables of Thermodynamic Data Values at the Temperatures of Isothermal and Isenthalpic Determinations (T = -147.4°F) 16

3a. Tables of Thermodynamic Data Values at the Pressures of Isobaric Determinations (Low Pressures) 17

3b. Tables of Thermodynamic Data Values at the Pressures of Isobaric Determinations (High Pressures) 18

AI.1 Mixture Compositions 33

AI.2 Extremes in Compositions Reported by Manker (47) and Mather (50) 34

AI.3 Conditions of Integral Isothermal Determinations by Dillard (25) 35

AI.4 Conditions of Reported Joule-Thomson Values of Budenholzer *et al* (9) 36

AI.5 Conditions of Reported Joule-Thomson Measurements by Head (32) 37

AI.6 Conditions of Reported Volumetric Data of Reamer, Sage and Lacey (56) 39

AI.7 Conditions of Reported Volumetric Data of Huang *et al* (37) 40

AII.1 Information Obtained at the Maximum in $C_p(T)$ 48

AII.2 Constants of Equation (AIII.6) Expressing Specific Heat in the Immediate Vicinity of the Bubble Point 57

AII.3 Values of C_p for the 5.18% C_3 in C_1 Mixture at 500 psia as Determined by Interpretation of Calorimetric Data at Other Conditions 58

AII.4 Values of $(\partial C_p/\partial T)_P$ Used to Extrapolate $C_p(T)$ to -280°F 61

AII.5 Empirical Data Obtained From Interpretation of Enthalpy Traverses 64

AIV.1 Thermodynamic Consistency Checks of Published Calorimetric Data for Methane at Low Temperatures 76

AIV.2 Maximum Percentage Adjustments in Published Calorimetric Data for Methane at Low Temperatures 80

AIV.3 Enthalpies of Pure Components as Ideas Gases at 200°F Relative to Saturated Liquid at -280°F 81

AV.1 Absolute Entropies of Pure Components as Ideal Gases at 25°C 89

AX.1 Comparison of Coefficients of the Series Giving Area Under a Curve Using Simpson's Approximation 119

LIST OF FIGURES

1. Temperatures and Pressures of Calorimetric Determinations on a Nominal 5% Propane in Methane Mixture (47,50) 3

2. Check of Thermodynamic Consistency of Experimental Enthalpy Determinations 6

3. Check of Thermodynamic Consistency of Entropy Differences Calculated from Calorimetric and Volumetric Data 9

4. Pressure-Temperature-Enthalpy Diagram For Nominal 5 Percent Propane in Methane Mixture (Low Temperatures) 19

5. Pressure-Temperature-Enthalpy Diagram For Nominal 5 Percent Propane in Methane Mixture (High Temperatures) 20

6. Mollier Diagram for Nominal 5 Percent Propane in Methane Mixture (Low Temperatures) 21

7. Mollier Diagram for Nominal 5 Percent Propane in Methane Mixture (High Temperatures) 22

8. Temperatures and Pressures of Volumetric Data for Methane-Propane Mixtures as Reported in the Literature 41

9. Isobaric Heat Capacity, C_p, at 1000 psia Illustrating Method of Interpreting Calorimetric Results 46

10. Isobaric Heat Capacity, C_p, at 1000 psia Above the Critical Point Illustrating Sharp Maximum . . 50

11. Check for Bias in Interpreting Isobaric Data Near the Maximum in $C_p(T)$ at 1000 psia 51

12. Check of Interpretation of Isobaric Data Near the Maximum in $C_p(T)$ at 1000 psia After Correcting for Bias 53

13. Plot of Excess Isobaric Heat Capacity, C_p^E, for the Purpose of Estimating C_p for the 5% Mixture at 500 psia Where Direct Measurements Are Not Available 56

14. Experimental Heat Capacities with Values Calculated from B-W-R Equation of State 59

15. Calorimetric Data Obtained Within and Through the Two-Phase Region 63

16. Isothermal Throttling Coefficient, ϕ, at -27°F Illustrating Method of Interpreting Isothermal Calorimetric Results 65

17. One Complete Check of Thermodynamic Consistency of Calorimetric Data Used to Evaluate Enthalpy Differences 69

18. Check of Thermodynamic Consistency of Published Calorimetric Data and Calculated Enthalpy Departures at Low Temperatures 77

19. Published Data on the Isobaric Heat Capacity of Methane as Saturated Liquid 79

20. Typical Plot of Compressibility Factor, Z, vs lnP at 91.6°F as Used to Evaluate $\int Z d\ln P$ 97

21. Typical Plot of Isobaric Density, ρ, for Liquid Methane-Propane Mixture for Interpolation fo Temperatures of Isothermal Calorimetric Data . . 98

22. Typical Plot of Specific Volume, $\underline{V} = 1/\rho$, of Liquid Methane-Propane Mixture for Interpolation to Composition of Mixture 99

23. Typical Plot Used to Evaluate Second (Residual) Term in Equation (V.9) in the Vicinity of the Peak in $C_p(T)$ at 1000 psia 102

24. Typical Plot Used to Evaluate Second (Residual) Term in Equation (V.9) in the Two-Phase Region . 104

25. One Complete Check of Thermodynamic Consistency of Calorimetric and Volumetric Data Used to Evaluate Entropy Differences 105

26. Typical Plot Used to Evaluate $\int \underline{V} dP$ in the Compressed Liquid Region 107

27. Area Under a Curve Using Trepezoidal Rule 116

28. Area Under a Curve Using Simpson's Rule 116

29. Simpson's Rule Used for Curve Fitting 121

INTRODUCTION

The continuing need for accurate thermodynamic data for natural gas mixtures and the components of natural gas has been accentuated by recent developments in the area of natural gas processing at cryogenic conditions including liquification. Accurate values of enthalpy and entropy for pure components and mixtures are required not only for direct use in design of heat exchangers, compressors and expanders but also to be used as a basis for testing and comparing various methods of prediction. Therefore the objective of this investigation was to develop accurate values of thermodynamic properties for one mixture approximating natural gas. This objective was to be met making maximum use of accurate calorimetric data and the basic definitions of classical thermodynamics so as to yield the most meaningful numbers.

COMPOSITION

The primary sources of calorimetric data are the theses of E. A. Manker (47) and A. E. Mather (50). The composition of mixtures used in these companion investigations varied somewhat during the course of the investigations and moreover did not correspond directly to any mixture for which volumetric data were available as indicated in Appendix 1. The following composition was taken as an average of those mixtures for which calorimetric data are available in relative abundance:

TABLE 1

COMPOSITION OF NOMINAL 5% PROPANE IN METHANE MIXTURE

	Composition
Methane, CH_4	0.9464
Ethane, C_2H_6	0.0006
Propane, C_3H_8	0.0518
Nitrogen, N_2	0.0006
Oxygen, O_2	0.0002
Carbon Dioxide, CO_2	0.0004
	1.0000

SOURCES OF DATA

Calorimetric Data

The basic calorimetric data used in preparing the tables of thermodynamic properties are the isobaric determinations of Manker (47) and the isobaric, isothermal and isenthalpic determinations of Mather (50). These determinations extend from -240 to +260°F at pressures between 100 and 2000 psia. The temperatures and pressures at which actual measurements were made are indicated on Figure 1. Other published calorimetric data were considered but did not enter directly into the calculations (See Appendix 1).

Volumetric Data

No volumetric data has been reported for the composition listed above. Extensive volumetric data have been reported for methane (1,27,44,58,65,66), propane (3,15,23,26,36,55,61)

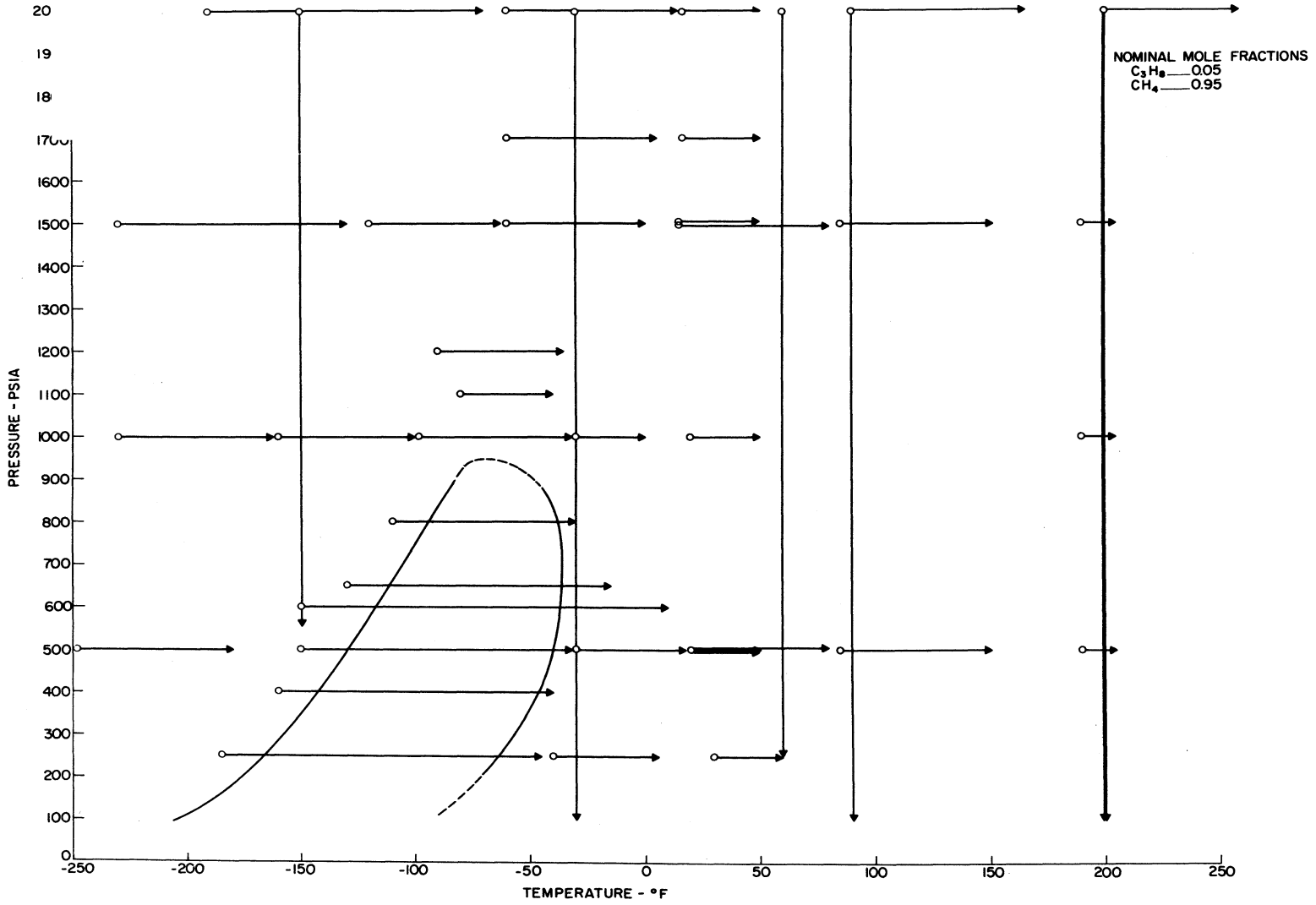

Figure 1. Temperature and Pressures of Calorimetric Determinations on a Nominal 5% Propane in Methane Mixture. (47,50)

and data are also reported for seven mixtures of these two components (36,56). The range of temperatures and pressures of volumetric data for the mixtures corresponding to those for the calorimetric data are presented later (Appendix 1).

CALCULATION PROCEDURES

Enthalpy, H, Isobaric Heat Capacity, C_p, and Isothermal Throttling Coefficient, Ø.

Values of C_p and Ø for this mixture (47,50) as well as three tables of H and three PTH diagrams (48,50,51) have been presented. There were reasons to question the interpretation of the basic data (70) even in the last of the three published tables both in the low temperature region and in the region just above the critical point for the mixture. Therefore, all data were reprocessed using improved techniques.

The basic methods of determining values of C_p from basic isobaric data and Ø from isothermal throttling data has been covered in detail elsewhere (46,47). The improved procedures are summarized in Appendix II. Likewise the methods of selecting bases for H and calculating values of H in the two-phase as well as the single-phase region has been discussed elsewhere (46,47) and are summarized in Appendix IV. The values of C_p, Ø and H reported in the skeleton table of thermodynamic data comprising the major part of this report are smoothed values which are thermodynamically self consistent. The procedure followed to insure this desirable feature is outlined below and presented in greater detail in Appendix II.

Graphical procedures are used. Smoothed curves are drawn through the basic isobaric and isothermal results to obtain a first estimate of C_p and ϕ respectively in the single phase region (Appendix II). A modified form of Simpson's rule (Appendix II) is applied to insure the best average fit of the experimental data. Values of $\Delta\underline{H}_p$ between experimental isotherms and $\Delta\underline{H}_T$ between experimental isobars are determined by again applying Simpson's rule over small intervals. The resulting numbers are summarized on Figure 2.

Enthalpy is a thermodynamic property and therefore, has the characteristics of an exact mathematical function. As a result the algebraic sum of all enthalpy differences around any closed loop, $\sum_i \Delta\underline{H}_i$, should be exactly equal to zero. The actual sum divided by the sum of the absolute values of the enthalpy differences,

$$\text{percentage deviation} = \frac{\sum \Delta\underline{H}_i}{\sum |\Delta\underline{H}_i|} \times 100 \qquad (1)$$

is an excellent measure of the consistency of the data. The results of such determinations are listed within each closed loop on Figure 2.

Adjustments were made on individual values of $\Delta\underline{H}_i$ as required to make $\sum_i \Delta\underline{H}_i = 0$ for all loops. These adjustments were made within the limits of precision of the basic data [C_p - $\pm$0.5%; ϕ - $\pm$1.0%]. The amount of the adjustment and the corrected values are presented in Figure 2. As indicated the magnitude of the corrections was generally much less than

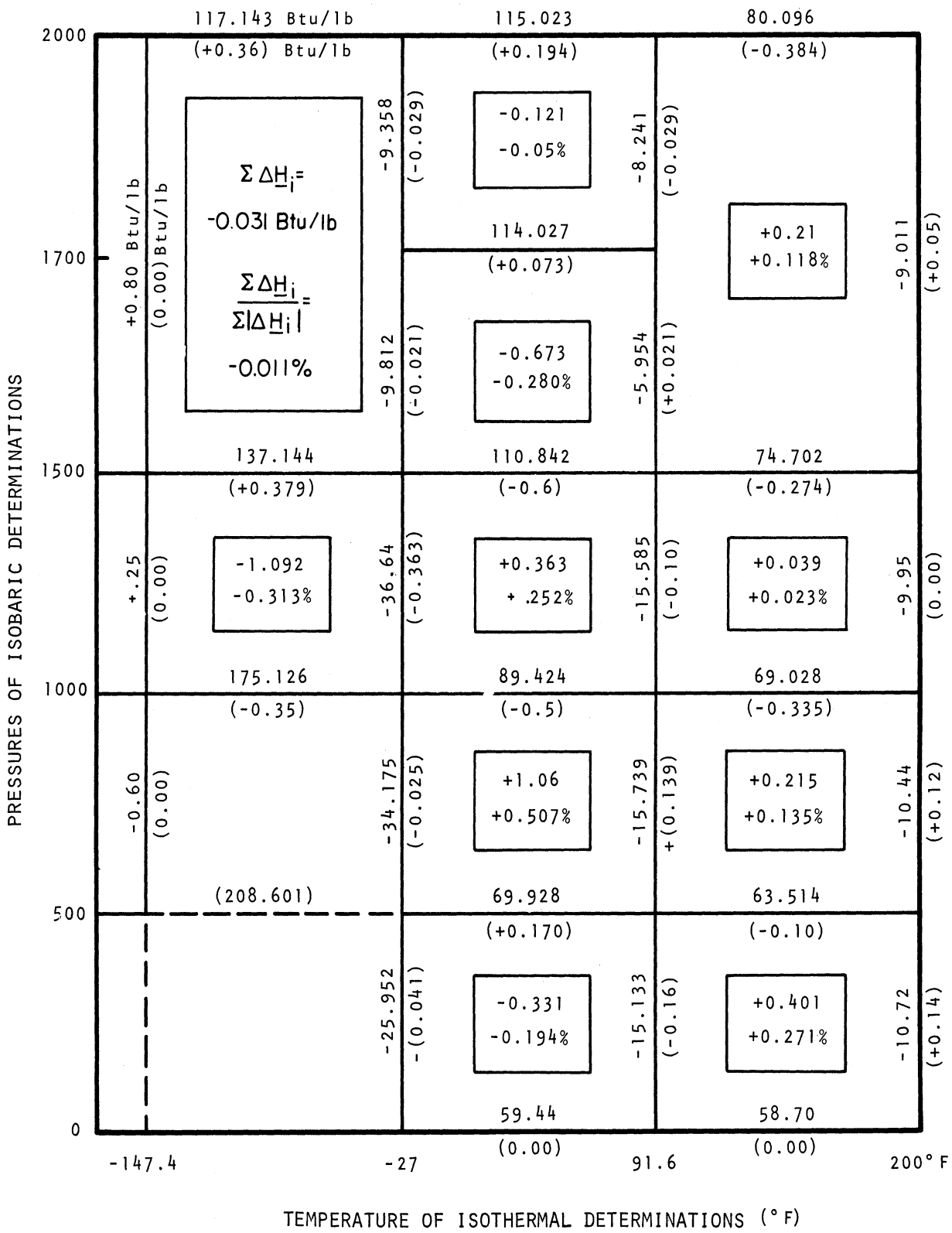

Figure 2. Check of Thermodynamic Consistency of Experimental Enthalpy Determinations.

the indicated precision. Finally, the smoothed curves for C_p and $\emptyset$ were adjusted so as to be consistent with the corrected values of ΔH_p and ΔH_T. Again such adjustments were made well within the limits of precision of the basic data. Values of C_p and $\emptyset$ reported in the skeleton tables and the adjusted smoothed curves were used to generate the intermediate values of H listed there.

As a result it is believed that the values of C_p are accurate to better than $\pm 0.2\%$, those for $\emptyset$ are better than $\pm 0.5\%$ and the H values are believed to accurate to better than 1 Btu/lb over the entire range of pressure and temperature. These statements must be tempered somewhat in various regions. Greater percentage errors are to be expected in the vicinity of $\emptyset = 0$. Higher errors for both C_p and $\emptyset$ also occur in the immediate vicinity of the critical point for the mixture where C_p and $\emptyset$ change very rapidly with both temperature and pressure (See Figures A-II-1, A-II-8) and at low temperatures below pressures of 1000 psia where complete data are lacking as described in Appendix II (See also Figure 1).

Entropy, S, Fugacity, f, and Specific Volume, V.

Two different advanced methods of interpolation were used to estimate values of specific volume for a binary mixture of methane and propane, which will be discussed in forthcoming publication. Interpolation was made primarily on Z in the gaseous region and on V in the liquid region. These were considered to be preliminary values and are not included as such in the skeleton tables.

Special equations were developed to make maximum use of the calorimetric data in determining both isobaric and isothermal differences in entropy as discussed in detail in Appendix VII. This is especially important because the interpolated values of the specific volume were not nearly accurate enough to yield meaningful values of either first or second derivatives such as $\left(\frac{\partial V}{\partial T}\right)_P$ and $\left(\frac{\partial^2 V}{\partial T^2}\right)_P$. (See Appendices VI and VII). As was done with enthalpy determinations, values of $\Delta\underline{S}_P$ were calculated between each pair of experimental isotherms and $\Delta\underline{S}_T$ values were evaluated between each pair of experimental isobars. The values thus calculated are summarized on Figure 3.

Entropy is also an exact function and therefore,

$$\text{percentage deviation} \equiv \frac{\sum_i \Delta\underline{S}_i}{\sum_i |\Delta\underline{S}_i|} \times 100 \qquad (2)$$

is a good measure of the thermodynamic consistency of the data. As indicated by the values of percentage deviation listed within the loops on Figure 3 the interpolated volumetric data are in remarkable agreement with the smoothed calorimetric data. Adjustments the volumetric values were made so as to make $\Delta\underline{S}_i = 0$ for each individual loop. All such adjustments were made within the anticipated limits of accuracy of the interpolated volumetric values ($\pm 0.5\%$). The corrections made to $\Delta\underline{S}_P$ and $\Delta\underline{S}_T$ are presented on Figure 3.

Note that the corrections are more or less random with respect to sign and are usually considerably less than $\pm 0.5\%$ indicating excellent agreement between the calorimetric and interpolated volumetric values.

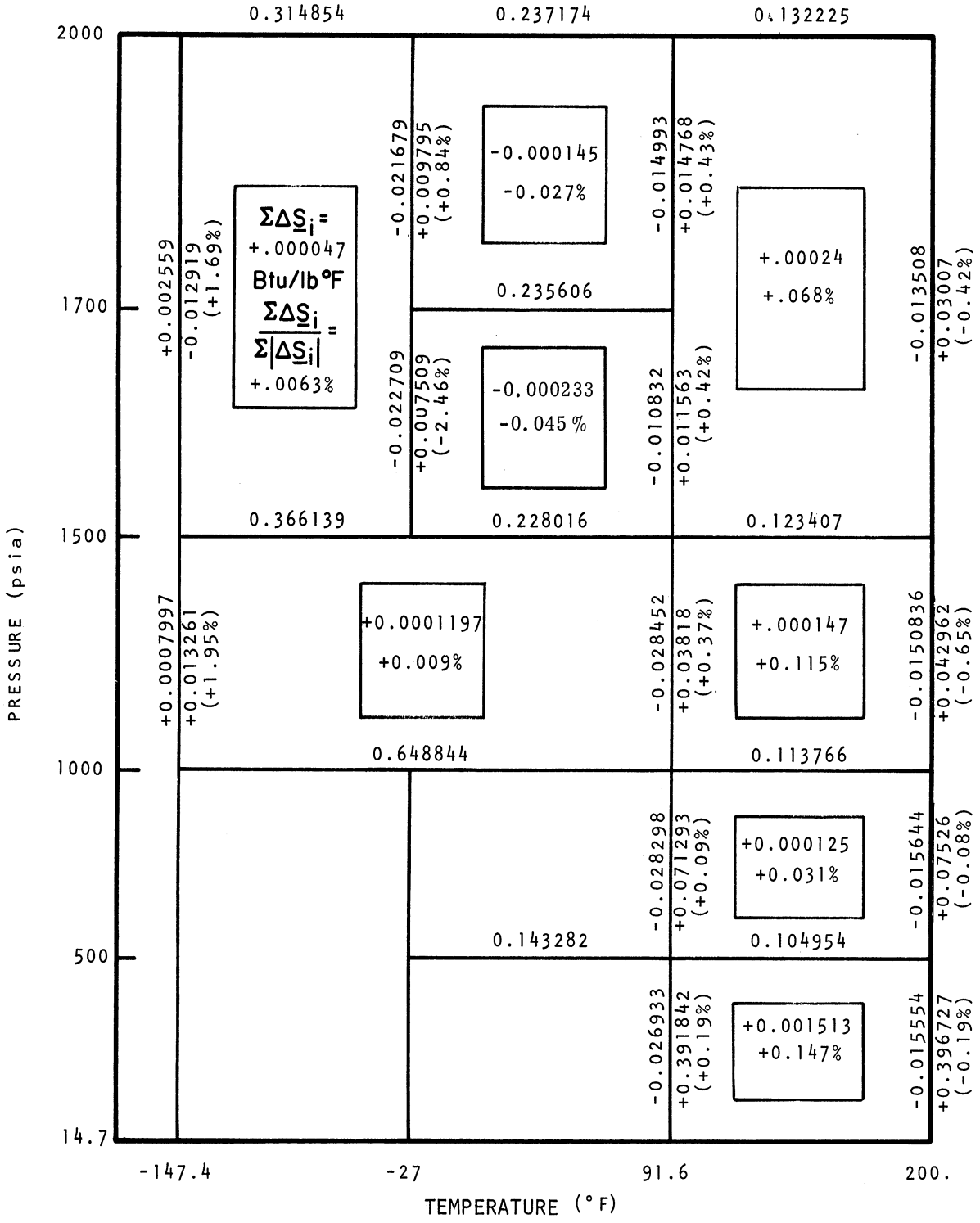

Figure 3. Check of Thermodynamic Consistency of Entropy Differences Calculated from Calorimetric and Volumetric Data.

The values of Z and $\underline{V}$ were modified so as to be consistent with the corrected values of $\Delta\underline{S}_P$ and $\Delta\underline{S}_T$. The corrected values of Z and $\underline{V}$ were used to calculate values of entropy at equal intervals of pressure along each experimental isotherm. This procedure yields values of $\emptyset$, $\underline{V}$ and $\underline{S}$ that are thermodynamically consistent with values of $\underline{H}$ determined from calorimetric data only. The consistency of the values should be better than 1 part in 1000.

The bases selected for the entropy determination are $\underline{S} = 0$ for each pure component as a perfectly oriented crystal at absolute zero on the temperature scale as described in detail in Appendix IX. As a result the values presented are for absolute entropy according to the third law of thermodynamics.

The smoothed and corrected values of $\underline{V}$ (and Z) were used to calculate values of fugacity, f, of the mixture at temperatures corresponding to each experimental isotherm according to fundamental definitions of classical thermodynamics as described in detail in Appendix V. It seems reasonable that these values are also thermodynamically consistent with other reported values to 1 part in 1000.

Skeleton Tables of Thermodynamic Values

The following tables contain the values developed from published calorimetric and volumetric data by the procedures described in preceeding sections.

The first four tables are for the temperatures of the isothermal and isenthalpic determinations as indicated on Figure 1. For each temperature, values of $\emptyset$, $\underline{H}$, $\underline{V}$, f and $\underline{S}$ are listed at atmospheric pressure and at intervals of 50 psia from zero to

2000 psia. The bases for enthalpy are $\underline{H} = 0$ for all compounds (including CO_2) as saturated liquids at -280°F. These choices are consistent with previously published values for methane (40,41), propane (70) and their mixtures (47,48,50,51,70,73). The bases for entropy are $\underline{S} = 0$ for all pure compounds as perfectly oriented crystals at absolute zero. Therefore, the values of $\underline{S}$ are absolute values in accordance with the third law of thermodynamics.

The pair of fold-out tables are principally for the pressures of the experimental isobars as indicated on Figure 1. Values at zero and atmospheric pressure are also included. These values are based primarily on tabular values listed by API Project 44 (1,58). At each pressure above atmospheric, values C_p, $\underline{H}$ and $\underline{S}$ are listed at intervals of 10°F between -280 and 300°F and at each of the temperatures of the isothermal and isenthalpic determinations. Values of $\underline{H}$ and $\underline{S}$ are listed within the two-phase region but values of C_p are not reported in this region. Values are reported only where experimental determinations were made or, in some cases, such as the low temperature region, where considerable care was taken in estimating these data by crossploting. Therefore, blanks in the table indicate lack of data at those particular conditions of pressure and temperature.

As indicated previously the values listed in the skeleton tables correspond in general to conditions of experimental determinations as represented on Figure 1. These values therefore

represent smoothed experimental values and are expected to be accurate on the order of 1 part per 1000. Therefore, these values can be used to advantage to test methods of prediction for all the properties.

Thermodynamic Diagrams

The values from the skeleton tables were plotted on large graph paper and smoothed so as to yield both PTH and Mollier (S, H) diagrams (See Figures 4 and 5). Both are presented as pairs of 11 x 17 diagrams so that values of H can be read to better than 1 Btu/lb and S can be read to better than 0.05 Btu/lb°F over the entire range of temperature and pressure.

ACKNOWLEDGMENTS

Richard J. Giszczak made significant contributions to this report by carrying out the interpolations of the volumetric data to yield values at the desired temperatures and compositions. This work was supported by a special grant from the Natural Gas Processors Association. The manuscript was typed by Diana Frinkel.

TABLES OF THERMODYNAMIC DATA

Table 2a

Mixture of Methane and Propane Containing Approximately 5.2 Percent Propane

Values at the Temperatures of Isothermal and Isenthalpic Determinations

T = 200°F

P	ø	H	V	f	S
psia	Btu/lb psi	Btu/lb	ft^3/lb	psi	Btu/lb°R
0	-0.02146	465.670		0.0	
14.7	-0.02144	465.356	27.46	14.868	2.697828
50	-0.02140	464.603	8.0377	49.59	2.558466
100	-0.02134	463.537	4.009	98.61	2.478786
150	-0.02129	462.474	2.6671	147.27	2.431625
200	-0.02123	461.412	1.9963	195.64	2.397760
250	-0.02117	460.353	1.5934	243.73	2.371185
300	-0.02112	459.296	1.3244	291.56	2.349234
350	-0.02105	458.241	1.1315	339.11	2.330484
400	-0.02100	457.188	0.9858	386.32	2.314078
450	-0.02096	456.138	0.8730	433.18	2.299481
500	-0.02090	455.090	0.7831	479.73	2.286308
550	-0.02086	454.043	0.7100	526.0	2.274246
600	-0.02081	452.999	0.6489	571.98	2.263147
650	-0.02076	451.958	0.5972	617.68	2.252844
700	-0.02071	450.920	0.5528	663.10	2.243215
750	-0.02067	449.885	0.5144	708.23	2.234168
800	-0.02061	448.854	0.4810	753.10	2.225634
850	-0.02058	447.827	0.4516	797.70	2.217544
900	-0.02050	446.804	0.4254	842.06	2.209843
950	-0.02043	445.784	0.4021	886.18	2.202495
1000	-0.02036	444.770	0.3811	930.07	2.195467
1050	-0.02028	443.750	0.3600	973.47	2.188744
1100	-0.02020	442.734	0.3428	1016.63	2.182270
1150	-0.02012	441.723	0.3273	1059.57	2.176046
1200	-0.02002	440.718	0.3131	1102.29	2.170028
1250	-0.01991	439.718	0.3001	1144.82	2.164216
1300	-0.01980	438.724	0.2880	1187.15	2.158589
1350	-0.01967	437.737	0.2768	1229.27	2.153126
1400	-0.01953	436.757	0.2664	1271.21	2.147838
1450	-0.01937	435.784	0.2567	1312.93	2.142696
1500	-0.01920	434.820	0.2477	1354.46	2.137698
1550	-0.01900	433.869	0.2403	1395.98	2.132894
1600	-0.01879	432.928	0.2325	1437.33	2.128158
1650	-0.01855	431.997	0.2251	1478.51	2.123536
1700	-0.01829	431.077	0.2183	1519.55	2.119028
1750	-0.01802	430.170	0.2118	1560.44	2.114635
1800	-0.01770	429.276	0.2058	1601.22	2.110359
1850	-0.01739	428.396	0.2000	1641.85	2.106180
1900	-0.01705	427.533	0.1946	1682.34	2.102102
1950	-0.01672	426.687	0.1895	1722.71	2.098124
2000	-0.01638	425.859	0.1846	1762.97	2.094248

TABLES OF THERMODYNAMIC DATA

Table 2b

Mixture of Methane and Propane Containing
Approximately 5.2 Percent Propane

Values at the Temperatures of Isothermal
and Isenthalpic Determinations

T = 91.6°F

P	Ø	H	V	f	S
psia	Btu/lb psi	Btu/lb	ft^3/lb	psi	Btu/lb°R
0	-0.03040	406.970			
14.7	-0.03042	406.523	22.94	14.67	2.60088
50	-0.03044	405.452	6.6985	49.50	2.46082
100	-0.03050	403.932	3.3291	98.11	2.380356
150	-0.03054	402.410	2.2081	146.07	2.332404
200	-0.03059	400.886	1.6476	193.44	2.297738
250	-0.03064	399.359	1.3106	240.25	2.270356
300	-0.03069	397.83	1.0851	286.66	2.247525
350	-0.03074	396.297	0.9233	332.30	2.227974
400	-0.03080	394.76	0.8016	377.22	2.210779
450	-0.03085	393.220	0.7073	421.60	2.195355
500	-0.03091	391.677	0.6324	465.34	2.181354
550	-0.03097	390.131	0.5703	508.45	2.168477
600	-0.03104	388.583	0.5197	551.03	2.156536
650	-0.03110	387.033	0.4768	593.11	2.145372
700	-0.03116	385.480	0.4394	634.61	2.134875
750	-0.03123	383.922	0.4070	675.52	2.124952
800	-0.03129	382.360	0.3789	715.87	2.115532
850	-0.03135	380.793	0.3542	755.69	2.106545
900	-0.03140	379.223	0.3326	795.00	2.097933
950	-0.03145	377.651	0.3133	833.83	2.089661
1000	-0.03148	376.077	0.2955	872.17	2.081701
1050	-0.03151	374.499	0.2786	910.00	2.074029
1100	-0.03152	372.922	0.2634	947.13	2.066613
1150	-0.03151	371.346	0.2504	983.78	2.059449
1200	-0.03149	369.771	0.2387	1020.0	2.052485
1250	-0.03144	368.197	0.2280	1055.74	2.045718
1300	-0.03137	366.626	0.2182	1091.11	2.039127
1350	-0.03127	365.059	0.2090	1126.08	2.032695
1400	-0.03115	363.497	0.2005	1160.68	2.026433
1450	-0.03101	361.441	0.1927	1195.31	2.020270
1500	-0.03084	360.392	0.1850	1229.13	2.014291
1550	-0.03062	358.852	0.1787	1262.67	2.008440
1600	-0.03036	357.327	0.1724	1295.86	2.002735
1650	-0.03005	355.815	0.1666	1328.72	1.997158
1700	-0.02966	354.319	0.1613	1361.29	1.991692
1750	-0.02915	352.847	0.1564	1393.62	1.986357
1800	-0.02844	351.418	0.1516	1425.70	1.981199
1850	-0.02752	350.029	0.1469	1457.49	1.976124
1900	-0.02658	348.685	0.1427	1489.01	1.971264
1950	-0.02559	347.391	0.1387	1520.28	1.966563
2000	-0.02459	346.147	0.1350	1551.35	1.962023

TABLES OF THERMODYNAMIC DATA

Table 2c

Mixture of Methane and Propane Containing Approximately 5.2 Percent Propane

Values at the Temperatures of Isothermal and Isenthalpic Determinations

T = -27°F

P	Ø	H	V	S
psia	Btu/lb psi	Btu/lb	ft^3/lb	Btu/lb°R
0	-0.04559	347.530		
14.7	-0.04589	346.858		
50	-0.04670	345.223		
100	-0.04791	342.858		
150	-0.04907	340.434		
200	-0.05033	337.948		
250	-0.05164	335.399		
300	-0.05305	332.781		
350	-0.05447	330.093		
400	-0.05598	327.332		
450	-0.05749	324.495		
500	-0.05921	321.578		
550	-0.06096	318.575		
600	-0.06288	315.479		
650	-0.06479	312.287		
700	-0.06681	308.997		
750	-0.06883	305.606		
800	-0.07084	302.115		
850	-0.07296	298.520		
900	-0.07487	294.824		
950	-0.07679	291.033		
1000	-0.07850	287.153	0.1645	1.898613
1050	-0.07970	283.193	0.1565	1.886046
1100	-0.08010	279.160	0.1474	1.873576
1150	-0.07990	275.196	0.1395	1.861264
1200	-0.07899	271.221	0.1312	1.849175
1250	-0.07707	267.319	0.1238	1.837426
1300	-0.07434	263.534	0.1165	1.836123
1350	-0.07111	259.898	0.1102	1.815302
1400	-0.06727	256.438	0.1046	1.805018
1450	-0.06293	253.183	0.09867	1.795323
1500	-0.05838	250.15	0.09419	1.786275
1550	-0.05351	247.356	0.08986	1.777851
1600	-0.04908	244.791	0.08586	1.770063
1650	-0.04474	242.446	0.08297	1.762844
1700	-0.04081	240.307	0.08041	1.756161
1750	-0.03729	238.354	0.07833	1.749955
1800	-0.03406	236.571	0.07625	1.744186
1850	-0.03104	234.943	0.07432	1.738821
1900	-0.02822	233.462	0.07256	1.733832
1950	-0.02529	232.124	0.07096	1.729209
2000	-0.02247	230.930	0.06936	1.724952

TABLES OF THERMODYNAMIC DATA

Table 2d

Mixture of Methane and Propane Containing Approximately 5.2 Percent Propane

Values at the Temperatures of Isothermal and Isenthalpic Determinations

T = -147.4°F

P	Ø	H	V	S
psia	Btu/lb psi	Btu/lb	ft^3/lb	Btu/lb°R
500	-0.0023	112.977	0.04805	1.448738
550	-0.0020	112.868	0.04783	1.446971
600	-0.0018	112.771	0.04765	1.445248
650	-0.0016	112.684	0.04751	1.443561
700	-0.0014	112.607	0.04733	1.441912
750	-0.0011	112.540	0.04716	1.440299
800	-0.0009	112.488	0.04700	1.438740
850	-0.0007	112.446	0.04685	1.437218
900	-0.0005	112.414	0.04671	1.435732
950	-0.00035	112.390	0.04656	1.434274
1000	-0.0002	112.377	0.04642	1.432856
1050	-0.0000	112.372	0.04626	1.431469
1100	0.0002	112.377	0.04610	1.430119
1150	0.0003	112.39	0.04596	1.428798
1200	0.0004	112.409	0.04581	1.42750
1250	0.0005	112.433	0.04568	1.426222
1300	0.0006	112.461	0.04552	1.424963
1350	0.0007	112.494	0.04539	1.423724
1400	0.0008	112.532	0.04527	1.422504
1450	0.00095	112.576	0.04514	1.421307
1500	0.0011	112.627	0.04498	1.420136
1550	0.0012	112.683	0.04471	1.418987
1600	0.0013	112.745	0.04437	1.417867
1650	0.0014	112.812	0.04369	1.416782
1700	0.0015	112.885	0.04301	1.415736
1750	0.0016	112.962	0.04248	1.414717
1800	0.0017	113.045	0.04197	1.413733
1850	0.0018	113.132	0.04146	1.412776
1900	0.0019	113.224	0.04100	1.411851
1950	0.00205	113.322	0.04065	1.410959
2000	0. 0022	113.427	0.04045	1.410098

TABLES OF THERMODYNAMIC DATA

Table 3a

Mixture of Methane and Propane Containing Approximately 5.2 Percent Propane

Values at the Pressures of Isobaric Determinations

Temperature °F	P = 0 psia C_p Btu/lb°F	P = 0 psia H Btu/lb	P = 14.7 psia H Btu/lb	P = 14.7 psia S Btu/lb°R	P = 250 psia C_p Btu/lb°F	P = 250 psia H Btu/lb	P = 250 psia S Btu/lb°R	P = 400 psia C_p Btu/lb°F	P = 400 psia H Btu/lb	P = 400 psia S Btu/lb°R	P = 500 psia C_p Btu/lb°F	P = 500 psia H Btu/lb	P = 500 psia S Btu/lb°R	P = 650 psia C_p Btu/lb°F	P = 650 psia H Btu/lb	P = 650 psia S Btu/lb°R	P = 800 psia C_p Btu/lb°F	P = 800 psia H Btu/lb	P = 800 psia S Btu/lb°R	Temperature °F
-280	0.460	228.97			0.7765	1.759	0.995950	0.7749	2.46	0.994819	-280	0.7730	2.98	0.995933	0.7718	3.633	0.994168	0.7702	4.16	0.991922	-280
-270	0.460	233.57			0.7779	9.459	1.037546	0.7759	10.26	1.036952	-270	0.7742	10.711	1.037702	0.7728	11.333	1.035764	0.7712	11.76	1.032972	-270
-260	0.461	238.17	236.25	2.115641	0.7795	17.259	1.07752	0.7771	18.06	1.076939	-260	0.7754	18.453	1.077448	0.7741	19.033	1.075228	0.7726	19.46	1.072442	-260
-250	0.462	242.77	240.75	2.13759	0.7826	25.159	1.116039	0.7800	25.96	1.115474	-250	0.7770	26.215	1.115326	0.7763	26.833	1.113274	0.7745	27.26	1.110492	-250
-240	0.462	247.37	245.25	2.158550	0.7887	33.159	1.153237	0.7857	33.86	1.152226	-240	0.7834	34.017	1.151610	0.7810	34.633	1.149557	0.7790	35.16	1.147241	-240
-230	0.463	252.07	249.85	2.179201	0.7960	41.359	1.189684	0.7922	41.86	1.187803	-230	0.7890	41.879	1.186549	0.7860	42.533	1.184668	0.7831	43.16	1.183787	-230
-220	0.463	256.67	254.45	2.198784	0.8080	49.659	1.224993	0.8030	49.96	1.222286	-220	0.7995	49.822	1.220288	0.7960	50.533	1.218715	0.7928	51.26	1.217262	-220
-210	0.464	261.27	259.05	2.217561	0.8242	58.059	1.259310	0.8169	58.06	1.255359	-210	0.8124	57.865	1.253053	0.8062	58.633	1.251708	0.8010	59.46	1.250732	-210
-200	0.464	265.87	263.75	2.2360	0.8435	66.659	1.29303	0.8332	66.26	1.287524	-200	0.8262	66.029	1.284999	0.8175	66.833	1.283795	0.8094	67.76	1.283277	-200
-190	0.465	270.47	268.45	2.253740	0.8692	75.459	1.32623	0.8485	74.66	1.319236	-190	0.8419	74.354	1.316351	0.8328	75.133	1.315053	0.8240	76.16	1.314979	-190
-180	0.466	275.07	273.15	2.270837	0.8847	84.459	1.358977	0.8724	83.26	1.35052	-180	0.8643	82.880	1.347290	0.8538	83.533	1.345535	0.8435	84.66	1.345902	-180
-170	0.466	279.77	277.95	2.287594	0.9150	93.659	1.391487	0.9028	92.06	1.381415	-170	0.8928	91.657	1.378003	0.8700	92.033	1.375296	0.8672	93.26	1.376083	-170
-160	0.467	284.47	282.75	2.303871	*	196.059	1.73836	0.9478	101.56	1.413622	-160	0.9313	100.771	1.408900	0.9100	100.633	1.404371	0.8918	102.06	1.405925	-160
-150	0.468	289.17	287.55	2.319605	*	221.059	1.82046	1.035	111.46	1.446072	-150	0.9833	110.327	1.440231	0.9557	109.633	1.433793	0.9305	111.06	1.435531	-150
-147.4	0.468	290.37	288.85	2.323781	*	233.459	1.83428		115.16	1.457954	-147.4	1.0004	112.977	1.448738	0.9690	112.133	1.441745	0.9390	113.46	1.443239	-147.4
-140	0.469	293.87	292.35	2.334845	*	237.759	1.87351	*	154.48	1.58283	-140	1.0624	120.477	1.472445	1.005	119.133	1.463761	0.9610	120.36	1.464986	-140
-130	0.470	298.57	297.15	2.349619	*	251.159	1.91478	*	222.34	1.79076	-130	1.2540	134.077	1.514281	1.123	130.933	1.500032	1.030	129.96	1.494463	-130
-120	0.471	303.27	301.95	2.363948	*	262.259	1.94793	*	243.03	1.85205	-120		209.177	1.737597	1.317	143.133	1.536348	1.150	140.36	1.525459	-120
-110	0.472	307.97	306.75	2.377862	*	271.959	1.97605	*	256.46	1.89062	-110		235.177	1.812626	*	168.533	1.60967	1.240	152.76	1.561342	-110
-100	0.473	312.67	311.55	2.39138	*	280.959	2.00141	*	267.26	1.92076	-100		251.677	1.858843	*	202.333	1.75978	1.760	167.76	1.603495	-100
- 90	0.474	317.37	316.35	2.404530	*	289.859	2.02580	*	276.84	1.94677	- 90		264.177	1.892889	*	242.833	1.81775	*	207.36	1.71163	- 90
- 80	0.475	322.17	321.15	2.417329	*	298.959	2.05006	*	286.11	1.97103	- 80		274.577	1.920453	*	257.533	1.85688	*	234.56	1.78423	- 80
- 70	0.477	326.87	325.95	2.429798	*	308.559	2.075011	*	295.49	1.99519	- 70		284.777	1.946788	*	269.633	1.88824	*	252.56	1.83103	- 70
- 60	0.478	331.67	330.75	2.441951	0.566	318.759	2.100860	*	305.49	2.02025	- 60		294.877	1.972203	*	281.033	1.91702	*	266.06	1.86515	- 60
- 50	0.480	336.47	335.55	2.453806	0.557	323.559	2.112698	*	315.78	2.04544	- 50		304.877	1.996736	*	292.033	1.94410	*	278.66	1.89620	- 50
- 40	0.482	341.27	340.45	2.465616	0.550	328.459	2.124512	0.490	322.62	2.061902	- 40	0.6453	314.177	2.020446	*	302.633	1.96956	*	289.96	1.92334	- 40
- 30	0.484	346.07	345.35	2.477147	0.548	333.459	2.136276	0.510	327.49	2.07334	- 30	0.6325	319.877	2.033855	0.785	310.833	1.989056	0.910	299.46	1.945535	- 30
- 27	0.485	347.57	346.85	2.480623	0.54	335.359	2.139752	0.527	329.0	2.076946	- 27	0.6300	321.579	2.038071	0.761	312.30	1.993459	0.878	302.10	1.950554	- 27
- 20	0.487	350.97	350.95	2.488413	0.539	338.959	2.148000	0.564	332.51	2.084965	- 20	0.6212	325.965	2.048122	0.711	317.033	2.003997	0.803	307.26	1.962388	- 20
- 10	0.489	355.77	355.85	2.499424	0.536	344.159	2.159684	0.564	337.97	2.097199	- 10	0.6102	332.116	2.061940	0.682	323.833	2.018604	0.756	314.46	1.978712	- 10
0	0.491	360.77	360.75	2.510192	0.534	349.359	2.171112	0.563	343.83	2.110019	0	0.6012	338.169	2.075242	0.663	330.133	2.032669	0.724	321.56	1.994456	0
10	0.494	365.67	365.65	2.520732	0.534	354.559	2.182509	0.563	349.59	2.122355	10	0.5941	344.149	2.088091	0.645	336.633	2.046433	0.697	328.56	2.009643	10
20	0.497	370.57	370.55	2.531050	0.535	359.859	2.193667	0.562	355.35	2.134432	20	0.5890	350.068	2.100551	0.633	342.933	2.059696	0.667	335.46	2.024303	20
30	0.500	375.57	375.45	2.541155	0.536	365.059	2.204802	0.562	361.01	2.146059	30	0.5849	355.940	2.112661	0.623	349.233	2.072686	0.661	342.36	2.038523	30
40	0.503	380.57	380.45	2.551257	0.537	370.459	2.215708	0.562	366.67	2.157451	40	0.5822	361.777	2.124450	0.617	355.433	2.085214	0.661	349.16	2.052266	40
50	0.506	385.67	385.45	2.561169	0.537	375.859	2.226599	0.561	372.23	2.168425	50	0.5804	367.591	2.135960	0.611	361.633	2.097493	0.642	355.86	2.06554	50
60	0.509	390.77	390.45	2.570879	0.538	381.359	2.237278	0.561	377.79	2.179186	60	0.5792	373.392	2.147218	0.607	367.833	2.109532	0.634	362.46	2.078363	60
70	0.512	395.87	395.45	2.580404	0.540	386.959	2.247945	0.561	383.25	2.189558	70	0.5787	379.182	2.158244	0.605	373.933	2.121148	0.628	368.86	2.09056	70
80	0.516	400.97	400.489	2.58975	0.543	392.559	2.258412	0.560	388.61	2.199554	80	0.5783	384.968	2.169058	0.604	380.033	2.132549	0.623	375.16	2.10234	80
90	0.519	406.17	405.721	2.599421	0.546	398.159	2.268687	0.560	393.87	2.209189	90	0.5778	390.752	2.179675	0.603	386.033	2.143555	0.619	381.36	2.113716	90
91.6	0.520	406.97	406.523	2.60088	0.546	399.359	2.270866	0.560	394.76	2.210779	91.6	0.5773	391.677	2.181354	0.603	387.033	2.145372	0.618	382.36	2.115532	91.6
100	0.523	411.37	410.917	2.608778							100	0.5771	396.531	2.190076							100
110	0.527	416.57	416.113	2.617974							110	0.5780	402.313	2.200304							110
120	0.531	421.87	421.408	2.627183							120	0.5795	408.109	2.210370							120
130	0.535	427.17	426.704	2.636235							130	0.5809	413.917	2.220294							130
140	0.539	432.57	432.10	2.645303							140	0.5829	419.739	2.230082							140
150	0.543	437.97	437.495	2.654210							150	0.5849	425.577	2.239740							150
160	0.547	443.37	442.876	2.662960							160	0.5871	431.433	2.249275							160
170	0.552	448.87	448.383	2.671773							170	0.5894	437.309	2.258686							170
180	0.556	454.47	453.983	2.680592							180	0.5921	443.209	2.267992							180
190	0.560	460.07	459.680	2.689268							190	0.5949	449.135	2.277195							190
200	0.565	465.67	465.356	2.697828							200	0.5981	455.09	2.286308							200
210	0.570	471.37	470.956	2.706249							210	0.6020	461.079	2.295333							210
220	0.574	477.07	476.656	2.714694							220	0.6058	467.104	2.304276							220
230	0.579	482.87	482.356	2.723014							230	0.6090	473.167	2.313142							230
240	0.584	488.67	488.156	2.731359							240	0.6123	479.268	2.321929							240
250	0.588	494.57	493.956	2.739586							250	0.6156	485.407	2.330636							250
260	0.593	500.47	499.856	2.747837							260	0.6190	491.584	2.339267							260
270	0.598	506.37	505.856	2.754112							270	0.6226	497.799	2.347829							270
280	0.603	512.37	511.956	2.764412							280	0.6262	504.052	2.356325							280
290	0.608	518.47	518.156	2.772734							290	0.6300	510.343	2.364755							290
300	0.613	524.57	524.456	2.781075							300	0.6340	516.672	2.373124							300

TABLES OF THERMODYNAMIC DATA

Table 3b

Mixture of Methane and Propane Containing Approximately 5.2 Percent Propane

Values at the Pressures of Isobaric Determinations

Temperature °F	P = 1000 psia C_p Btu/lb°F	H Btu/lb	S Btu/lb°R	P = 1100 psia C_p Btu/lb°F	H Btu/lb	S Btu/lb°R	P = 1200 psia C_p Btu/lb°F	H Btu/lb	S Btu/lb°R	P = 1500 psia C_p Btu/lb°F	H Btu/lb	S Btu/lb°R	P = 1700 psia C_p Btu/lb°F	H Btu/lb	S Btu/lb°R	P = 2000 psia C_p Btu/lb°F	H Btu/lb	S Btu/lb°R	Temperature °F
-280	0.7694	5.442	0.990754							0.7630	7.865	0.986385				0.7580	10.288	0.982389	-280
-270	0.7704	13.136	1.032348							0.7640	15.505	1.027635				0.7585	17.873	1.023400	-270
-260	0.7714	20.840	1.071883							0.7650	23.145	1.066795				0.7590	25.458	1.062319	-260
-250	0.7745	28.564	1.109558							0.7660	30.795	1.104105				0.7595	33.043	1.099326	-250
-240	0.7765	36.318	1.145629							0.7680	38.465	1.139776				0.7605	40.638	1.134663	-240
-230	0.7805	44.113	1.180278							0.7720	46.165	1.174007				0.7625	48.253	1.168504	-230
-220	0.7885	51.958	1.213660							0.7765	53.905	1.206938				0.7665	55.898	1.201030	-220
-210	0.7925	59.863	1.245907							0.7825	61.695	1.238725				0.7705	63.583	1.232389	-210
-200	0.8015	67.848	1.277217							0.7875	69.545	1.269496				0.7765	71.318	1.262730	-200
-190	0.8145	75.933	1.307711							0.7955	77.465	1.299363				0.7825	79.113	1.292156	-190
-180	0.8316	84.148	1.337566							0.8070	85.475	1.328474				0.7925	86.988	1.320797	-180
-170	0.8516	92.564	1.367094							0.8215	93.615	1.357035				0.8029	94.962	1.348788	-170
-160	0.8726	101.135	1.396150							0.8390	101.910	1.385148				0.8139	103.046	1.376202	-160
-150	0.9030	109.993	1.425195							0.8580	110.038	1.412918				0.8259	111.260	1.403135	-150
-147.4	0.9062	112.377	1.432856							0.8630	112.627	1.420136				0.8310	113.427	1.410098	-147.4
-140	0.9231	119.145	1.454261							0.8789	119.050	1.440437				0.8426	119.618	1.429667	-140
-130	0.9780	128.676	1.483573							0.9055	127.965	1.467825				0.8672	128.114	1.455811	-130
-120	1.0494	138.806	1.513815							0.9376	137.172	1.495309				0.8767	136.780	1.481675	-120
-110	1.1412	149.714	1.545463							0.9787	146.750	1.523084				0.8993	145.657	1.504838	-110
-100	1.2974	161.820	1.579576							1.0288	156.778	1.551331				0.9253	154.775	1.533065	-100
- 90	1.6277	176.260	1.619080				1.2939	170.978	1.598847	1.0930	167.369	1.580342				0.9544	164.174	1.558794	- 90
- 80	2.4152	196.028	1.671691	1.6048	188.525	1.648935	1.4920	184.858	1.635853	1.1697	178.672	1.610485				0.9875	173.884	1.584687	- 80
- 70	2.4631	220.723	1.735743	2.1077	207.585	1.698431	1.7332	201.069	1.677944	1.2605	190.816	1.642027	1.1297	187.174	1.626945	1.0231	183.935	1.610800	- 70
- 60	1.9321	242.649	1.791286	1.9966	228.361	1.751010	1.8523	219.261	1.723975	1.3557	203.905	1.675166	1.1902	198.771	1.656319	1.0592	194.347	1.637160	- 60
- 50	1.4700	259.404	1.832686	1.7554	247.196	1.797520	1.7402	237.444	1.768904	1.4299	217.856	1.709617	1.2447	210.958	1.686407	1.0933	205.100	1.663693	- 50
- 40	1.2206	272.746	1.864843	1.3725	262.488	1.834382	1.4710	253.505	1.807620	1.4319	232.217	1.744219	1.2807	223.605	1.716888	1.1229	216.184	1.690390	- 40
- 30	1.0609	284.101	1.891536		275.498	1.864997	1.2288	266.924	1.839202	1.3607	246.218	1.777159	1.2807	236.445	1.747111	1.1390	227.509	1.717027	- 30
- 27	1.0220	287.153	1.898613		279.201	1.873576	1.1768	271.227	1.849175	1.3292	250.150	1.786275	1.2710	240.318	1.756086	1.1408	230.930	1.724952	- 27
- 20	0.9487	294.274	1.914909							1.2621	259.324	1.807260	1.2358	249.141	1.776300	1.1364	238.902	1.743217	- 20
- 10	0.8731	303.353	1.935299							1.1761	271.516	1.834645	1.1797	261.229	1.803470	1.1239	250.201	1.768613	- 10
0	0.8169	311.785	1.953827							1.0970	282.872	1.859603	1.1182	272.717	1.828718	1.0948	261.289	1.792922	0
10	0.7756	319.729	1.970904							1.0205	293.453	1.882379	1.0547	283.589	1.852100	1.0568	272.047	1.816110	10
20	0.7438	327.315	1.986864							0.9439	303.256	1.903021	0.9926	293.816	1.873631	1.0162	282.404	1.837902	20
30	0.7180	334.623	2.001923							0.8752	312.334	1.921742	0.9396	303.465	1.893526	0.9751	292.350	1.858405	30
40	0.6986	341.697	2.016207							0.8285	320.834	1.938917	0.8926	312.627	1.912043	0.9356	301.906	1.877707	40
50	0.6852	348.607	2.029890							0.7977	328.957	1.955004	0.8505	321.343	1.929304	0.9005	311.081	1.895877	50
60	0.6702	355.361	2.043023							0.7743	336.811	1.970258	0.8170	329.675	1.945481	0.8695	319.926	1.913052	60
70	0.6603	362.003	2.055678							0.7554	344.456	1.984820	0.7930	337.721	1.960807	0.8424	328.481	1.929346	70
80	0.6513	368.566	2.067943							0.7385	351.922	1.998773	0.7745	345.555	1.975453	0.8194	336.785	1.944866	80
90	0.6444	375.050	2.079837							0.7256	359.239	2.012198	0.7585	353.215	1.989484	0.8044	344.879	1.959720	90
91.6	0.6426	376.077	2.081701							0.7242	360.392	2.014291	0.7562	354.417	1.991692	0.7950	346.147	1.962023	91.6
100	0.6389	381.467	2.091408							0.7159	366.446	2.025202	0.7435	360.725	2.003066	0.7788	352.752	1.973911	100
110	0.6359	387.836	2.102685							0.7074	373.559	2.037798				0.7643	360.464	1.987568	110
120	0.6339	394.175	2.113715							0.7004	380.594	2.050036				0.7524	368.047	2.000767	120
130	0.6339	400.514	2.124559							0.6930	387.561	2.061949				0.7424	375.531	2.013568	130
140	0.6339	406.842	2.135201							0.6855	394.458	2.073542				0.7335	382.916	2.025985	140
150	0.6329	413.170	2.145665							0.6795	401.285	2.084843				0.7260	390.211	2.038050	150
160	0.6319	419.490	2.155943							0.6750	408.052	2.095849				0.7195	397.436	2.049803	160
170	0.6319	425.810	2.166060							0.6715	414.780	2.106630				0.7146	404.601	2.061273	170
180	0.6326	432.130	2.176016							0.6690	421.487	2.117177				0.7101	411.717	2.072485	180
190	0.6334	438.450	2.185815							0.6660	428.164	2.127531				0.7066	418.803	2.083474	190
200	0.6342	444.770	2.195467							0.6656	434.820	2.137698				0.7055	425.859	2.094250	200
210	0.6350	451.105	2.204993							0.6658	441.500	2.147743				0.7045	432.924	2.104872	210
220	0.6358	457.445	2.214387							0.6660	448.180	2.157640				0.7030	439.964	2.115300	220
230	0.6365	463.800	2.223664							0.6665	454.855	2.167383				0.7010	446.974	2.125534	230
240	0.6390	470.175	2.232837							0.6670	461.525	2.177080				0.7000	453.974	2.135606	240
250	0.6440	476.585	2.241930							0.6675	468.195	2.186542				0.7000	460.974	2.145535	250
260	0.6470	483.035	2.250951							0.6685	474.875	2.195885				0.7010	467.984	2.155337	260
270	0.6490	489.515	2.259889							0.6715	481.575	2.205127				0.7015	474.994	2.165005	270
280	0.6500	496.015	2.268733							0.6740	488.295	2.214270				0.7020	482.004	2.174544	280
290	0.6520	502.525	2.277472							0.6765	495.050	2.223338				0.7022	489.019	2.183959	290
300	0.6550	509.055	2.286121							0.6785	501.830	2.232318				0.7025	496.039	2.193258	300

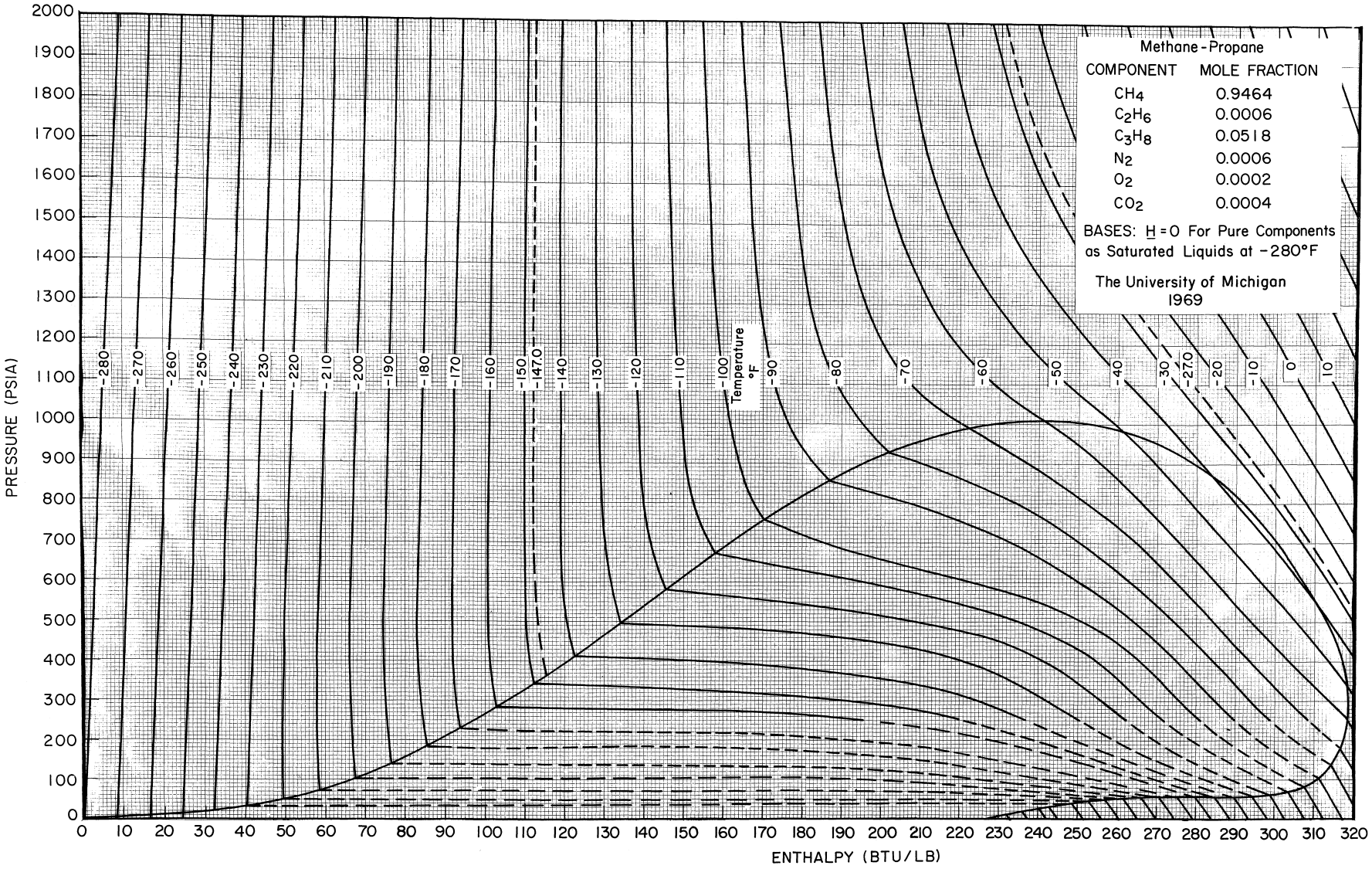

Figure 4a. Pressure-Temperature-Enthalpy Diagram for Nominal 5 Percent Propane in Methane Mixture (Low Temperatures)

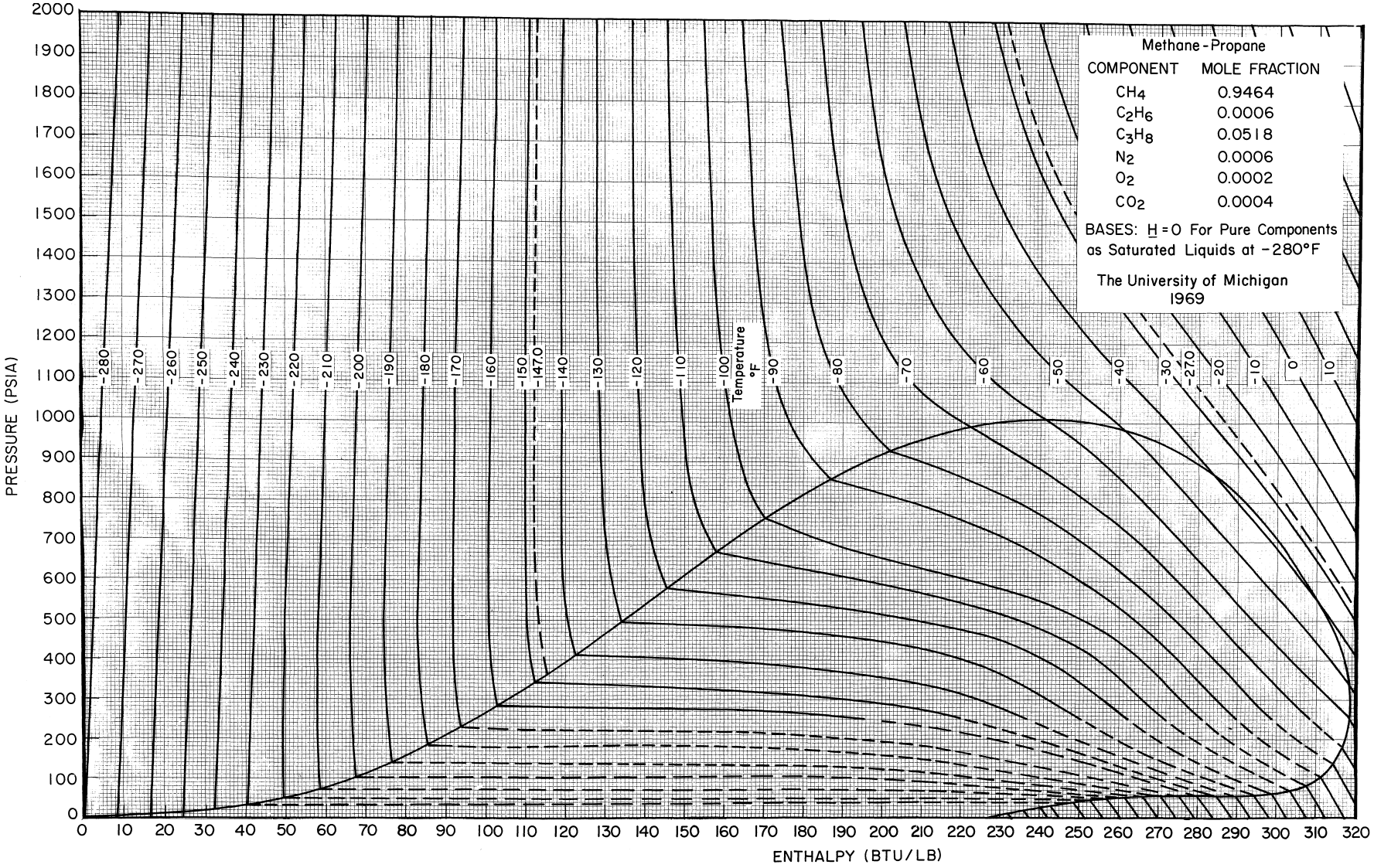

Figure 4a. Pressure-Temperature-Enthalpy Diagram for Nominal 5 Percent Propane in Methane Mixture (Low Temperatures)

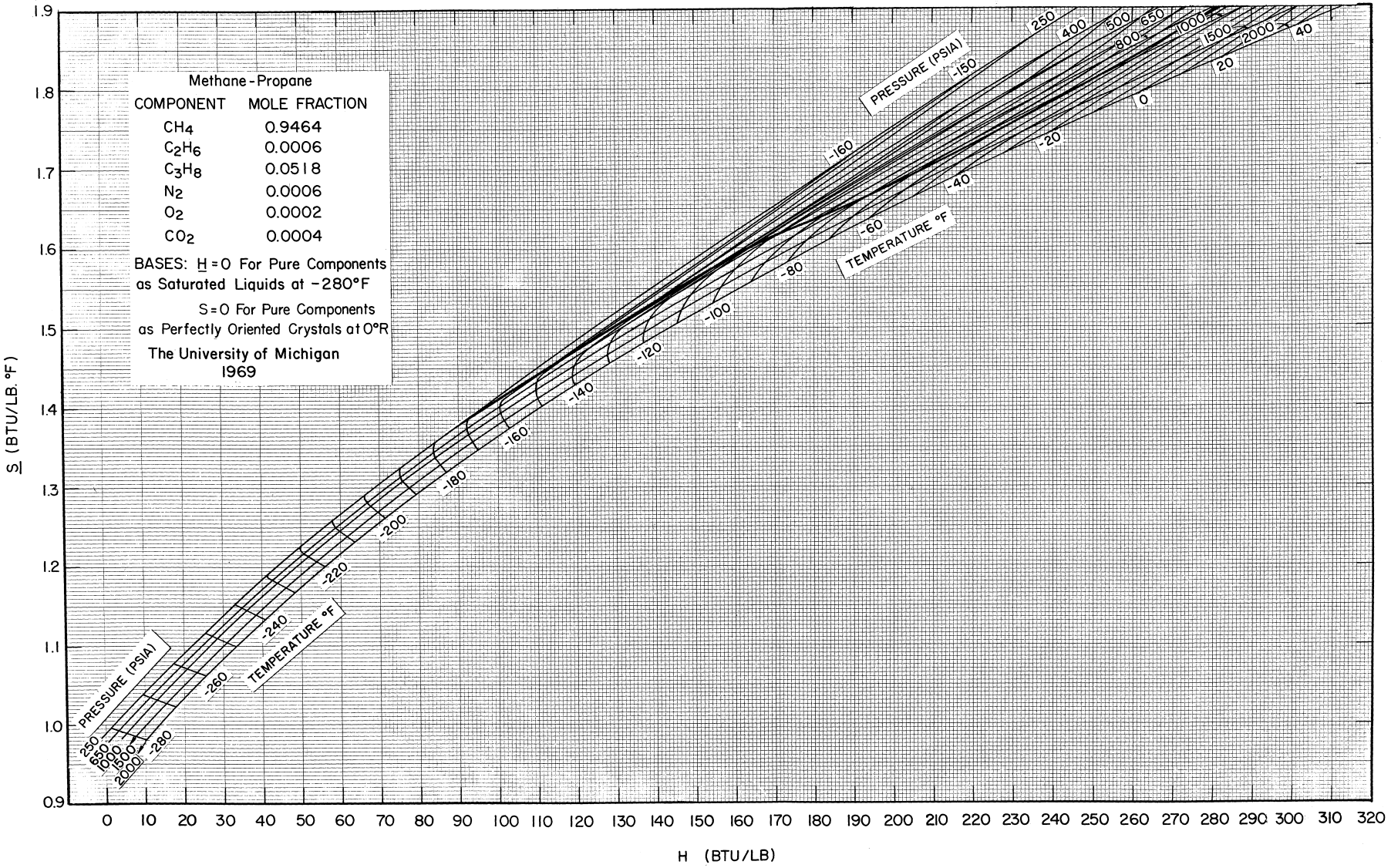

Figure 5a. Mollier Diagram for Nominal 5 Percent Propane in Methane Mixture (Low Temperatures)

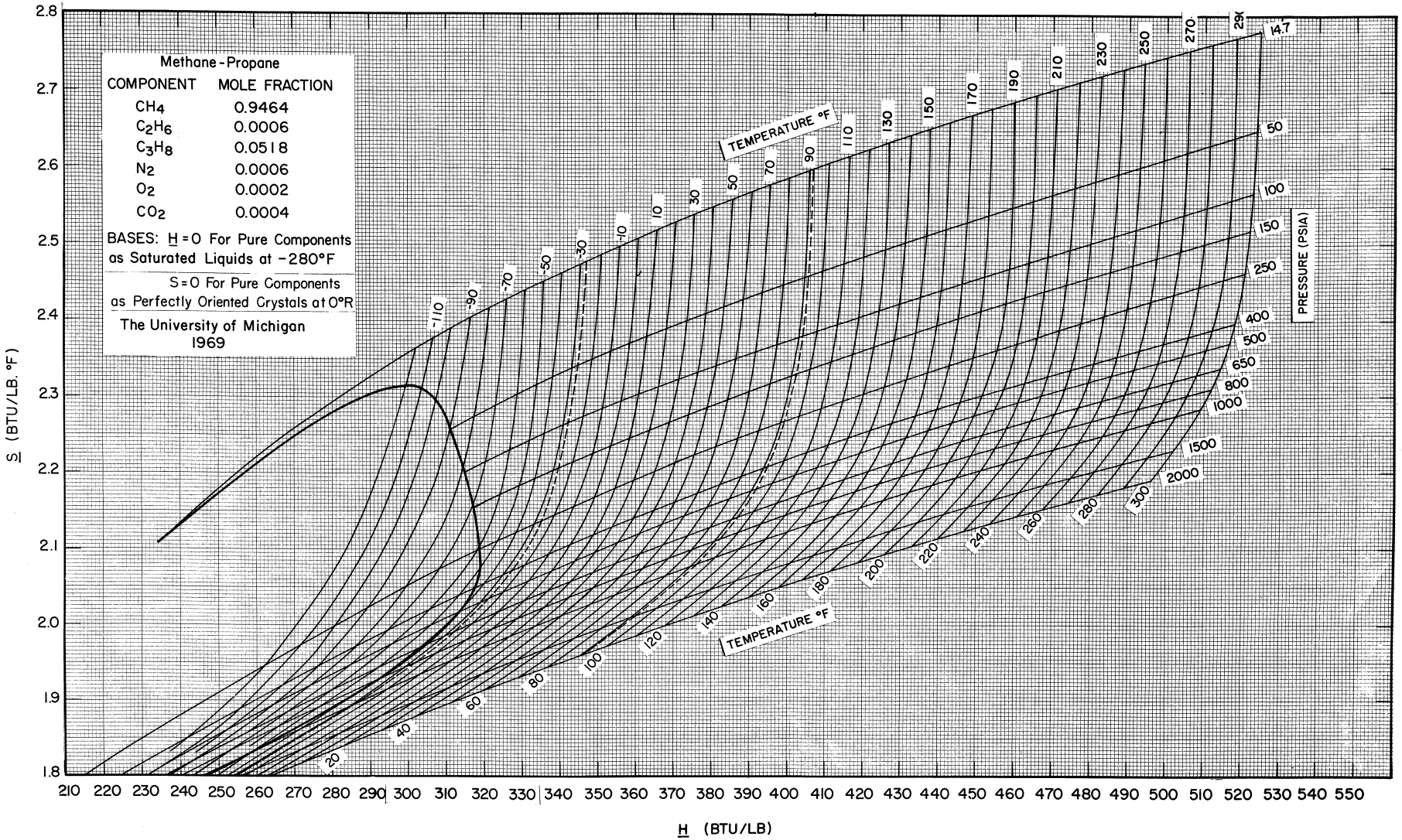

Figure 5b. Mollier Diagram for Nominal 5 Percent Propane in Methane Mixture (High Temperatures)

NOTATION

a,b	constants used in Equation (II.6)
a_i	coefficient in a polynomial
A	area under a curve
B	second virial coefficient in volume polynomial virial equation (Units of $\underline{V}$)
B_m	second virial coefficient of a mixture
B'	second virial equation in pressure polynomial virial equation (Units of P)
B_{11}	second virial coefficient of component 1
B_{12}	second virial coefficient of interaction between a molecul of component 1 and a molecule of component 2
B_{22}	second virial coefficient of component 2
C	third virial coefficient of volume polynomial virial equation (Units of $\underline{V}^2$)
C'	third virial coefficient in pressure polynomial virial equation (Units of P^2)
C_p	isobaric heat capacity $= (\partial \underline{H}/\partial T)_p$, (Btu/lb)
C_{pm}	isobaric heat capacity of a mixture (Btu/lb)
$C_{ps.l.}$	isobaric specific heat of saturated liquid (Btu/lb)
C_p^E	excess isobaric heat capacity (Btu/lb)
f	fugacity (psia)
$\underline{G}$	specific free energy (Btu/lb)
$\underline{H}$	specific enthalpy (Btu/lb)
$\underline{H}_B$	specific enthalpy at the beginning (Btu/lb)
$\underline{H}_i$	specific enthalpy of ith component (Btu/lb)
$\underline{H}_m$	specific enthalpy of the mixture (Btu/lb)

$\underline{H}^\circ$ specific enthalpy at zero pressure (Btu/lb)

$\underline{H}^\circ_T$ specific enthalpy at zero pressure and temperature T (Btu/lb)

IGM ideal gas mixture

n integer

P pressure (psia)

P_B pressure at the beginning (psia)

R gas constant

RGM real gas mixture

$\underline{S}$ specific entropy (Btu/lb°F)

$\underline{S}^\circ$ specific entropy of ideal gas (cal/gm mole°C)

$\underline{S}_i$ specific entropy in the ith state (Btu/lb°F)

T temperature (°F or °R)

T_B temperature at the beginning (°F or °R)

T_i temperature in ith state (°F or °R)

T_S bubble point (°F)

$\underline{U}$ specific internal energy (Btu/lb)

$\underline{V}$ specific volume (ft^3/lb or cc/g)

x mole fraction or mass fraction or an independent variable

y dependent variable

Z compressibility factor $\frac{PV}{RT}$

Z_m compressibility factor of a mixture

Greek Notation

$\Delta\underline{H}_i$ change in the specific enthalpy between two states (Btu/lb)

$\Delta\underline{H}_p$ change in specific enthalpy between two temperatures at constant pressure (Btu/lb)

$\Delta\underline{H}_T$ change in the specific enthalpy between two pressures at constant temperature (Btu/lb)

$\underline{\Delta H}_{vap}$ specific enthalpy of vaporization (Btu/lb)

$\underline{\Delta S}_i$ change in the specific entropy between two states (Btu/lb°F)

$\underline{\Delta S}_p$ change in specific entropy at constant pressure between two temperatures (Btu/lb°F)

$\underline{\Delta S}_T$ change in specific entropy at constant temperature between two pressures (Btu/lb°F)

μ Joule-Thomson coefficient

$\mathcal{L}$ fugacity coefficient (= f/p)

ρ density (g/cc or lb cu ft)

$\emptyset$ isothermal throttling coefficient $= \left(\frac{\partial \underline{H}}{\partial P}\right)_T$

Subscripts

B conditions at start

i component in a mixture or a running variable

j a running variable

m mixture

O outlet conditions

p pressure

s.l. saturated liquid

T temperature

vap vaporization condition

1 inlet condition or component 1

11 component 1

12 interaction condition between a molecule of component 1 and a molecule of component 2

2 component 2 or outlet condition

22 component 2

3 component three or a state 3

Superscripts

E	excess value
0	zero pressure value

BIBLIOGRAPHY

1. API Research Project No. 44., "Selected Values of Physical and Thermodynamic Properties of Hydrocarbons and Related Compounds," A and M College of Texas, College Station, Texas (1953)

2. Barnard, A.J., S.P. Luthra, D.M. Newitt and M.U. Pai, Proc. Roy Soc. (London) A209, 143 (1951)

3. Beattie, J.A., W.C. Kay and J. Kaminsky, J. Am. Chem. Soc. 59, 1589 (1937)

4. Beenakker, J.J.M., B. Van Eijnbergen, M. Knoester, K.W. Taconis and P. Zandbergen, Symp. Thermophys. Prop., Papers, 3rd, Lafayett, Ind., p. 114, 1965

5. Benedict, M., G.B. Webb and L.C. Rubin, J. Chem. Phys., 8, 334 (1940)

6. Benedict, M., G.B. Webb, and L.C. Rubin, J. Chem. Phys., 10, 747 (1942)

7. Bicher, L.B., and D.L. Katz, Ind. Eng. Chem. 35 754 (1943)

8. Brewer, J., Project No. 975-01, Air Force Office of Scientific Research, Arlington, Virginia, Dec. 1967

9. Budenholzer, R.A., D.F. Botkin, B.H. Sage and W.N. Lacey, Ind. Eng. Chem., 34, 878 (1942)

10. Budenholzer, R.A., B.H. Sage and W.N. Lacey, Ind. Eng. Chem., 35, 1214 (1943)

11. Canjar, L.N. and F.S. Manning, Hydrocarbon Process. Petrol. Refiner, 41 No. 8 121-3 (1962)

12. Canjar, L.N. and F.S. Manning, "Thermodynamic Properties and Reduced Correlations for Gases", Gulf Publishing Co. Houston, Texas 1967

13. Canjar, L.N., N.R. Patel and F.S. Manning, Hydrocarbon Process. Petrol. Refiner, 41, No. 11, 203-4 (1962)

14. Canjar, L.N., V.M. Tejada and F.S. Manning, Hydrocarbon Process. Petrol. Refiner, 41, No. 9, 253-4 (1962) ibid No. 10 149-50 (1962)

15. Chu, J.C., N.F. Mueller, R.M. Busche, and A.S. Jennings, Pet. Processing, 1203 (1950)

16. Collins, S.C. and F.G. Keyes, Proc. Am. Acad. Arts Sci., 72, 283 (1938)

17. Collins, S.C. and F.G. Keyes, J. Phys. Chem. 43 5 (1939)

18. Colwell, J.H., E.K. Gill and J.A. Morrison, J. Chem.Phys. 39, 635 (1963)

19. Curl, R.E., Personal Communications

20. Cutler, A.J.B. and J.A. Morrison, Trans. Farad. Soc., 61, 429 (1965)

21. Dana, L.I., A.C. Jenkins, J.N. Burdick and R.C. Timm, Refrig. Engr. 12, 387 (1926)

22. Dantzler, E.M., C.M. Knobler and M.L. Windsor, J. Phys. Chem. 72, No. 2 676 (1968)

23. Deschner, W.W., and G.G. Brown, Ind. Eng. Chem. 32 836 (1940)

24. Dillard, D.D., M.S. Thesis, Oklahoma State Univ. (1966)

25. Dillard, D.D., W.C. Edmister, J.H. Erbar and R.L. Robinson, A.I.Ch.E. J., 14 923 (1968)

26. Dittmar, P., F. Schultz and G. Strese, Chemie-Ing. Techn. 34, 437 (1962)

27. Douslin, D.R., R.H. Harrison, R.T. Moore and J.P. McCullough, J. Chem. Eng. Data 9, 358 (1964)

28. Ernst, G., Dr. Ing. Dissertation, Universitat Karlsruhe, Germany 1967.

29. Eucken, A. and W. Berger, Z. ges Kalte-Ind., 41 145 (1934)

30. Finn, D., Ph.D. Thesis, Univeristy of Oklahoma (1965)

31. Frank. A. and K. Clusius, Z. Physik. Chem., B36, 291 (1937)

32. Head, J.F., Ph.D. Thesis. University of London. 1960

33. Helgeson, N.L. and B.H. Sage, J. Chem. Eng. Data 12, 47 (1947)

34. Hestermans, P., and D. White, J. Phys. Chem. 65 362 (1961)

35. Hoover, A.E., I. Nagata, T.W. Leland, Jr. and Riki Kobayashi, J. Chem. Phys. 48 No. 6, 2633 (1968)

36. Huang, E.T.S., Ph.D. Thesis, University of Kansas, (1966)

37. Huang, E.T.S., G.W. Swift and F. Kurata, AIChE J., 13 846 (1967)

38. Huff, J.A., and T.M. Reed, III, J. Chem. Eng. Data, 8, 306 (1963)

39. Hujsak, K.L., H.R. Froning, and C.S. Goddin, Chem. Eng. Prog. Symp. Ser., 59, No. 44, 88 (1963)

40. Jones, M.L., Jr., Ph.D. Thesis, University of Michigan (1961)

41. Jones, M.L., D.T. Mage, R.C. Faulkner and D.L. Katz, Chem. Eng. Prog. Symp. Ser. 59 (44), 52 (1963)

42. Kemp, J.D. and C.J. Egan, J. Am. Chem. Soc. 60 1521 (1938)

43. Klaus, R.L. and H.C. Van Ness, Personal Communications

44. Kobayashi, Riki, Personal Communications

45 Lane, Ralph E.,"The Extension of Jenkins' Fifth-Difference Modified Osculatory Interpolation Formula for Unequal Intervals," Unpublished Report, Military Physics Laboratory, University of Texas.

46. Mage, D.T., Ph.D. Thesis, University of Michigan, (1964)

47. Manker, E.A., Ph.D. Thesis, University of Michigan (1964)

48. Manker, E.A., D.T. Mage, A.E. Mather, J.E. Powers and D.L. Katz, Proc. Ann. Conv., Natl. Gas Process. Assoc., Tech. Papers 43, 3 (1964)

49. Manning, F.S. and L.N. Canjar, J. Chem. Eng. Data 6 364-5 (1961)

50. Mather, A.E., Ph.D. Thesis, University of Michigan (1967)

51. Mather, A.E., V.F. Yesavage, J.E. Powers and D.L. Katz, Proc. Ann. Conv., Natl. Gas Process. Assoc., Tech. Papers, 45, 12 (1966)

52. Mather, A.E., V.F. Yesavage, J.E. Powers and D.L. Katz, Proc. Ann. Conv., Natl. Gas Process. Assoc., Tech. Papers, 46, 13 (1967)

53. Mickley, H.S., T.K. Sherwood, and G.E. Reed, "Applied Mathematics in Chemical Engineering," McGraw-Hill Book Company, Inc., New York, 1957

54. Pena, M.D., and E.Cerverar, Thermodynamics Symposium, Hydelberg, W. Germany, Sept. 1967, No. 3, 10

55. Reamer, H.H., B.H. Sage and W.N. Lacey, Ind. Eng. Chem. 41, 482 (1949)

56 Reamer, H.H., B.H. Sage and W.N. Lacey, Ind. Eng. Chem. 42, 534 (1950). See corrections, Ind. Eng. Chem. 42, 1258 (1950)

57. Roebuck, J.R., Phys. Rev. 2, 299 (1913)

58. Rossini, F.D., et al., "Selected Values of Physical and Thermodynamic Properties of Hydrocarbons and Related Compounds," Carnegie Press, Pittsburgh, Pas., 1953

59. Sage, B.H., H.D. Evans and W.N. Lacey, Ind. Eng. Chem. 31 763 (1939)

60. Sage, B.H., E.R. Kennedy and W.N. Lacey, Ind. Eng. Chem. 28, 601 (1936)

61. Sage, B.H., J.G. Schaafsma and W.N. Lacey, Ind. Eng. Chem. 26, 1218 (1934)

62. Sahgal, P.N., J.M. Geist, A. Jambhekar, and G.M. Wilson, Intern. Advan. Cryogen. Eng. 10, 224 (1965)

63. Sehgal, I.J.S., V.F. Yesavage, D.L. Katz and J.E. Powers, Hydrocarbon Process. 8, (8) 137 (1968)

64. Stull, D.R., E.F. Westrum, Jr., and G.C. Sinke, "The Chemical Thermodynamics of Organic Compounds," John Wiley and Sons, Inc., New York, 1969

65. Vennix, A.J., Ph.D. Thesis, Rice University (1966)

66. Vennix, A.J., T.W. Leland and Riki Kobayashi, Submitted for Publication in J. Chem. Phys.

67. Wiebe, R. and N.J. Brevoort, J. Am. Chem. Soc. 52 622,(193(

68. Wiener, L.D., Paper presented at 58th National AIChE Meeting, Dallas, 1966

69. Yarborough, L. and W.C. Edmister, AIChE J. 11, 492 (1965)

70. Yesavage, V.F., Ph.D. Thesis, University of Michigan (1968)

71. Yesavage, V.F., A.W. Furtado, D.L. Katz and J.E. Powers, "Enthalpy Data for a Mixture Containing 77 Mole Percent Propane in Methane and Comparison with Prediction," To be published in AIChE J.

72. Yesavage, V.F., A.W. Furtado, and J.E. Powers, Proc. Ann. Conv., Natl. Gas Process Assoc., Tech. Papers, 47,3 (1968)

73. Yesavage, V.F., D.L. Katz and J.E. Powers, Fourth Symposium on Thermophysical Properties, A.S.M.E., New York (1968)

74. Yesavage, V.F., D.L. Katz and J.E. Powers, J. Chem. Eng. Data 14, No. 2 (1969) 137

75. Yesavage, V.F., D.L. Katz and J.E. Powers, "Enthalpy Data for a Mixture Containing 51 Mole Percent Propane in Methane" To be published in AIChE J.

76. Yesavage, V.F., A.E. Mather, D.L. Katz and J.E. Powers, Ind. Eng. Chem. 56 35 (1967)

Appendix I

Review of Literature

A number of investigators have reported both calorimetric and PVT data for methane, propane and their mixtures. Brief resumes of the most pertinent references are given in this Appendix.

Calorimetric Data

Although a number of different investigators have reported calorimetric data for methane (9,18,29,31,34,39,40,41,46,62,68), propane (21,28,30,33,59,60,69,70,73,74), and their mixtures (9,24,25,32,47,48,50,51,52,70,71,54) the results of E.A. Manker (47) and A. E. Mather (50) were used almost exclusively for the following reasons:

1) The data of these two investigators were obtained with mixtures of almost identical composition.

2) These experimental investigations cover an extensive range of both temperatures and pressures - certainly those of primary interest to the natural gas processing industry (-240°F to +250°F at pressures up to 2000 psia).

3) These data are thermodynamically consistent to ±0.2%.

4) No other data reported in the literature were obtained at exactly the same composition.

Manker (47) and Mather (50).- The calorimetric data used in making all calculations were obtained directly from the theses of Manker (47) and Mather (50). Manker reported isobaric data over a range of temperature from -240 to +90°F with some relatively crude Joule-Thomson determinations at 60°F up to 2000 psia. Mather obtained supplementary isobaric data between 90 and 250°F at pressures between 500 and 2000 psia, isothermal results between 100 and 2000 psia at -27, 91.6 and 200°F and isothermal and isenthalpic data at -147°F between 600 and 1800 psia. The temperatures and pressures of experiments made by these investigators are illustrated in Figure 1.

The average compositions of the mixtures as reported by these two investigators are summarized in Table AI.1.

TABLE AI.1

Mixture Compositions Reported by
Manker (47) and Mather (50)

Component	Manker (47)	Mather (50)
Methane, CH_4	0.9464	0.9463
Ethane, C_2H_6	0.0006	0.0006
Propane, C_3H_8	0.0518	0.0510
Nitrogen, N_2	0.0006	0.0007
Oxygen, O_2	0.0002	0.0001
Carbon Dioxide, CO_2	0.0004	0.0003
	1.0000	1.0000

There was some variation in composition during the course of the investigations as determined by periodic chromatographic determinations. The extremes of such variations are indicated in terms of the propane mole fractions in Table AI.2.

TABLE AI.2

Extremes in Compositions of Manker (47) and Mather (50)

	Mole Fraction Propane		
Investigator	Lowest Value	Average Value	Highest Value
Manker (47)	0.0491	0.0518	0.0521
Mather (50)	0.051	0.0510	0.052

The greatest variation in composition occurred during runs made through the two-phase region. No attempt was made to correct for variation in composition for individual runs. The average composition reported by Manker (47) as given in Table AI.1 was used as the base composition because the majority of Mather's runs were made at temperatures relatively far removed from the critical region and therefore, small variation in composition would be expected to have a negligible effect.

Dillard, et al (25).- Results from a series of isothermal determinations with methane and methane-propane mixtures have been reported by Dillard (24) and Dillard, et al (25). The equipment was designed to yield integral measurements of

isothermal changes in enthalpy between elevated pressures and atmospheric. Results were reported for methane and two methane-propane mixtures as indicated in Table AI.3.

TABLE AI.3

Conditions of Integral Isothermal Determinations of Dillard (25)

Mole Fraction Propane in Methane	Inlet Pressures (psia)	Temperature Range (°F)
0.0000	500 to 2000	150
0.051	500 to 2000	90
		150
		200
0.126	500 to 2000	90
		150
		200

Replicates were reported for most runs. The precision of the experiments as indicated by analysis of the replicates is ±30%. The mean of all the determinations made at one set of conditions is consistent with data obtained by Mather (50) within ±5%. Mather (50) made use of these results to justify use of calculated values based on the BWR equation of state (5,6) in publishing PTH diagrams for binary mixtures containing 11.7 and 28.0 mole percent propane in methane. The results

reported by Dillard et al (25) are considered to be at least one order of magnitude less accurate than those of Manker and Mather and therefore, were not given further consideration in preparing this report.

Budenholzer et al (9).- Joule-Thomson data for mixtures of methane and propane have been reported. The range of composition, temperatures and pressures of these reported values is summarized in Table AI.4.

TABLE AI.4

Conditions of Reported Joule-Thomson Values of Budenholzer et al (9)

Mass Fraction Methane	Temperature (°F) high	Temperature (°F) low	Pressure (psia) high	Pressure (psia) low
0.2458	310	70	1500	0
0.4934	310	70	1500	0
0.7552	310	70	1500	0

As indicated in Table AI.4, Budenholzer et al have reported values of the Joule-Thomson coefficient for mixtures of methane and propane. In addition, Sage, Kennedy and Lacey (60) have published values for propane and Budenholzer et al (10) report values for methane so that these data could be used to interpolate with respect to composition.

Joule-Thomson data, μ, can be used with values of isobaric heat capacity, C_p, to calculate the isothermal throttling coefficient, ϕ.

$$\phi \equiv \left(\frac{\partial H}{\partial P}\right)_T = - \mu C_p \qquad \text{(AI.1)}$$

Values of the isothermal enthalpy departures are obtained by integration.

$$(H-H^\circ)_T = \int_{P=0}^{P} \phi \, dP_T \qquad \text{(AI.2)}$$

Comparisons made by several investigators (49,50) have illustrated that the Joule-Thomson data covered in Table AI.4 are thermodynamically inconsistent with values calculated from PVT data and published values of C_p° (11), as well as the results of Manker (47) Mather (50), Dillard et al (25) and values calculated from the BWR equation of state (5,6). Therefore, no attempt was made to incorporate these experimental data on the Joule-Thomson coefficient in the results of this report.

Joule-Thomson data for mixtures of methane and propane have also been reported by Head (32). The range of composition temperatures and pressures of these reported values is summarized in Table AI.5.

TABLE AI.5

Conditions of Reported Joule-Thomson Measurements of Head (32)

Fraction Methane	Temperature (°K)		Pressure (atm)	
0.489	high	low	high	low
	360	258	40.06	1.71

For a mixture containing approximately 51 mole percent propane in methane at 152.2°F the values of μ reported by Head (32) are consistent to within 3% with values interpolated to that composition from data published by Budenholzer et al (9) as reported by Yesavage, Katz and Powers (75). However, values of ϕ calculated using Equation (AI.1) disagree with the values of Yesavage et al by -8% at zero pressure and +9% at 600 psia (71). These calculated values based on the data of Head (32) also disagree with values of ϕ calculated from PVT data for the mixture (69) and with data calculated by the BWR equation of state (5,6). Therefore, no attempt was made to incorporate the Joule-Thomson values of Head into the enthalpy and entropy values of this report.

Volumetric Data

A great deal of volumetric data has been reported for pure methane and pure propane. Only two investigators have reported PVT data for mixtures. The published results for the mixtures will be reviewed first and then the data for pure methane and propane used for purposes of interpolation with respect to composition will be mentioned.

Reamer, Sage and Lacey (55,56). These investigators reported smoothed values of volumetric data on several binary mixtures of methane and propane. The compositions and range of temperatures covered by this report are listed in Table AI.6.

TABLE AI.6

Conditions of Reported Volumetric Data of Reamer, Sage and Lacey (56)

	Temperature (°F)	Pressure (psia)
Low	40	200
High	466	10,000

Composition

Mixture	Mole Fraction Methane	Mole Fraction Propane
1	0.10	0.90
2	0.20	0.80
3	0.30	0.70
4	0.40	0.60
5	0.50	0.50
6	0.60	0.40
7	0.70	0.30
8	0.80	0.20
9	0.90	0.10

Huang et al (37). The conditions corresponding to values reported for methane-propane mixture are reported in TABLE AI.7

TABLE AI.7

Conditions of Reported Volumetric Data of Huang et al (37)

	Temperature (°F)	Pressure (psia)
Low	-238	50
High	100	5,000

	Composition	
Mixture	Mole Fraction Methane	Mole Fraction Propane
1	0.221	0.779
2	0.500	0.500
3	0.753	0.247

The ranges covered by the volumetric data of Reamer, Sage and Lacey (56) and Huang et al (37) are indicated in Figure AI.1.

Volumetric Data for Methane. None of the volumetric data listed above are for the composition of the mixture investigated by Manker (47) and Mather (50) In fact, all mixtures reported contain substantially more propane than 5 mole %. Therefore, it was necessary to utilize volumetric data for methane to interpolate with respect to composition to the desired value.

The published data for the volumetric behavior of methane is much too extensive to be reviewed in its entirety. Instead, use was made of the most recent compilations of volumetric data.

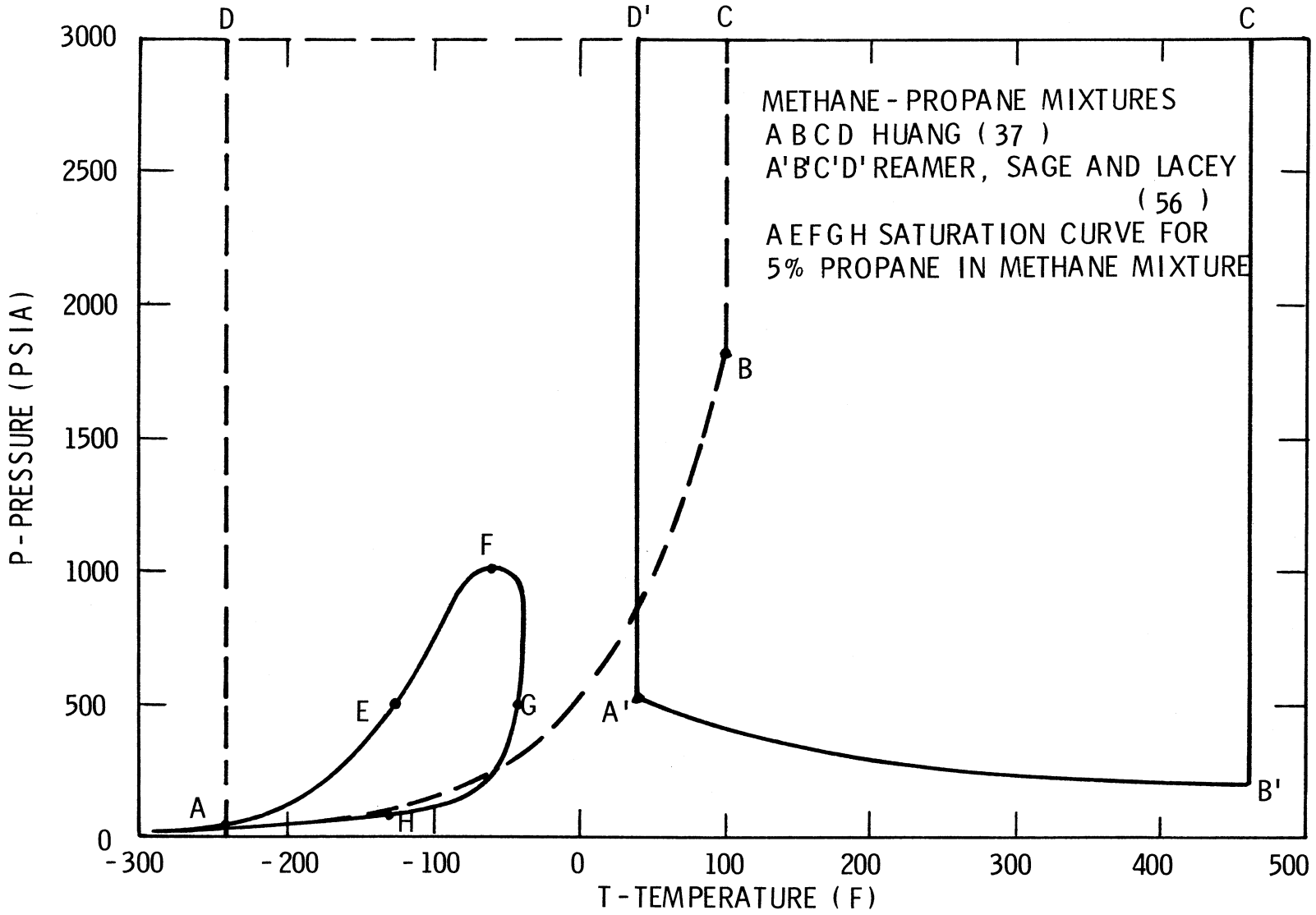

Figure AI.1 Temperatures and Pressures of Volumetric Data for Methane-Propane Mixtures as Reported in the Literature

API Project 44. A recent supplement of API Project 44 (1,58) lists values of the volumetric data for gaseous methane from -115 to 2140°F at pressures up to 15,000 psia. These values were used for the purposes of interpolation primarily as a matter of convenience.

Vennix et al. The API supplement does not include the published data of Vennix (65,66) and of Douslin et al (27). The data of these two recent investigations are remarkably consistent (±0.02%) at the temperature of overlap (0°C) and have been combined to yield a single equation of state (44). Values calculated using this equation of state were found to be in very good agreement with values interpolated from the API values.

Volumetric Data for Propane. The interpolation procedure used to obtain volumetric data for a mixture containing 5 mole % propane is relatively insensative to the values selected for pure propane. Whereas extensive consideration of all published volumetric data is planned subject to availability of funds, values for propane published by Reamer, Sage and Lacey (56) were used in connection with this report because they appear to be reasonably consistent with other published data and were in a form that is convenient for interpolation.

Appendix II

Basic Interpretation of Calorimetric Data

The calorimetric results of Manker (47,48) have been interpreted twice in the past to yield tables and graphs of enthalpy values (48.50,51) and the combined results of Manker (47) and Mather (50) have been so interpreted once (50,51). Unfortunately eventhe latest interpretation (50,51) appears to be in question for two principle reasons:

1) The isotherms at low temperatures as drawn by Mather (50) exhibit a sharp curvature at low pressures that is not in evidence in the PTH diagrams for methane (40,41), nitrogen (46), propane (70) or any of their mixtures (47,50,70,71,72,73,74,75) which have been produced from results obtained in the Thermal Properties of Fluids Laboratory.

2) The correlational efforts of Yesavage (70) were very successful in fitting the enthalpy data for all five binary mixtures of methane and propane except the 5% propane in methane mixture at low temperatures where deviations of more than 4 Btu/lb were noted.

In an attempt to resolve these apparent discrepancies a complete reinterpretation of the original data was undertaken to insure that the resulting enthalpy values (and the entropy data obtained therefrom) would be as meaningful as possible. The purpose of this Appendix is to provide detailed descriptions

of the procedures used to reinterpret the basic data to provide the bases for an improved estimate of the enthalpy behavior of this mixture with particular emphasis on changes which were incorporated in the analysis.

Isobaric Determinations

Manker (47) reported the results of 325 isobaric determinations both in the single-phase region and within the two-phase region. Mather (50) presented 28 isobaric data points in the single-phase region at elevated temperatures.

Single-Phase

General procedure. In making measurements in the single-phase region, determinations are usually made with a common inlet temperature and temperature increases varying from 10 to 100°F. In processing the data to yield smoothed values of $C_p(T)$, mean values of $\hat{C}_p$ are calculated from the measured isobaric increases in enthalpy and temperature.

$$\hat{C}_p \equiv \frac{(\underline{H}_{T_2} - \underline{H}_{T_1})_P}{T_2 - T_1} \qquad \text{(II.1)}$$

Values thus calculated are plotted over the temperature interval $T_1 \rightarrow T_2$. Typical values appear on Figure AII.1 as solid horizontal lines extending over the experimentally measured temperature intervals.

For isobaric enthalpy differences measured with a common inlet temperature, T_1, a difference in enthalpy between two outlet temperatures, T_2 and T_3, can be calculated:

$$(\underline{H}_{T_3} - \underline{H}_{T_2})_P = (\underline{H}_{T_3} - \underline{H}_{T_1})_P - (\underline{H}_{T_2} - \underline{H}_{T_1})_P \qquad \text{(II.2)}$$

Such differences can be used to calculate additional values of $\hat{C}_p$. Typical values are plotted as dashed lines on Figure AII.1.

Point values of C_p can be determined from a plot of $\hat{C}_p$ vs T by applying the identities

$$\underline{H}_{T_j} - \underline{H}_{T_i} \equiv \hat{C}_p(T_j - T_i) \qquad \text{(II.3)}$$

$$= \int_{T_i}^{T_j} C_p dT \qquad \text{(II.4)}$$

where T_i and T_j are used to indicate any two experimental values of temperature.

Thus the integral of the function $C_p(T)$ between T_i and T_j must equal the experimentally measured values of $\underline{H}_{T_j} - \underline{H}_{T_i}$ and the product $\hat{C}_p(T_j - T_i)$. Graphical procedures were applied to determine $C_p(T)$ by an iterative procedure.

The interative procedure employed was based entirely on graphical procedures. A draftsman's spline was used to plot a first approximation of $C_p(T)$. Integrations were made between each experimentally determined temperature interval as indicated by Equation (II.4). Simpson's rule (See Appendix X) was used to obtain integral values both accurately and rapidly. Adjustments

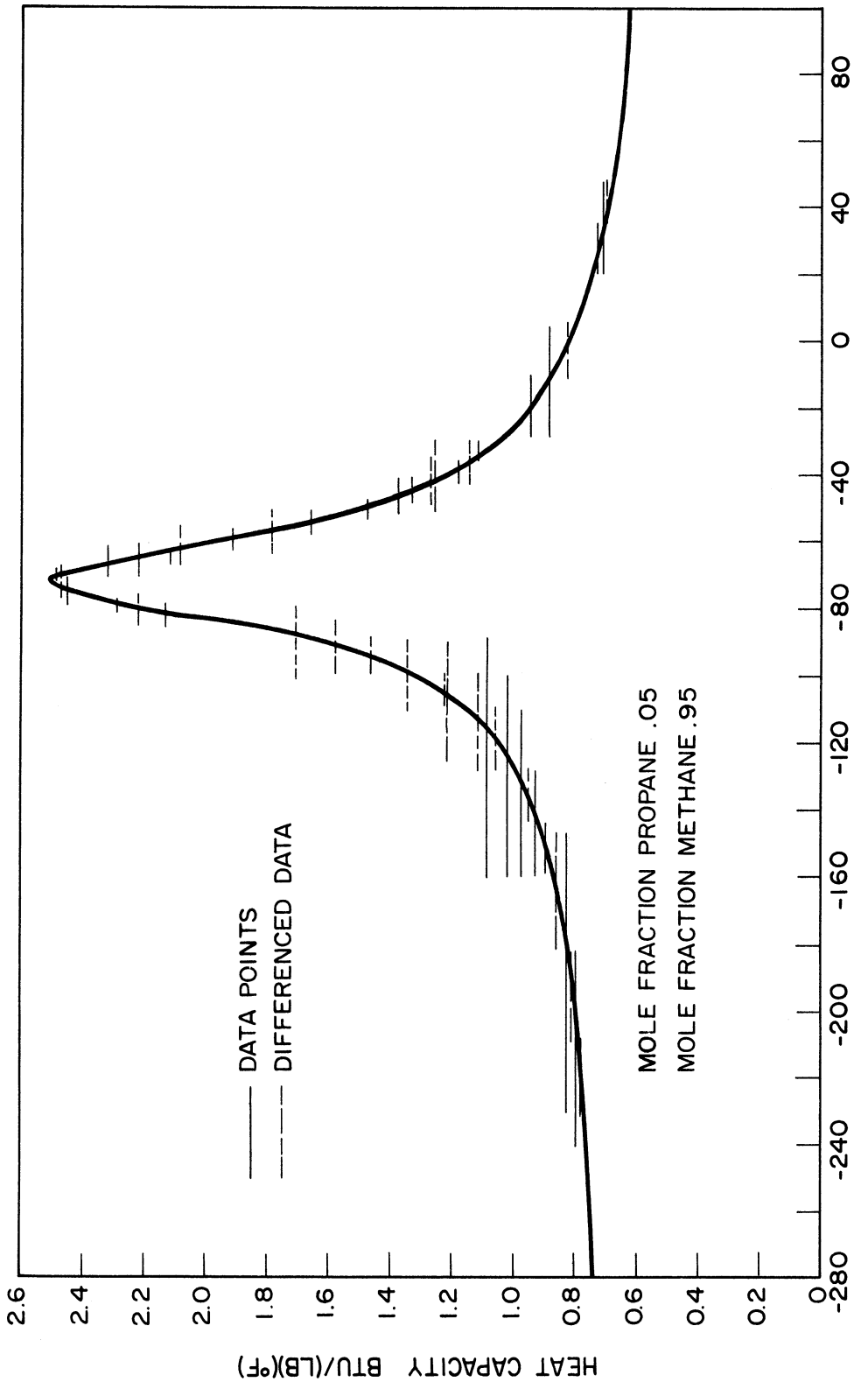

Figure AII.1 Isobaric Heat Capacity, Cp, at 1000 psia Illustrating Method of Interpreting Calorimetric Results.

were made in the curve representing $C_p(T)$ until the deviations between the experimental values of enthalpy difference and the values determined by graphical integration showed random variation. In general the agreement between experimental and calculated values was on the order of $\pm 0.2\%$ or better.

After the iterative graphical procedure described above yielded the desired preliminary relation for $C_p(T)$, Simpson's rule was applied to evaluate isobaric enthalpy differences over temperatures intervals other than those noted experimentally. In particular, enthalpy differences were evaluated over uniform intervals of 10°F to aid in preparation of the tables and graphs and between temperatures corresponding to isothermal determinations made with this mixture (See Figure 1). The latter calculations are used to check the thermodynamic consistency of the two types of data (isobaric and isothermal) obtained for this mixture as will be described in detail in Appendix III.

The general procedure described above was applied to determine approximations of $C_p(T)$ and isobaric enthalpy differences at all pressures from 1100 psia to 2000 psia over the temperature interval studied at each pressure (See Figure 1). Special care was taken in interpreting the data over the temperature intervals in which C_p exhibits a maximum. Table AII.1 summarizes information on the peak values (including that at 1000 psia).

TABLE AII.1

Information Obtained at the Maximum in $C_p(T)$

Pressure	Temperature at Peak °F	$C_{p\ max}$ Btu/lb°F
2000	-25.5±1.0	1.139
1700	-35.5±1.0	1.2572
1500	-44.5±1.0	1.434
1200	-60.5±0.6	1.8502
1100	-67.5±0.5	2.12
1000	-72.5±0.2	2.564

Additional efforts were expended at pressures of 1000 psia and below and to extrapolate the reported values upward in temperature to +300°F and downward to -280°F.

Interpretation of the data at 1000 psia. Over much of the temperature range of experiments at 1000 psia (-240 to +205°F) it was possible to obtain good agreement between calculated and experimental values using the general graphical procedure described in the preceeding section. Manker (47,48) reported an unusually heavy concentration of data points in the immediate vicinity of the maximum of $C_p(T)$ at 1000 psia. This peak is quite sharp ($C_p \approx 2.5$ Btu/lb°F at the peak) and large values of C_p are in evidence between -120 and -30°F (See Figure AII.1). Thus the enthalpy difference between these two temperatures is exceptionally large and interpretation of the data over this range of temperature exerts a disproportionate

influence on the enthalpy values calculated for low temperatures and low pressures where rather large discrepancies were noted in earlier interpretations. Therefore, special efforts were taken to interpret the data in the vicinity of the peak.

A plot with expanded scales for both temperature and C_p was made. The working drawing measured 70 in. by 30 in. A reproduction in reduced form is presented as Figure AII.2.

As in the general case, a curve representing $C_p(T)$ was drawn using a spline and the results of integrations by Simpson's rule were used to make adjustments and obtain a better estimate of the function $C_p(T)$. A more sensitive procedure was used in making the next adjustment:

1) The adjusted curve for $C_p(T)$ was integrated over small temperature intervals and enthalpy differences were calculated corresponding to each experimental temperature interval $(\underline{H}_{T_o} - \underline{H}_{T_i})_{calc}$.

2) Difference between the calculated and experimental enthalpy differences were evaluated

$$\Delta(\Delta H) \equiv (\underline{H}_{T_o} - \underline{H}_{T_i})_{calc} - (\underline{H}_{T_o} - \underline{H}_{T_i})_{expt}$$

and plotted against $(\underline{H}_{T_o} - \underline{H}_{T_i})_{calc}$. The first plot thus prepared is presented as Figure AII.3. Note that all differences are positive indicating a bias.

3) A dotted line was drawn through the differences and through the origin exhibit random scatter instead of a bias. The curve representing $C_p(T)$ was then adjusted to satisfy this condition.

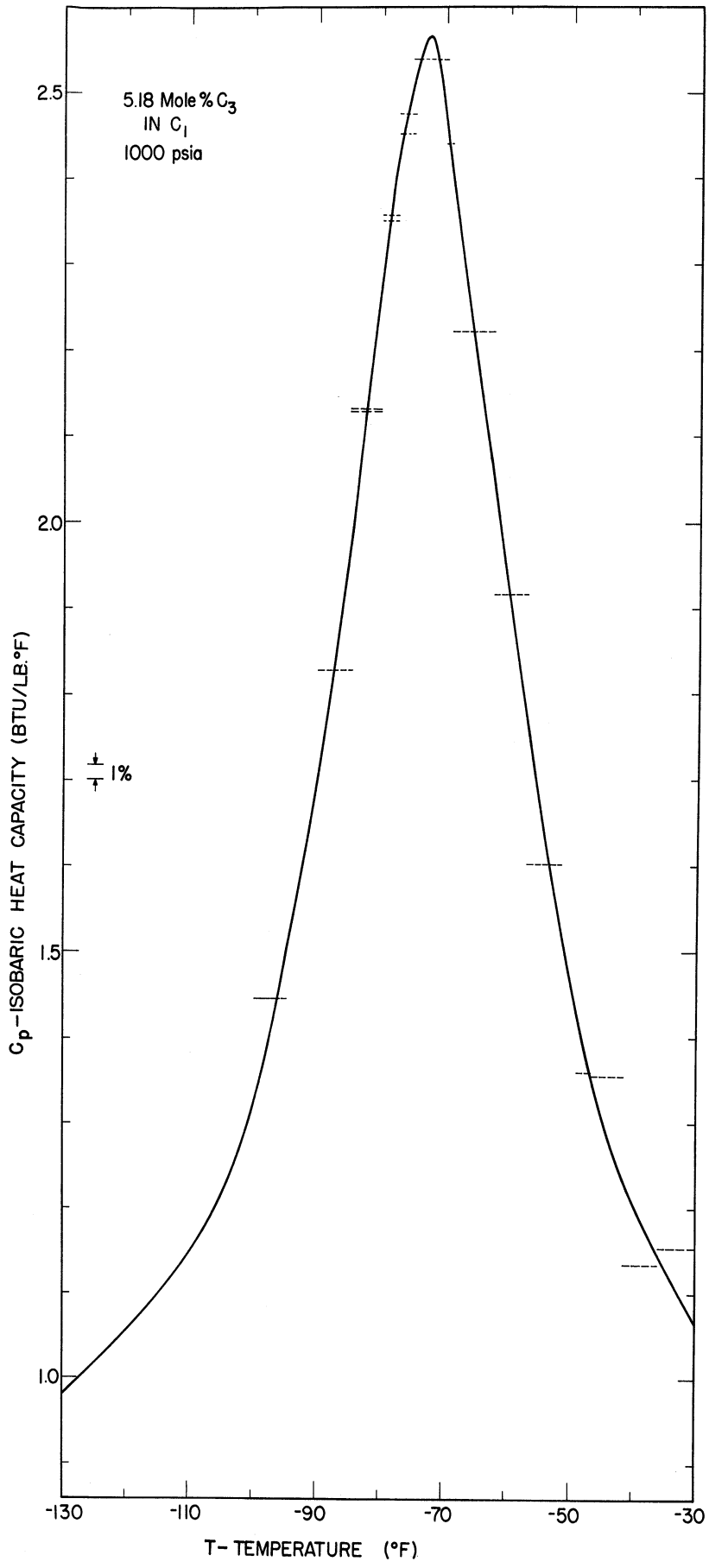

Figure AII.2 Isobaric Heat Capacity, C_p, at 1000 psia the Critical Point Illustrating Sharp Max

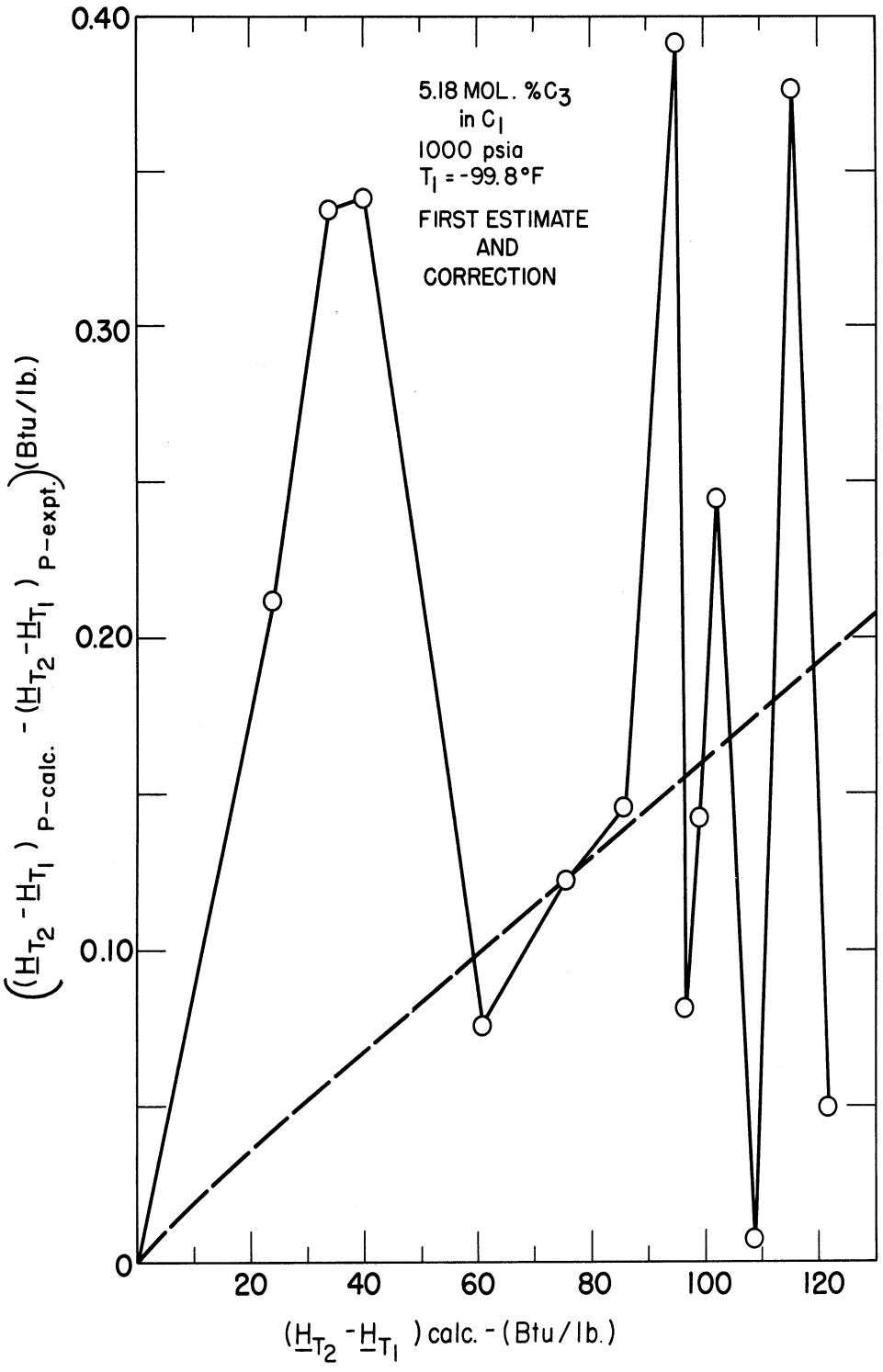

Figure AII.3 Check for Bias in Interpreting Isobaric Data Near the Maximum in $C_p(T)$ at 1000 psia.

4) Simpson's rule integrations were again performed using the adjusted curve of $C_p(T)$ and new values of $(\underline{H}_{T_o} - \underline{H}_{T_i})_{calc}$ determined for direct comparison with the experimental values. The resulting plot is presented as Figure AII.4. By using this special procedure it was possible to represent the experimental data by means of a smoothed curve of $C_p(T)$ well within the limits of precision of the experimental data ($\pm 0.3\%$).

Interpretation of the data at 500 psia. Although both Manker (47) and Mather (50) give indication in their theses that enthalpy traverses were made at 500 and 600 psia and Mather (50) presents the results of a check of thermodynamic consistency that incorporates the enthalpy travers at 500 psia, no data for these runs are included in Manker's thesis. The data for these runs were included in the Proceedings of the NGPA (600 psia) (48). The results were not included in Manker's thesis because of unresolved problems with respect to the flowmeter calibrations associated with these runs.

Another problem associated with attempting to establish the enthalpy behavior of the mixture at low temperatures and pressures below 1000 psia can be understood by considering Figure 1; the isobaric run made between -250 and -180°F at 500 psia does not overlap the enthalpy traverse through the two phase region nor does it intersect the isothermal run made at -147.4°F. Estimation of C_p is difficult near the two-phase region because C_p changes in value relatively rapidly

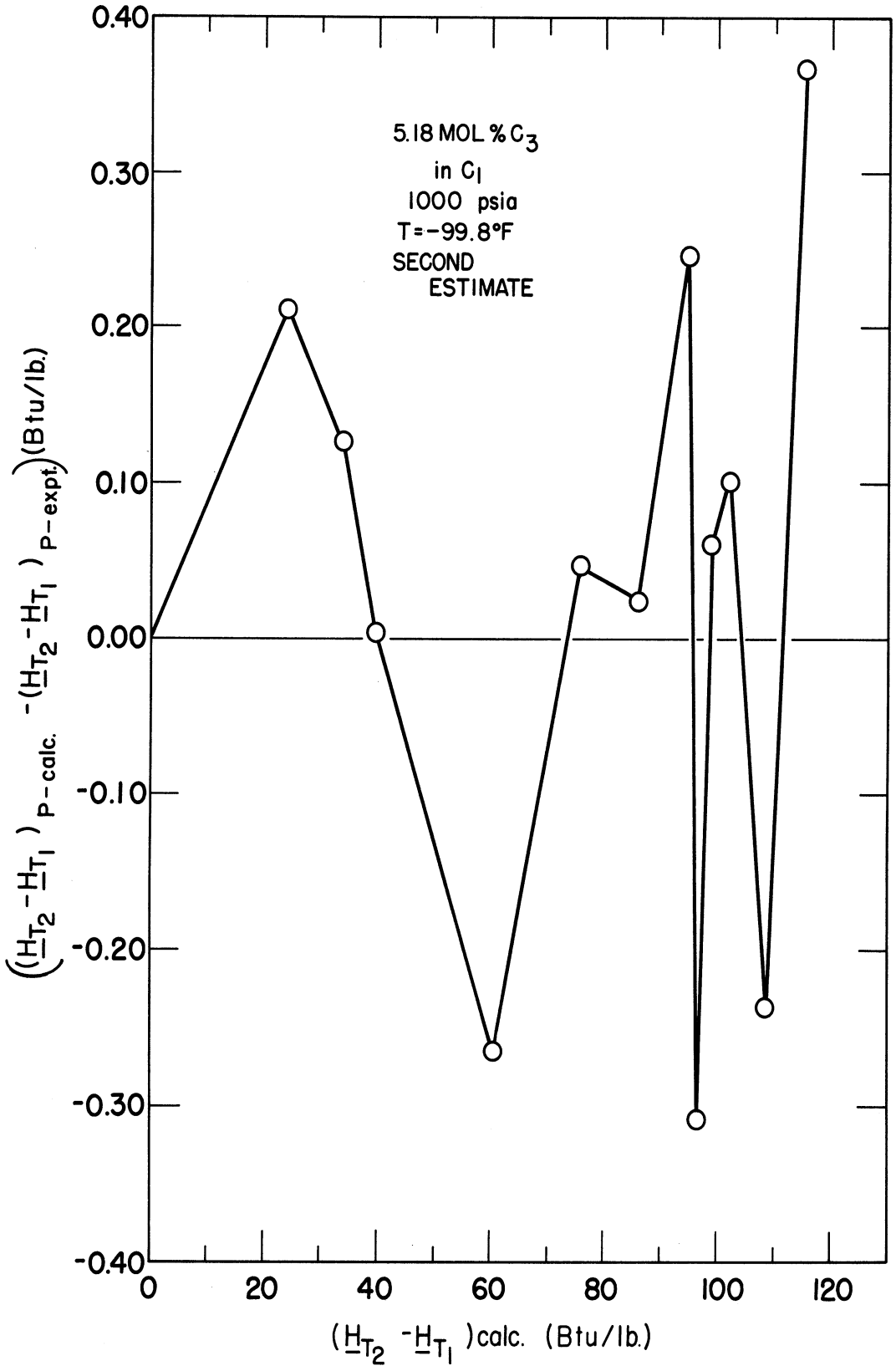

Figure AII.4 Check of Interpretation of Isobaric Data Near the Maximum in $C_p(T)$ at 1000 psia after Correcting for Bias.

in this region. Considerable effort was expended in an attempt to establish the enthalpy behavior at 500 psia and low temperatures because the results of previous interpretations may have been misleading.

Resolution of the problems associated with estimation of the enthalpy change across the two-phase region at 500 psia will be described later in this Appendix because it involves use of the isothermal data. The method of establishing values of C_p up to the bubble point at 500 psia is presented in the paragraphs that follow.

As indicated in Figure 1, isobaric data were obtained in the temperature range from -245 to -175°F. The bubble point is at -128°F at this pressure. As indicated in the previous section the results obtained from -140°F across the two-phase region at 500 psia are suspect. Therefore, a procedure was developed to estimate $C_p(T)$ at 500 psia at low temperatures which does not rely on the values reported by Manker (47).

Reliable values of $C_p(T)$ are available at 500 psia over the temperature of interest for methane (40,41), propane (70), and four other mixtures of methane and propane [11.7% C_3(50), 28.0% C_3(50), 50.6% C_3(70) and 76.6% C_3(70)]. Therefore, it is possible to plot C_p vs composition at various values of T at 500 psia and interpolate to obtain a good estimate of C_p for the 5% mixture. Interpolations with respect to composition are aided by working with excess quantities; in this case the excess heat capacity, C_p^E;

$$C_p^E \equiv C_{pm} - \sum_{i=1,3} x_i C_{pi} \qquad \text{(II.5)}$$

where C_{pm} refers to the mixture and C_{pi} refers to the pure components, methane and propane in this case. A typical plot is presented as Figure AIII.5. Note that the values are plotted vs mass fraction C_3 in C_1 because it was found that the plot was much less skewed when thus plotted than when plotted against mole fraction. Smoothed values of C_p^E were read from the plot at 5.18 mol % C_3(0.1306mass fraction C_3) and values of C_{pm} were calculated using Equation AII-5 making use of the published C_p values for methane (40,41) and propane (70)

Experimental data are reported by Manker (47) in the single-phase region near the bubble points at 250,400,650 and 800 psia. Two experiments were reported in the liquid phase at 250 psia and four values are given at each of the other pressures. It was assumed that C_p is a linear function of temperature near the bubble point. The data were individually fitted to the equation

$$C_p = a + b(T_S - T) \qquad \text{(II.6)}$$

where T_S refers to the bubble point temperature at the given pressure. The results are summarized in Table AII.2.

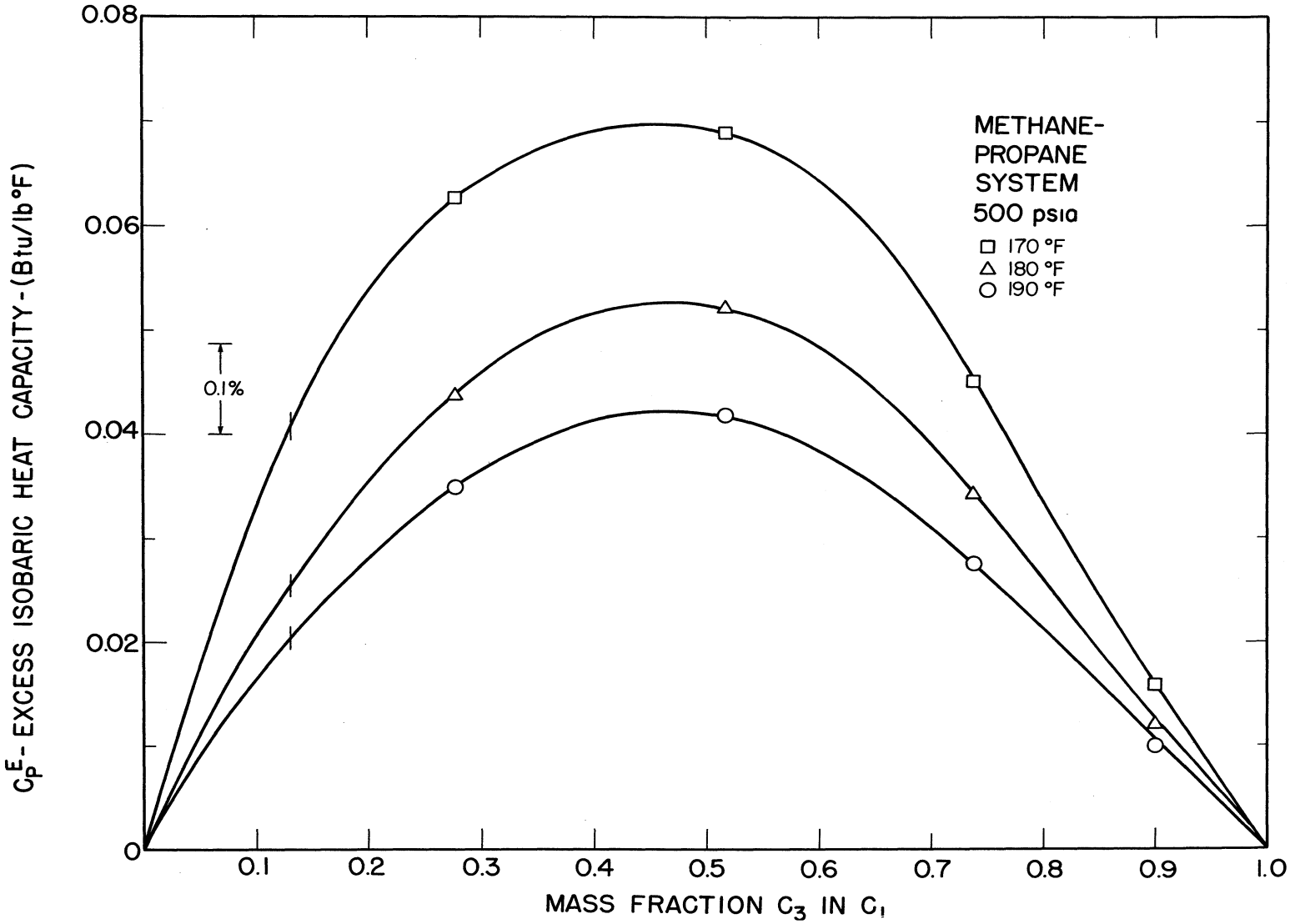

Figure AII.5 Plot of Excess Isobaric Heat Capacity, C_p^E, for the Purpose of Estimating C_p for the 5% Mixture at 500 psia Where Direct Measurements are not Available.

TABLE AII.2

Constants of Equation (AII-6), Expressing

Specific Heat in the Immediate Vicinity of Bubble Point

Pressure (psia)	T_S (°F)	a (Btu/lb°F)	b (Btu/lb°F^2)
250	-167	1.06	0.015
400	-141.65	1.23	0.0216
500	-128.1	1.36*	0.025*
650	-111.87	1.60	0.033
800	- 96.0	2.22	0.0758

* interpolated value

Plots were made of a and b versus pressure and the values estimated at 500 psia are reported in Table AII.2.

The straight line relation was employed to estimate $C_p(T)$ at 500 psia between -150 and -128°F. Comparison with the values reported in the NGPA Proceedings (48) at 500 psia between -140 and -128°F indicates that the experimental values for this enthalpy traverse as reported were too low by about 5% probably as a result of an error in the calibration of the flowmeter. The values of C_p in the range -240 to -128°F determined as described above are summarized in Table AII.3.

TABLE AII.3

Values of C_p for the 5.18% C_3 in C_1 Mixture at 500 psia as Determined by Interpretation of Calorimetric Data at Other Conditions.

Temp. (°F)	-240	-230	-220	-210	-200	-190
C_p $\left(\frac{Btu}{lb\,°F}\right)$	0.772	0.782	0.795	0.809	0.826	0.844

Temp. (°F)	-180	-170	-160	-150	-140	-130	-128.1
C_p $\left(\frac{Btu}{lb\,°F}\right)$	0.866	0.894	0.928	0.972	1.037	1.182	1.36

Extrapolation with respect to temperature. It was decided to report values between -280°F and +300°F although experimental determinations were limited to the interval from -245°F to +250°F. It was felt that such extrapolations could be made accurately.

Extrapolation to elevated temperatures was based on blending experimental values with ones calculated using the BWR equation of state. The nature of the agreement is illustrated on Figure AII.6. The C_p values at elevated temperatures reported in the thesis of Mather (50) were obtained by blending the results of BWR calculations with experimental values and therefore these values were used directly in this region.

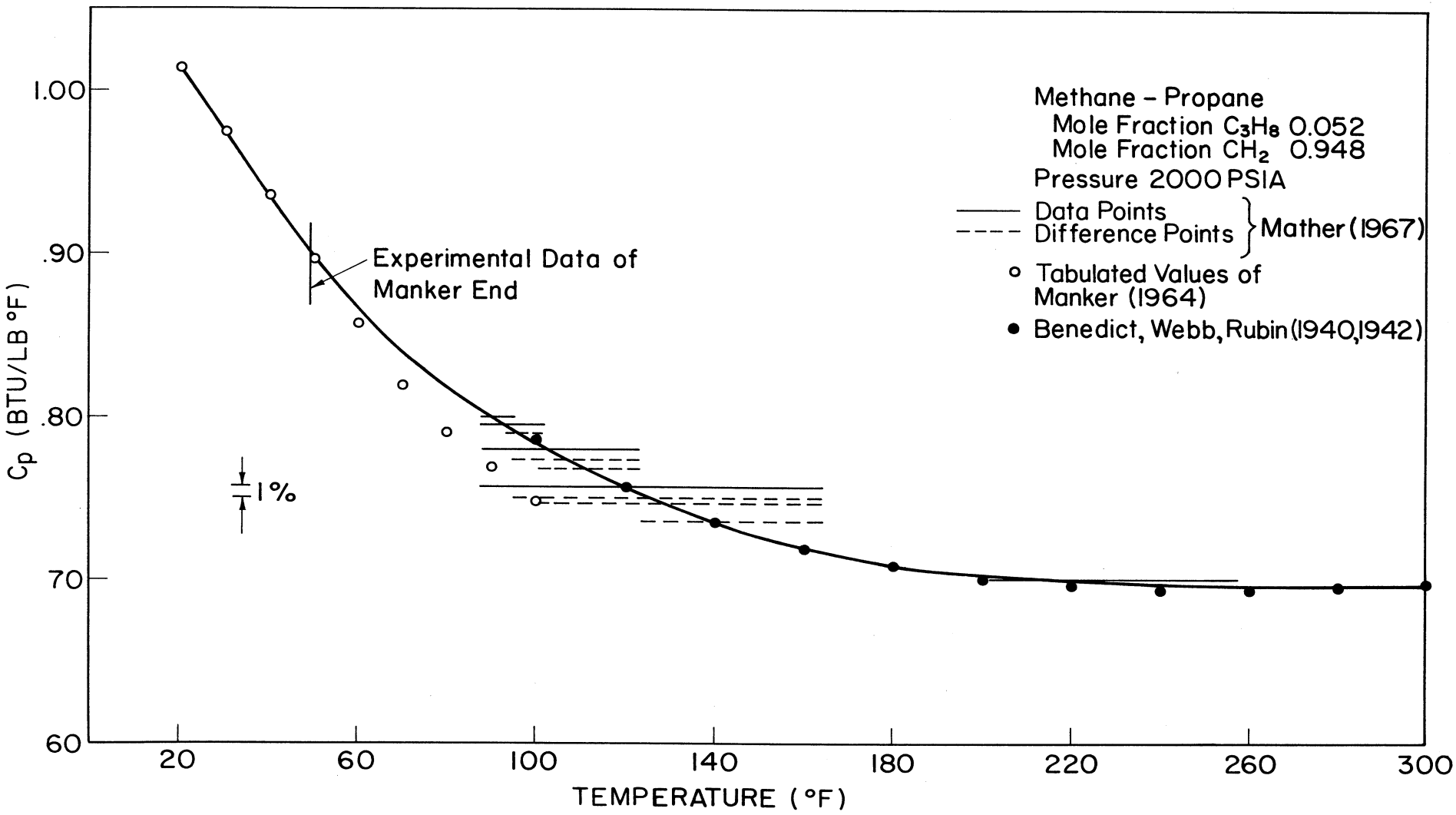

Figure AII.6 Experimental Heat Capacities with Values Calculated from B-W-R Equation of State.

The BWR equation - as well as most other published equations of state - generally yields erroneous results at high densities especially at low temperatures. On the other hand $C_p(T)$ tends to approach a constant value at low temperatures as indicated in Figure AII.1. Therefore, an empirical approach was used to extrapolate $C_p(T)$ to lower temperatures.

By definition

$$C_p(T_2) - C_p(T_1) = \int_{T_1}^{T_2} \left(\frac{\partial C_p}{\partial T}\right)_P dT_p \qquad \text{(II.7)}$$

Values of $(\partial C_p/\partial T)_P$ were approximated by taking differences in tabulated values

$$\left(\frac{\partial C_p}{\partial T}\right)_P = \frac{C_p(T_2) - C_p(T_1)}{T_2 - T_1} \qquad \text{(II.8)}$$

Values of differences thus calculated were plotted at each pressure and smoothed. The resulting values are listed in Table AII.4.

In estimating the values of $(\partial C_p/\partial T)_P$ at low temperatures as indicated by underlined values, note was made of the trends in $(\partial^2 C_p/\partial T^2)_P$ with temperature and of the observation that C_p is essentially independent of pressure at low temperatures (40,70).

TABLE AII.4

Values of $(\partial C_p/\partial T)_P$ Used to Extrapolate $C_p(T)$ to -280°F

$(\partial C_p/\partial T)_P$ in Btu/lb(°F)^2 x 10

Temperature (°F)	Pressure (psia) 500	1000	1500	2000
-160	0.635			
-170	0.44	0.186	0.175	0.13
-180	0.335	0.170	0.155	0.11
-190	0.25	0.15	0.12	0.08
-200	0.20	0.13	0.09	0.06
-210	0.16	0.10	0.07	0.05
-220	0.12	0.08	0.01	0.04
-230	0.10	0.06	0.05	0.03
-240	0.08	0.05	0.04	0.02
-250	0.06	0.04	0.03	0.01
-260	0.04	0.03	0.02	0.00
-270	0.02	0.02	0.01	0.00
-280	0.01	0.01	0.00	0.00

Two-Phase (Enthalpy traverses)

Manker (47) reported isobaric determinations made near the boundaries as well as within the limits of the two-phase region. Experimental data have been reported at 250, 400, 650 and 800 psia (47) as well as at 500 and 600 psia (48) (See Figure 1). As indicated in the previous section of this Appendix, the values reported at 500 and 600 psia are suspect probably because of an error in the flowmeter calibration.

The data at 250, 400, 650 and 800 psia were interpreted to yield enthalpy values both within the two-phase region and the single-phase region near the bubble- and dew-points. The procedure used also yielded values of the bubble- and dew-points.

Experimental enthalpy traverses at each pressure were made by feeding liquid at constant temperature to the calorimeter and adding varying amounts of electrical energy until the outlet material was determined to be completely vaporized. By making minor corrections for the fact that the inlet temperature does vary slightly it is possible to calculate enthalpy differences from a common inlet temperature. Plots of such enthalpy differences are illustrated on Figure AII.7. Note the breaks in the curves indicating both bubble- and dew-points for this mixture at the various pressures. Values of bubble- and dew-points determined in this manner are listed in Table AII.5. Isobaric enthalpy differences between the bubble- and dew-points can be read directly from these plots and values thus determined are also listed in Table AII.5. Enthalpy differences within the two-phase region were also noted at intervals of 10°F at pressures of 250, 400, and 800 psia for use in preparing the final PTH diagram and tables. The data at 650 psia was not suitable for this purpose because few points were reported within the two-phase region except very near the bubble- and dew-points. The method used to incorporate these results in preparation of the PTH diagram will be discussed in detail in Appendix III.

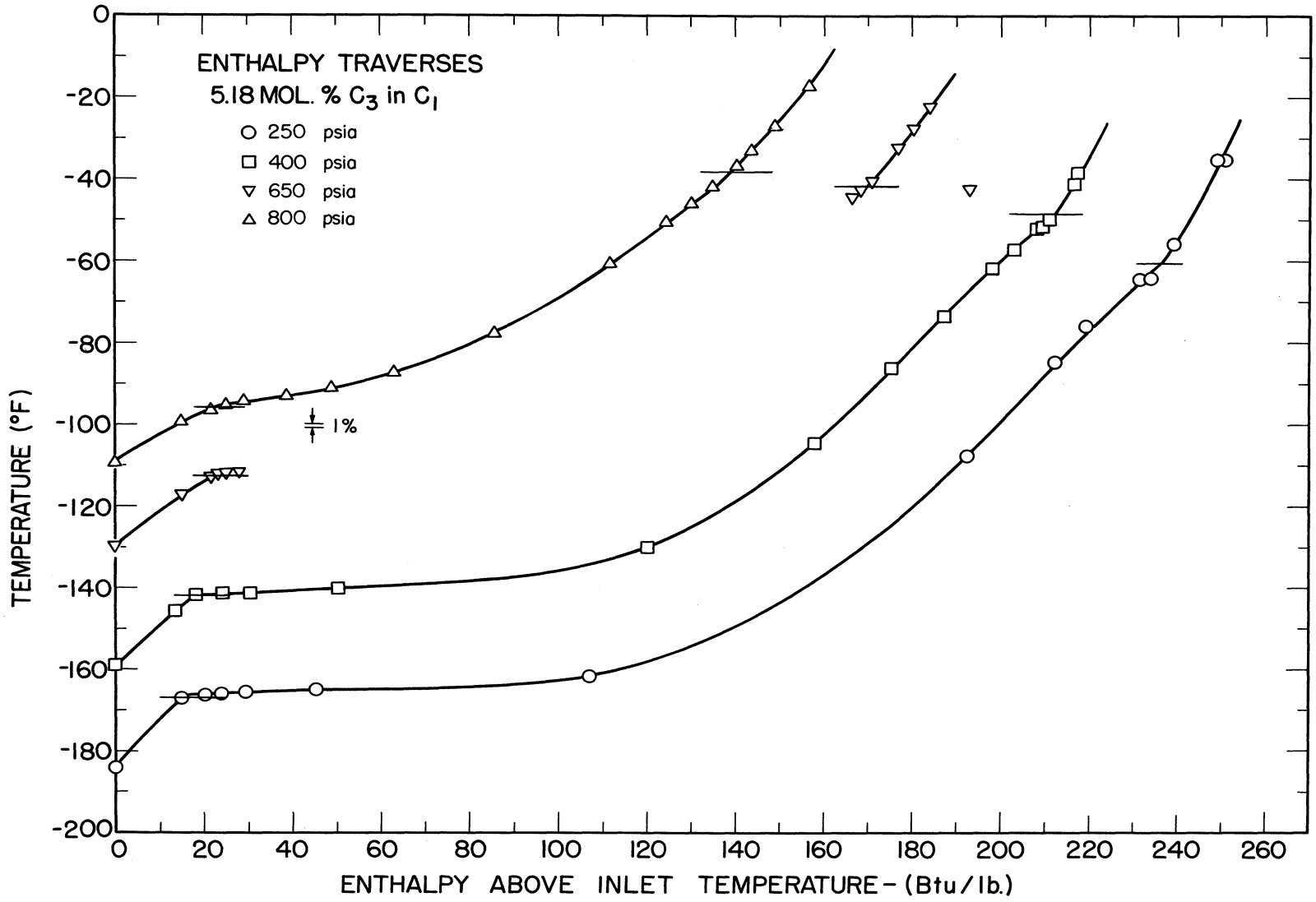

Figure AII.7 Calorimetric Data Obtained Within and Through the Two-Phase Region.

TABLE AII.5

Empirical Data Obtained From Interpretation of Enthalpy Traverses

Pressure psia	Bubble Point °F	Dew Point °F	ΔH_{vap} Btu/lb
250	-166.5	-60.5	221.0
400	-141.7	-48.0	194.3
500	-128.1	-41.4	178.5*
650	-111.8	-40.3	147.4
800	- 95.2	-37.5	116.1

* Calculated (See Thermodynamic Consistency Checks)

Isothermal Determinations (Single-Phase)

Mather (50) reported the results of isothermal calorimetric determinations in the single-phase region for this mixture at -147.4, -27.0, 91.6 and 200°F. (See Figure 1). The basic procedures used to interpret the data to yield values of

$$\phi \equiv (\partial \underline{H}/\partial P)_T \qquad \text{(II.9)}$$

and isothermal enthalpy differences are similar to those used to interpret the isobaric data as described in the previous section.

A typical plot of

$$\hat{\phi} \equiv \frac{(\underline{H}_{P_2} - \underline{H}_{P_1})_T}{P_2 - P_1} \qquad \text{(II.10)}$$

is illustrated in Figure AII.8. An iterative graphical procedure involving use of Simpson's rule for integration was used to yield $\phi = f(P)$. The values of ϕ at low pressure listed by Mather (50) were used to define the curve between 0 and 100 psia.

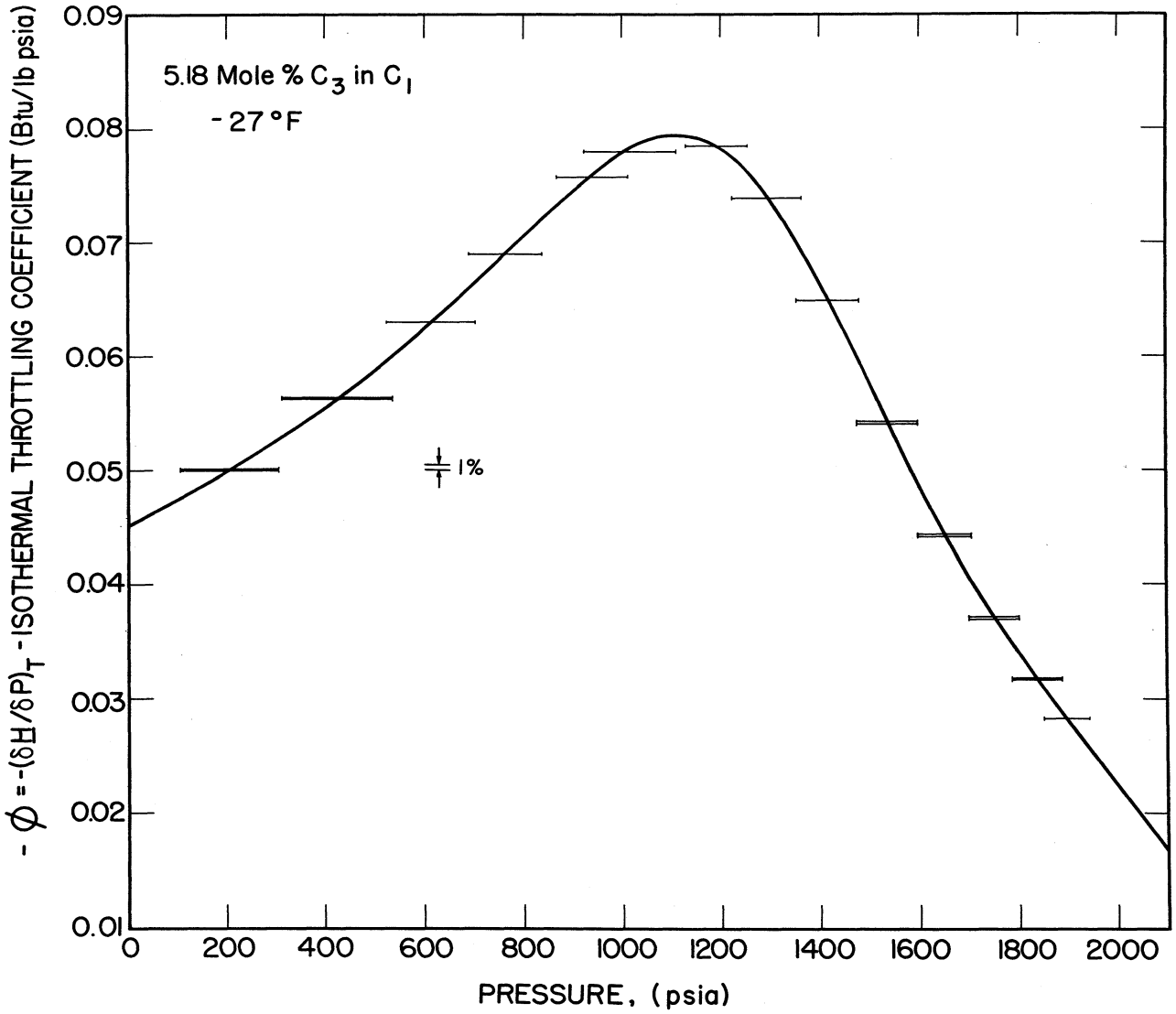

Figure AII.8 Isothermal Throttling Coefficient, ϕ, at -27°F Illustrating Method of Interpreting Isothermal Calorimetric Results.

A curve for $\emptyset = f(P)$ was generated over the entire range of experimental pressures so as to yield random variation in differences between experimental and calculated values of isothermal enthalpy differences. The resulting curves were then integrated to yield values of enthalpy difference for every 50 psi interval to aid in making the final tabulation and between experimental isobars for use in making the thermodynamic consistency checks to be described in Appendix III. At -147.4°F the data extend only from 509 to 1791 psia. In interpreting these data extrapolations were made to 500 and 2000 psia but not beyond these pressures.

The values of C_p, $\emptyset$ and isobaric and isothermal enthalpy differences determined by the iterative graphical procedures described in this Appendix were considered to be good estimates subject to small corrections as required to obtain thermodynamic consistency of all experimental results. The tests for thermodynamic consistency and adjustment of values are described in Appendix III.

Appendix III

Thermodynamic Consistency Checks and Final Adjustment of Values of C_p and ϕ

Thermodynamic Consistency Checks

Enthalpy is a state thermodynamic property and is therefore represented by an exact mathematical function. This fact provides a severe test of the thermodynamic consistency of the isobaric and isothermal data obtained for this mixture.

The exactness of the enthalpy function is readily expressed in the form of a mathematical restriction. If one begins at a thermodynamic state designed by T_B and P_B such that

$$\underline{H}_B = f(T_B, P_B) \qquad \text{(III.1)}$$

and considers a number of changes in enthalpy, $\Delta\underline{H}_i$ corresponding to sequential changes in state such that the final state is identical to the initial state, then the algebraic sum of such changes must be identically equal to zero.

$$\Sigma\Delta\underline{H}_i = 0 \qquad \text{(III.2)}$$

If independent experimental data are used to evaluate the sequential enthalpy differences in such a closed loop experimental errors will almost always yield a non-zero value for their algebraic sum. A measure of the experimental error on a percentage basis is provided by the equation

$$\text{percentage deviation} = \frac{\Sigma\Delta\underline{H}_i}{\Sigma|\Delta\underline{H}_i|} \times 100 \qquad \text{(III.3)}$$

The isobaric and isothermal determinations carried out with this mixture were made so as to provide a number of checks of the thermodynamic consistency of the data. With reference to Figure 1, note that isobaric data are reported at 1500 psia from -240 to +150°F and at 1000 psia from -240 to +40°F. In addition, isothermal determinations were made at -147.4°F between 500 and 1000 psia and at -27°F between 100 and 1950 psia. A "loop" of four independent experimental determinations is thus formed by the isobaric determinations at 1000 and 1500 psia between -147.4 and -27°F and the two isothermal determinations at -147.4 and -27°F between 1000 and 1500 psia. This particular loop is illustrated as Figure AIII.1

In carrying out the interative graphical procedures to yield $C_p(T)$ and $\phi(P)$ as described in Appendix II, values of $\Delta\underline{H}_i$ corresponding to the four individual sides of the loop of Figure AIII.1 were determined.

$$\Sigma\Delta\underline{H}_i = [+(137.144)+(36.64)-(175.126)+(-0.25)] \text{ Btu/lb}$$
$$= -1.092 \text{ Btu/lb}$$

Therefore, the net result of experimental error for this particular closed loop is -1.092 Btu/lb as expressed within the box enclosed within the loop.

In expressing this error on a percentage basis the sum of the absolute values of all differences is taken as denomenator as expressed by Equation (III.3)

$$\Sigma|\Delta\underline{H}_i| = [(137.144)+(36.64)+(175.126)+(0.25)] \text{ Btu/lb}$$
$$= 349.16 \text{ Btu/lb}$$

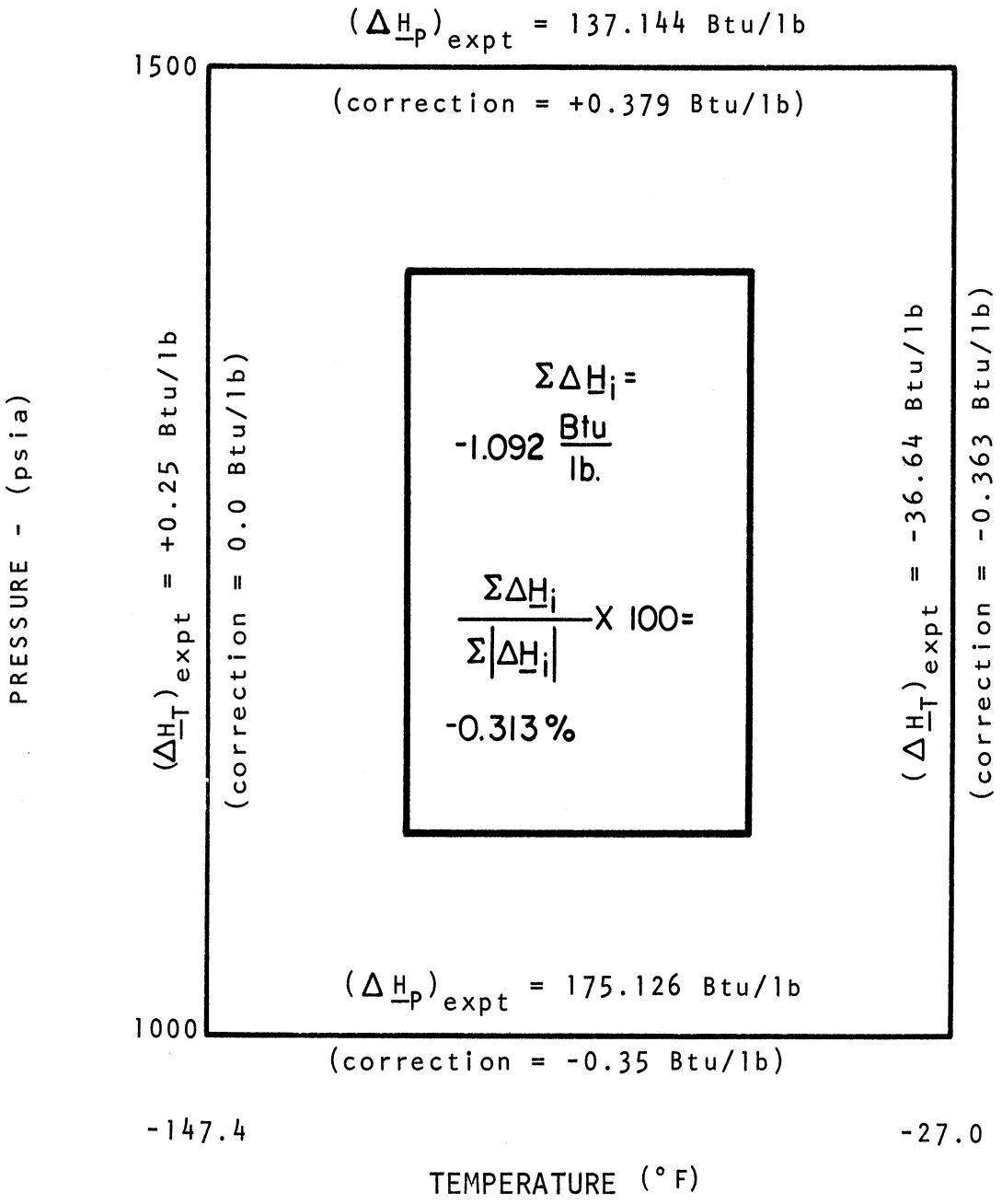

Figure AIII.1 One Complete Check of Thermodynamic Consistency of Calorimetric Data Used to Evaluate Enthalpy Differences.

Therefore, the average percentage error of this set of four experimental determinations is given by

$$\text{percentage deviation} = \frac{-1.092 \text{ Btu/lb}}{349.16 \text{ Btu/lb}} \times 100 = -0.313\%$$

This result is also included within the box enclosed by the loop in Figure AIII.1.

The result of all checks of thermodynamic consistency of the enthalpy determinations are summarized in Figure 2. Associated with each leg is the value of ΔH_i determined from the raw data as described in Appendix II. Each completed loop encloses a box containing the value of experimental deviation expressed both as actual error (Btu/lb) and percentage error.

Adjustment of Value of ΔH_i

The enthalpy differences of each leg were adjusted that that $\Sigma \Delta H_i = 0$ for each closed loop. Note the adjustment of legs that are common to two loops effects the error in both loops. In all cases an attempt was made to limit such corrections to the anticipated experimental errors associated with the precision of the data. Experience has shown this to be about $\pm 0.3\%$ for the isobaric data. A value of $\pm 0.8\%$ was used as the expected precision of the isothermal data because of the limitations of the differential pressure balance of Roebuck (57) which was used in making the isothermal measurements. The values of the corrections are listed for the one loop on Figure AIII.1, and for all loops in Figure 2.

In some cases it was necessary to apply corrections in excess of the anticipated limits on precision as indicated above. Corrections of about 0.5% were made to the isobaric data between -27.0 and 91.6°F at pressures of 1000 and 1500 psia. As noted with reference to Figure 1 there are regions over which no data were obtained over these ranges of conditions. Thus some of this larger correction was probably required to adjust for incorrect estimates where data were lacking. A correction of 1% was made on the isothermal leg at -27.0°F between 1000 and 1500 psia. This correction is made in the region of the maximum in $\emptyset$ (See Figure AII.).

Adjustment of Values of C_p and $\emptyset$

As indicated earlier, the experimental values of $\Delta\underline{H}_i$ listed on Figures AII.1 and Figure 2 were determined by graphical integration of the functions $C_p(T)$ and $\emptyset(P)$ as estimated by iterative graphical procedures described in Appendix II. The adjusted values of $\Delta\underline{H}_i$ as developed to satisfy the condition $\Delta\underline{H}_i = 0$ for each loop are therefore inconsistent with the functions $C_p(T)$ and $\emptyset(P)$ as originally developed from the basic experimental data, i.e. these original estimates are thermodynamically inconsistent by approximately $\pm$ 0.2% on the average. Therefore, the functions $C_p(T)$ and $\emptyset(P)$ were adjusted so as to be consistent with the adjusted values of $\Delta\underline{H}_i$. The corrected values of C_p and $\emptyset$ are shown on all figures and are listed at temperatures and pressures corresponding to experimental conditions on Tables IIa,b,c,d and IIIa,b. Extrapolated values are included with corrections.

Appendix IV

Preparation of PTH Tables and Diagrams

In preparing the final table and diagram of enthalpy values for the mixture every attempt was made to incorporate accurate data reported in the literature for the pure components as a final check on the accuracy of the results reported by Manker (47) and Mather (50). The following steps are followed in order:

1) Arbitrary reference states are selected for each pure component in the mixture.

2) Data for the pure components at relatively low pressures are used to determine the enthalpy of each component as an ideal gas at zero pressure and at an elevated temperature corresponding to one of the sets of isothermal calorimetric determinations reported for this mixture.

3) The enthalpy of the mixture in the ideal gas state at zero pressure and temperature of the isothermal determination is calculated assuming no heat of mixing under these conditions.

4) The isothermal and isobaric enthalpy differences determined by interpretation of the calorimetric data at elevated pressures as described in Appendices II and III are used to calculate values of enthalpy at pressures and temperatures of experimental determinations.

5) The thermodynamic consistency of the data at low pressures from the literature and at elevated pressures from the Thermal Properties of Fluids Laboratory is checked by determining the enthalpy of the liquid mixture at low temperature and pressure. Adjustments are then made to satisfy the condition that $\Delta \underline{H}_i = 0$ around the closed loop of the enthalpy diagram.

In preparing the last published PTH diagram for this mixture, Mather (50) chose to "close the loop" by drawing isotherms at low temperatures and pressures which exhibited unusual (and unacceptable) curvature. Jones (40) had a similar problem in attempting to obtain such closure when working with the enthalpy data for pure methane. He chose to resolve this discrepancy by applying a correction of 4 Btu/lb to the values at low pressures as calculated using data from the literature.

It was decided to take exceptional care with respect to every step of the reprocessing of the data in order to obtain values of the highest accuracy obtainable from the data. This Appendix is devoted to detailed descriptions of the procedures that were followed.

Selection of Arbitrary Reference States

The specification of arbitrary reference states for each pure component is a matter of convenience. It was therefore, specified that $\underline{H} = 0$ for pure liquid methane and propane at their saturation pressures at -280°F. This choice was made for two reasons:

1) The choice is consistent with reference states selected for methane (40,41), propane (70) and several mixtures (47,50,51,70) by previous investigators.

2) All values at -280°F and above will be positive, i.e.> 0.

It was necessary to consider the effects of minor impurities in preparing the final PTH diagram. For consistency, it was specified that $\underline{H}$ = 0 at -280°F and the corresponding vapor pressures for the impurities N_2, O_2, C_2H_6 and CO_2 in the liquid state.

Therefore, all pure components were specified to have the same reference condition; $\underline{H}$ = 0 for saturated liquid at -280°F.

Determination of $\underline{H}_i$ for Pure Components as Ideal Gases at +200°F

Relatively little effort was spent to determine $\underline{H}$ for the minor components in the mixture:

Propane. Yesavage (70) gave detailed consideration to published data from the literature and calculated a value of $\underline{H}$ = 298.7 Btu/lb for pure propane at 200°F and zero pressure. He found this value to be consistent with interpretation of his calorimetric data at elevated pressures and therefore, this value was accepted as published.

Impurities. Values of $\underline{H}$ at 200°F and zero pressure relative to the pure saturated liquids at -280°F for nitrogen and oxygen were calculated from values listed by Canjar and Manning (12). Carbon dioxide does not exist as a pure liquid at -280°F and therefore, a value was estimated from the values of N_2 and

O_2 by assuming that $\underline{H}$ at 200°F and zero pressure is a linear function of molecular weight. A value for ethane was obtained as the arithmetic average of the ones for propane and that for methane (the determination of which is described in detail in the pargraphs to follow).

The estimation of $\underline{H}_i$ for CO_2 and C_2H_6 as ideal gases at 200°F is admittedly relatively crude but the total mole fractions of these two components is .001 so that extended efforts to estimate these values was not considered to be justified.

Methane. As noted previously, both Jones (40) and Mather (50) had difficulty in their attempts to establish the thermodynamic consistency of their data with published data for the pure components at low pressures. The fact that both investigators had similar difficulties led to the conclusion that the published data for methane might be somewhat in error. Therefore, the published data were themselves checked for thermodynamic consistency.

Values of enthalpy differences for methane at low pressures are available from a variety of sources. These include values of C_p of the saturated liquid (20,31,34), calorimetric determinations of the heat of vaporization (18,31), values of enthalpy departures for the vapor $(\underline{H}^\circ - \underline{H})$ (1) and the enthalpy behavior of methane at zero pressure, $\underline{H}^\circ$. (58). These data can be used to calculate enthalpy differences between two fixed states. Such differences should be independent of the data used to evaluate the difference thereby providing a test of thermodynamic consistency.

The various paths selected to evaluate the enthalpy difference between saturated liquid at 100°K and the ideal gas state at 150°K are illustrated on Figure AIV.1. Each such difference is evaluated as the sum of the enthalpy difference required to increase the temperature of the saturated liquid from 100°K to the temperature at which vaporization occurs. ($\int C_{ps.l} dT$), the heat of vaporization at that temperature ($\Delta \underline{H}_{vap}$), the enthalpy change associated with the isothermal change from a saturated vapor to the ideal gas state at zero pressure ($-(H^\circ - H)$) and finally the change in enthalpy of the ideal gas methane from the temperature of vaporization to 150°K ($\underline{H}^\circ_{150°K} - \underline{H}^\circ_{T}$)

TABLE AIV.1

THERMODYNAMIC CONSISTENCY CHECKS OF PUBLISHED CALORIMETRIC DATA FOR METHANE AT LOW TEMPERATURES

T	$\int_{100}^{T}$ Cpsidt	ΔHvap	$\underline{H}^\circ - \underline{H}$	$\underline{H}^\circ_{150} - \underline{H}_T$	$\underline{H}^\circ_{150} - \underline{H}_{100}$
°K	Ca/l gmol	Cal/gmol	Cal/gmol	Cal/gmol	Cal/gmol
100	0	2030 (-1.3)	13.8 (-4.8)	397.1 (-0.8)	2440.9
110	129.3	1963 (+1.1)	26.0 (-2.5)	317.7 (-0.6)	2436.0
120	261.7	1888 (+1.8)	45.7 (-1.0)	238.3 (-0.5)	2433.7
130	399.0 (0)	1800 (+2.1)	74.3	158.9 (-0.3)	2432.2
140	542.8 (-1.0)	1698 (+1.0)	113.9	79.5 (-0.2)	2434.2
150	693.7 (-2.0)	1577 (-1.8)	167.1	0	2437.8

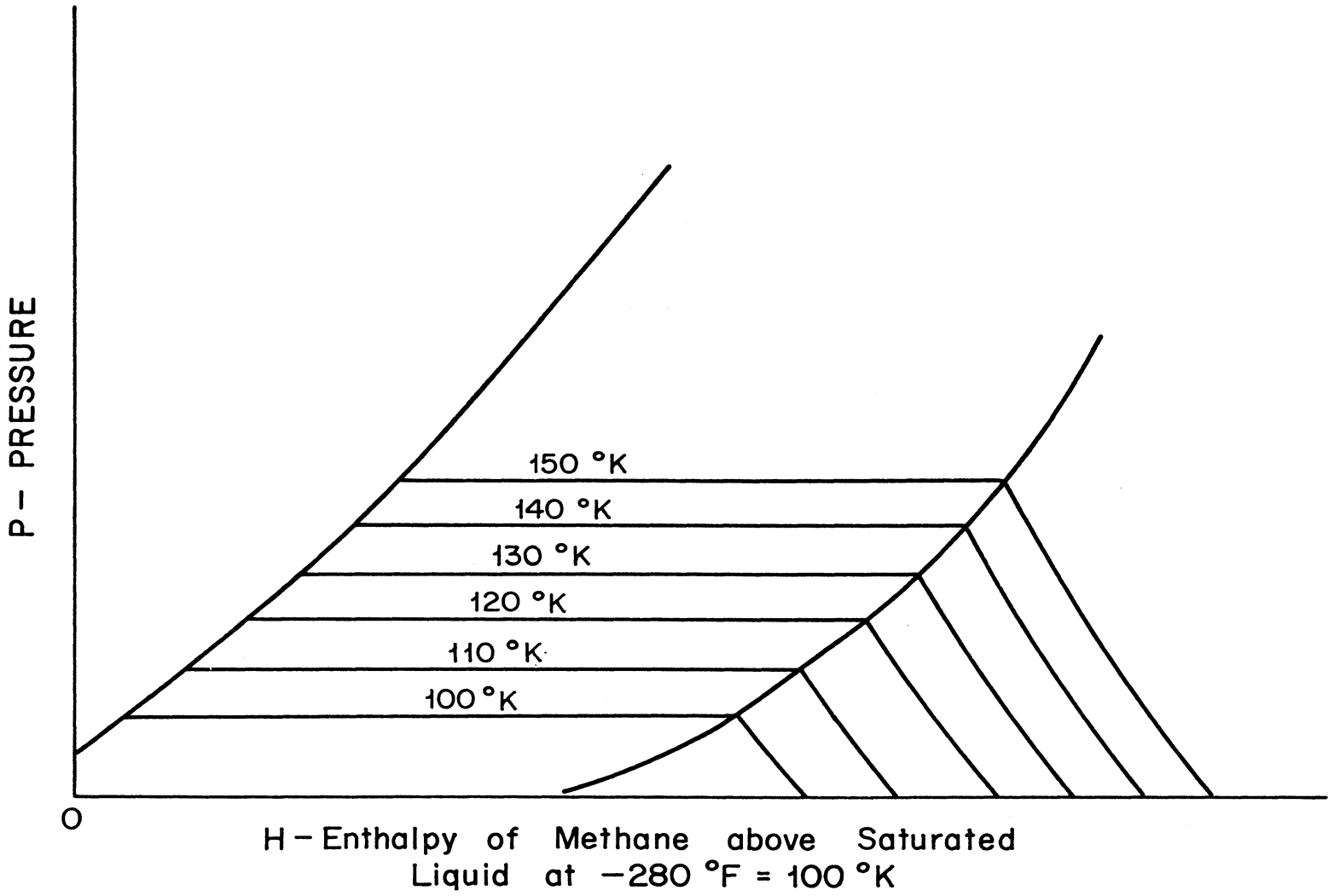

Figure AIV.1 Check of Thermodynamic Consistency of Published Calorimetric Data and Calculated Enthalpy Departures at Low Temperatures.

1. ($\int C_{ps.l.} dT$). Values of the heat capacity of saturated liquid methane, $C_{ps.l.}$, as reported in the literature (20,31,34) were plotted vs T as illustrated in Figure AIV.2. A smooth curve was drawn through the points giving primary emphasis to the results of Frank and Clusius (31), Hestermans and White (34) and Cutler and Morrison (20). The integral was determined by Simpson's rule for every interval of 10°K. The results are summarized in the second column of Table AIV.1.

2. ($\Delta \underline{H}_{vap}$). Values of $\Delta \underline{H}_{vap}$ listed as the third column of Table AIV.1 are based primarily on the calorimetric data reported by Hestermans and White (34). These data have been shown to be in good agreement with values calculated from data on the vapor pressure and volumetric behavior of methane (34). The values listed at 100°K is the lowest possible value within the combined limits of accuracy of the independent results of Hestermans and White (34), Frank and Clusius (31) and Colwell, Gill and Morrison (18).

3. ($\underline{H}^\circ - \underline{H}$). Values of ($\underline{H}^\circ - \underline{H}$) obtained from the latest API tabulation for methane (158) are included as column four in Table AIV.1. No value was listed for 100°K and therefore, a value was estimated by differencing the tabular values.

4. ($\underline{H}^\circ_{150} - \underline{H}^\circ_T$). A value of 397.1 cal/gmol was determined directly from values listed in the API 44 tables published in 1952 (158). This value was found to be inconsistent with the values of C_p° listed in the same publication but, nonetheless,

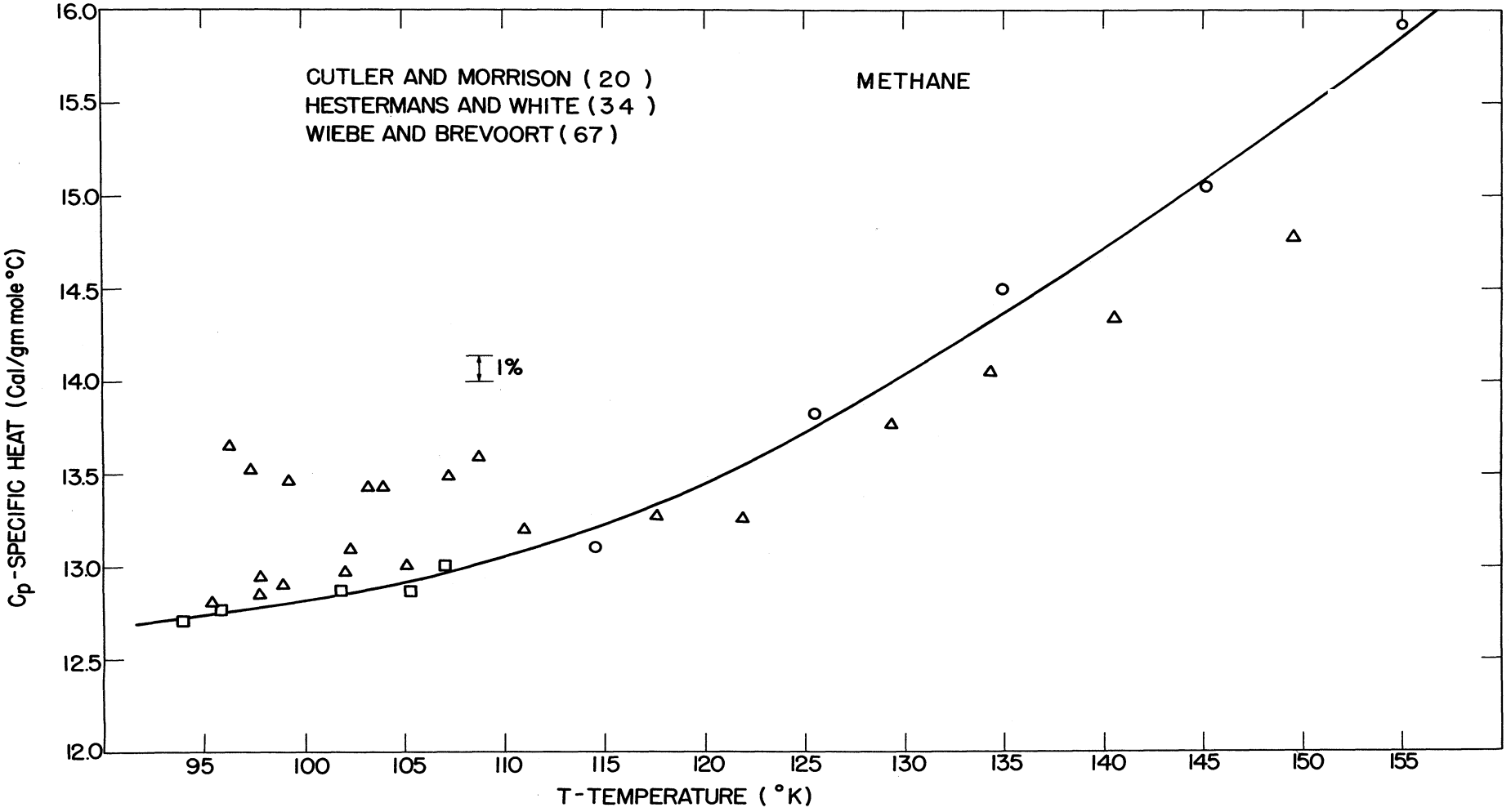

Figure AIV.2 Published Data on the Isobaric Heat Capacity of Methane as Saturated Liquid.

C_p° values were used for purposes of interpolation. The values thus determined are listed in the next-to-last column in Table AIV.1.

The sum of all differences is listed in the last column of Table AIV.1. The values differ by as much as 8.7 cal/gmol or about 0.4%.

All values were made to equal 2434 cal/gmol by applying the corrections included in the parentheses in Table AIV.1. Maximum percentage adjustments are indicated in Table AIV.2.

TABLE AIV.2

MAXIMUM PERCENTAGE ADJUSTMENTS IN PUBLISHED CALORIMETRIC DATA FOR METHANE AT LOW TEMPERATURE

	Type of Data	Adjustment
1.	$\int C_{ps.l.} dT$	0.9%
2.	$\Delta \underline{H}_{vap}$	0.1%
3.	$\underline{H}^\circ - \underline{H}$	35. %
4.	$\underline{H}^\circ_{150} - \underline{H}_T$	0.2%

The large percentage correction of $\underline{H}^\circ$-$\underline{H}$ is justified on the basis that this value was calculated using the BWR equation of state at low temperatures where large errors of extrapolation have been noted in other systems (62,72,76). Note also that little or no corrections are required for ($\underline{H}^\circ$-$\underline{H}$) at temperatures of 130°K and above.

Tabular values of $\underline{H}°$ from API 44 were used together with the result of the above interpretation to determine the enthalpy of methane as an ideal gas at 200°F. The results are summarized as follows:

	Btu/lb
$\underline{H}$ as saturated liquid at -280°F	0
Latent heat of vaporization at -280°F	227.72
Effect of Pressure on Enthalpy (5 → 0 psia at -280°F)	1.01
Increase in temperature as an ideal gas	
-280°F to -190°F	44.47
-190°F to +200°F	203.33
	476.53

In contrast Mather used a value of 477.79 Btu/lb.

The values of $\underline{H}_i$ resulting from these considerations are summarized in Table AIV.3.

TABLE AIV.3

Enthalpies of Pure Components as Ideal Gases at 200°F Relative to Saturated Liquid at -280°F

	Mole Fraction	H_i Btu/lb	Molecular Weight
Methane	0.9464	476.53	16.042
Ethane	0.0006	(437.5)	30.068
Propane	0.0518	398.68	44.094
Nitrogen	0.0006	195.6	28.016
Oxygen	0.0002	192.6	32.016
Carbon Dioxide	0.0004	(184)	44.011

Calculation of $\underline{H}_m$ for the Mixture as Ideal Gas at +200°F

At zero pressure gases behave ideally in that there is little or no heat of mixing. Therefore, the enthalpy of the mixture in the ideal gas state at 200°F can be calculated by applying the equation

$$\underline{H}_m = \Sigma\, x_i\, \underline{H}_i \qquad \text{(AIV.1)}$$

Note that x_i is listed as mole fraction whereas $\underline{H}_i$ is given on a mass basis in Table AIV.2. The value calculated by applying Equation (AIV.1) together with the values listed in Table AIV.2 is 465.67.

Incorporation of Isobaric and Isothermal Enthalpy Differences at Elevated Pressures.

The base temperature of 200°F was selected because isothermal data were obtained at this temperature. Making use of isothermal enthalpy differences evaluated as described in Appendixes II and III, values of enthalpy of the mixture as an actual gas were determined at intervals of 50 psia which includes every pressure at which isobaric determinations had been made. At these pressures the isobaric enthalpy differences were utilized to establish values of enthalpy over the entire temperature range at elevated pressures. Because of the adjustments which had been made to the isothermal and isobaric enthalpy differences as described in Appendix III, all enthalpy values were consistent at the intersection of isothermal and isenthalpic determinations. However, in spite

of the fact that considerable care had been used in interpreting the data at elevated pressures, slight additional corrections were required to obtain complete agreement with published data at -280°F.

Corrections to Obtain Complete Agreement at -280°F

The procedure described above yielded values of enthalpy for the mixture at -280°F at pressures of 2000, 1500, 1000 and 500 psia. Cutler and Morrison (20) report data on the heat of mixing of methane and propane at 100°K (-280°F) and these data indicate that the liquid mixture at low pressures has an enthalpy of 0.268 Btu/lb.

It is possible to draw a curve connecting the individual values at 200, 1500, 1000, 500 and about zero psia, but such a curve does not appear to have the correct curvature at low pressures. The points at 2000, 1500, and 1000 are fit very well with a straight line but the extension of this line misses the point at 500 psia by about 1 Btu/lb and the point at saturation pressure by 2.5 Btu/lb. An arbitrary decision was made to consider the isotherm at -280°F to be a straight line. A final adjustment of 0.54 Btu/lb was made on the values at 2000 psia and 1000 psia with somewhat smaller corrections at 1500 psia. These corrections applied over the entire temperature interval for which the enthalpy changed by about 430 Btu/lb so that the final correction was 0.13%. Uniform adjustments of this amount was applied to values of C_p so that the final tabulated values of C_p and $\underline{H}$ are consistent.

Interpolation to Intermediate Values of Temperature and Pressure

A large scale (20" x 8') graph was prepared and all adjusted values of enthalpy plotted. Isotherms were then drawn through points of common temperature. The data at 1700 psia was readily incorporated because it joined with isothermal data at -27°F. Slight extrapolation of the data at 1100 and 1200 psia was required in order to incorporate these data.

Experimental data obtained with partial vaporization of the mixture was used to determine the location of the isotherms within the two-phase region. The data obtained at 800 psia was readily incorporated because it intersected the isotherm at -27°F. The isobar at 650 psia likewise intersected this isotherm but very few points were obtained within the two-phase region at this pressure. The data at 800 and 650 psia were used to guide the extrapolation of the curves at 400 and 250 psia to -27°F. The extrapolations are illustrated on Figure AII.7.

Tabulated values of enthalpy are presented on Tables IIa and IId and IIIa, IIIb. The PTH diagrams were photo reduced and are presented as Figures 4a and 4b.

Appendix V

Equations Used in Calculating Values of Entropy and Fugacity.

The availability of an extensive table of adjusted values of enthalpy made it possible to calculate isobaric entropy differences quite precisely. These values also permitted utilization of published volumetric data to maximum advantage in calculating isothermal entropy differences. As a matter of convenience, the basis for all entropy values was taken to be a pure, perfectly oriented crystals at absolute zero. The equations used in making the calculations are summarized in this Appendix.

The Basic Property Relation

Entropy is related to other thermodynamic properties by the fundamental Gibb's relation. In the absence of significant changes in surface area, and other miscellaneous effects, this relation is written as

$$d\underline{U} = Td\underline{S} - Pd\underline{V} \qquad (V.1)$$

Incorporating the definition of enthalpy

$$\underline{H} \equiv \underline{U} + P\underline{V} \qquad (V.2)$$

yields an equavalent expression

$$d\underline{H} = Td\underline{S} + \underline{V}dP \qquad (V.3)$$

Similarly incorporation of the definition of Gibb's free energy, $\underline{G}$,

$$\underline{G} \equiv \underline{H} - T\underline{S} \qquad (V.4)$$

yields

$$d\underline{G} = -\underline{S}dT + \underline{V}dP \qquad (V.5)$$

These relations serve as the basis for all calculations of entropy differences made for this report using calorimetric and volumetric data for the mixture.

Isobaric Changes in Entropy

If pressure is held constant Equation (V.3) reduces to

$$d\underline{H}_p = Td\underline{S}_p \qquad (V.6)$$

Thus isobaric entropy differences are evaluated as

$$(\underline{S}_{T_2} - \underline{S}_{T_1})_P = \int_{T_1}^{T_2} d\underline{S}_p = \int_{T_1}^{T_2} \frac{d\underline{H}_p}{T} \qquad (V.7)$$

The most common form of this relation is

$$\int_{T_1}^{T_2} \frac{d\underline{H}_p}{T} = \int_{T_1}^{T_2} \frac{C_p}{T}\, dT_p \qquad (V.8)$$

In addition to data on C_p values of $(\underline{H}_{T_2} - \underline{H}_{T_1})_P$ have been determined as described in Appendix II. As noted there, considerable care was taken in the region of the peaks. Rather than repeat such integrations and run the risk of introducing computational errors, Equation (V.7) was modified so as to permit maximum utilization of the adjusted enthalpy values. Integrating the last terms of Equation (V.7) by parts yields

$$(\underline{S}_{T_2} - \underline{S}_{T_1})_P = \frac{\underline{H}_{T_2} - \underline{H}_{T_1}}{T_2} + \int_{T_1}^{T_2} \frac{\underline{H}_T - \underline{H}_{T_1}}{T^2}\, dT \qquad (V.9)$$

This is the relation that was used to calculate isobaric entropy difference so as to obtain values that are as consistent as possible with the tabulated enthalpy values.

Isothermal Changes in Entropy

In evaluating isothermal entropy differences it is common practice to utilize Equation (V.5) to obtain the Maxwell's identity

$$\left(\frac{\partial \underline{S}}{\partial P}\right)_T = -\left(\frac{\partial \underline{V}}{\partial T}\right)_P \qquad (V.10)$$

and then make use of published volumetric data to evaluate isothermal differences in entropy

$$\Delta \underline{S}_T = \int_{P_1}^{P_2} \left(\frac{\partial \underline{V}}{\partial T}\right)_P dP \qquad (V.11)$$

This procedure requires differentiation of volumetric data and a resulting loss of accuracy. An alternative procedure was developed to permit maximum utilization of the calorimetric data which were obtained with this mixture.

Under isothermal conditions Equation (V.3) can be rewritten as

$$d\underline{S}_T = \frac{d\underline{H}}{T} - \frac{\underline{V}dP}{T} \qquad (V.12)$$

Integration serves to yield values of isothermal entropy differences in terms of isothermal enthalpy differences and integrals of the volumetric function.

$$(\underline{S}_2 - \underline{S}_1)_T = \frac{(\underline{H}_2 - \underline{H}_1)_T}{T} - \frac{1}{T}\int_{P_1}^{P_2} \underline{V} dP_T \qquad (V.13)$$

Values of the enthalpy differences were obtained from the tables of adjusted values. Volumetric data from the literature were used to evaluate the integral term.

For liquids, $\underline{V}$ is relatively independent of pressure and therefore, the integration was carried out graphically using values of $\underline{V}$ directly. In the gaseous region $\underline{V}$ changes greatly with P and graphical integration is awkward. Therefore, a simple transformation was made. The compressibility factor Z is defined by

$$Z = \frac{PV}{RT} \qquad (V.14)$$

Therefore

$$(\underline{S}_{P_2} - \underline{S}_{P_1})_T = \frac{(\underline{H}_{P_2} - \underline{H}_{P_1})}{T} - R\int_{P_1}^{P_2} Z d\ln P_T \qquad (V.15)$$

Thus isothermal entropy differences were evaluated by application of Equation (V.12) with integration of the volumetric contribution being determined by either Equation (V.13) or (V.15) as appropriate.

Absolute Entropy Values

In order to tabulate values of entropy it is necessary to establish a value at some condition of temperature and pressures. It is especially conveinent in working with mixtures to have all mixtures referred to common bases for the pure components. Further convenience is provided if the bases are selected to

yield values of absolute entropy in accordance with the third law of thermodynamics. This procedure was followed in calculating absolute values of entropy for the mixture.

Values of absolute entropy for pure components as ideal gas at atmospheric pressure and 25°C have been tabulated recently by Stull, Westrum and Sinke (64). Values taken from these tables are listed in Table AV.1.

TABLE AV.1

Absolute Entropies of Pure Components as Ideal Gases at 25°C

Component	x_i mol fraction	$\underline{S}^\circ$ (cal/gmol°K)
Methane	0.9464	44.52
Ethane	0.0006	54.85
Propane	0.0518	64.51
Nitrogen	0.0006	45.767
Oxygen	0.0002	49.003
CO_2	0.0004	51.07
	1.0000	

The absolute entropy of the mixture under study as a mixture of ideal gases at 25°C is calculated by applying the equation

$$(S_M)_{IG} = \Sigma x_i \underline{S}^\circ + \Sigma x_i \ln x_i \qquad (V.16)$$

wherein the second term takes into account the entropy of mixing of ideal gases.

Applying Equation (V.16) together with the values listed in Table AV.1 yields $\underline{S}^{\circ}_{M-298} = 45.347$ cal/gmole°K. Using the molecular weight of the mixture, 17.525, yields $\underline{S}^{\circ}_{M-298} = 2.5876$ Btu/lb°F.

Next corrections must be applied to account for the fact that the mixture is not composed of ideal gases even at a pressure as low as one atmosphere and a temperature as high as 25°C.

Equation (V.12) applied for a real gas mixture. An equivalent expression can be written for an ideal gas mixture.

$$(\underline{S}_2 - \underline{S}_1)_{IGM} = -\frac{\underline{H}_1 - \underline{H}_2}{T} - \frac{1}{T}\int_{P_1}^{P_2} \underline{V}dP \qquad (V.17)$$

For a mixture of ideal gases, enthalpy is independent of pressure at constant temperature and therefore, Equation (V.17) reduces to

$$(\underline{S}_2 - \underline{S}_1)_{IGM} = -R\int_{P_1}^{P_2} d\ln P \qquad (V.18)$$

Written in the same form by combining Equations (V.12) and (V.14) the expression for the actual gas mixture is given by

$$(\underline{S}_2 - \underline{S}_1)_{RGM} = -\frac{(\underline{H}_1 - \underline{H}_2)_{RGM}}{T} - R\int_{P_1}^{P_2} Z_m d\ln P \qquad (V.19)$$

Subtracting the two equations yields

$$(\underline{S}_{2RGM} - \underline{S}_{2IGM}) - (\underline{S}_{1RGM} - \underline{S}_{1IGM}) = - \frac{(\underline{H}_1 - \underline{H}_2)_{RGM}}{T} - R \int_{P_1}^{P_2} \frac{(Z_m - 1)}{P} \, dP \qquad (V.20)$$

At zero pressure the entropy of the actual gas mixture is equal to that of an ideal gas mixture. Therefore, setting $P_1 = 0$ eliminates the second term on the left of Equation (V.20) and yields a value for the enthalpy departure, $(\underline{H}^\circ - \underline{H}_2)$ on the right hand side. Further P_2 is set equal to 1 atmosphere

$$\underline{S}_{RGM,1\ atm} - \underline{S}^\circ_{IGM} = \frac{(\underline{H}^\circ - \underline{H}_{1\ atm})_{RGM}}{T} - R \int_0^1 \frac{(Z_m - 1)}{P} \, dP \qquad (V.21)$$

In evaluating the difference the enthalpy departure $(\underline{H}_{1\ atm} - \underline{H}^\circ)_{298\text{-}RGM}$ is determined from the detailed analysis of the enthalpy behavior. The volumetric contribution at this low pressure is readily evaluated by application of the virial equation of state

$$\frac{PV}{RT} = 1 + \frac{B}{V} + \frac{C}{V^2} + \text{----} \qquad (V.22)$$

Expressed in a different form

$$Z = 1 + B'P + C'P^2 + \text{----} \qquad (V.23)$$

The coefficients of these two series are related mathematically

$$B' = B/RT$$

$$C' = (C - B^2)/(RT)^2 \qquad (V.24)$$

At low pressure Equation (V.23) reduces to

$$Z = 1 + B'P \qquad (V.25)$$

This relation can be utilized to evaluate volumetric term in Equation (V.21) at low pressures

$$\underline{S}_{RGM,\ 1\ atm} - \underline{S}^{\circ}_{IGM} = \frac{-(\underline{H}^{\circ} - \underline{H}_{1\ atm})_{RGM}}{T} - R\int_{0}^{1} B_m dP \qquad (V.26)$$

In estimating the second virial coefficient for the mixture it is considered that it is a binary mixture of methane and propane.

$$B_{mix} = x_1^2 B_{11} + 2x_1 x_2 B_{12} + x_2^2 B_{22} \qquad (V.27)$$

Equations (V.16) and (V.26) are used in combination with the value of $\underline{S}^{\circ}_m$ to determine the absolute entropy of the mixture at 25°C and 1 atm. Values of absolute entropy at other temperatures and pressures are then determined by applying Equation (V.9) to calculate isobaric entropy differences and Equations (V.13) to evaluate isothermal entropy differences

The Fugacity Function

Fugacity is defined by the equations

$$d\underline{G}_T = RTd\ln f \qquad (V.28)$$

$$\frac{f}{p} \rightarrow 1 \text{ as } P \rightarrow 0$$

At constant temperature Equation V.5 reduces to

$$d\underline{G}_T = \underline{V}dP_T \qquad (V.29)$$

Therefore

$$RTd\ln f_T = \underline{V}dP_T \qquad (V.30)$$

Incorporating the definition of Z [Equation (V.14)] and subtracting $d\ln P_T$ from both sides of Equation (V.30) yields

$$d\ln\left(\frac{f}{P}\right)_T = (Z-1)d\ln P_T \qquad (V.31)$$

Incorporating the limit expressed by Equation (V.30) permits one to evaluate values of fugacity coefficient $\gamma = (f/p)$ at any pressure and thereby determine f.

The integral term is difficult to evaluate graphically at low values of pressure. The substitution of Equation (V.25) is appropriate in such cases. Therefore, the integral expression is evaluated in two parts, one from P = 0 to 1 atm and the second applies at higher pressures.

Appendix VI

Primary Interpretation of Data from the Literature to Estimate the Volumetric Behavior of the 5% Mixture.

As indicated in Appendix V, accurate volumetric data are required in order to determine the isothermal effect of pressure on enthalpy. The procedures used to estimate the volumetric behavior of the mixture will be described in this Appendix.

The sources of volumetric data for methane, propane and their mixtures are reviewed in Appendix I. The four isothermal runs at -147.4, -27.0, 91.6 and 200°F were divided into two sets of two each in keeping with the availability of data at high temperatures from several sources (27,55,56,65,66) and at low temperatures from only one source (36,37).

Isotherms at 91.6 and 200°F

Reamer, Sage and Lacey (55,56) report values of Z for nine methane-propane mixtures over a fairly wide range of temperatures and pressures, none of which coincides with the compositions of the binary under study. The methane data tabulated by API Project 44 (1,58) and the propane data of Reamer, Sage and Lacey (55) were used to permit interpolation to the composition of the mixture.

The choice of the propane values is not critical in attempting to establish the volumetric behavior of a mixture containing 95 mole percent methane. Conversely, the values used for methane will exert a significant influence. Therefore,

the values obtained from the API tables (1,58) were checked against values calculated using the Vennix-Kobayashi equation of state for methane (44). The results of these computations were furnished by Kobayashi (44) and were found to be in excellent agreement with the values used in the calculations ($\pm$0.1%).

Tabulated values of Z from the three sources mentioned above were interpolated using a large digital computer. First interpolations were made of methane, propane and the nine mixtures to yield values at the two desired temperatures 91.6 and 200°F. Next interpolations were made with respect to composition to 5.18 mole percent propane in methane. The values thus obtained were considered to be preliminary values suitable for calculation of a first approximation of entropy differences as will be discussed in Appendix VII.

Use of digital computers to interpolate tabular values is subject to considerable error. Therefore, two independent methods were used; the method of Lane (45) and that of Klaus and Van Ness (43). Both do not necessarily go through the data points but do insure continuity of both first and second derivatives over the entire range of the table. Considerable modification of the Lane method was required as will be described in a subsequent publication. The method of Klaus and Van Ness was used to check the validity of the values calculated by the Lane method. Good agreement was obtained which was taken to mean that both interpolation methods probably yield reliable values.

The interpolated values of Z were plotted vs lnP to facilitate evaluation of the integral expressions in Equations (V.14) and (V.28). A typical curve is shown on Figure AVI.1.

Isotherms at -147.4 and -27.0°F

The only data for mixtures at these low temperatures are the relatively crude values (±1%) reported by Huang (36) and Huang and Kurata (37). These contributors also report values for propane and methane. These data for the pure components was used for purposes of interpolation with respect to composition because it was felt that use of more accurate values for methane (27) was not justified.

The data are reported at temperature intervals of 20°C from -150°C to 0°C and at intervals of 1000 psia up to 5000 psia with some intermediate values at 500 psia and at the bubble point of some mixtures. Data are tabulated for four mixtures.

The comparitive paucity of tabulated values in the range of primary interest (-147.4 and -27.0°F up to 2000 psia) required that graphical procedures be used for interpolation. Therefore, density was plotted vs temperature at constant pressure and composition as illustrated in Figure AVI.2. Values read from such plots at -147.4 and -27.0°F were plotted as isobars with composition as ordinate. A typical plot is presented as Figure AVI.3.

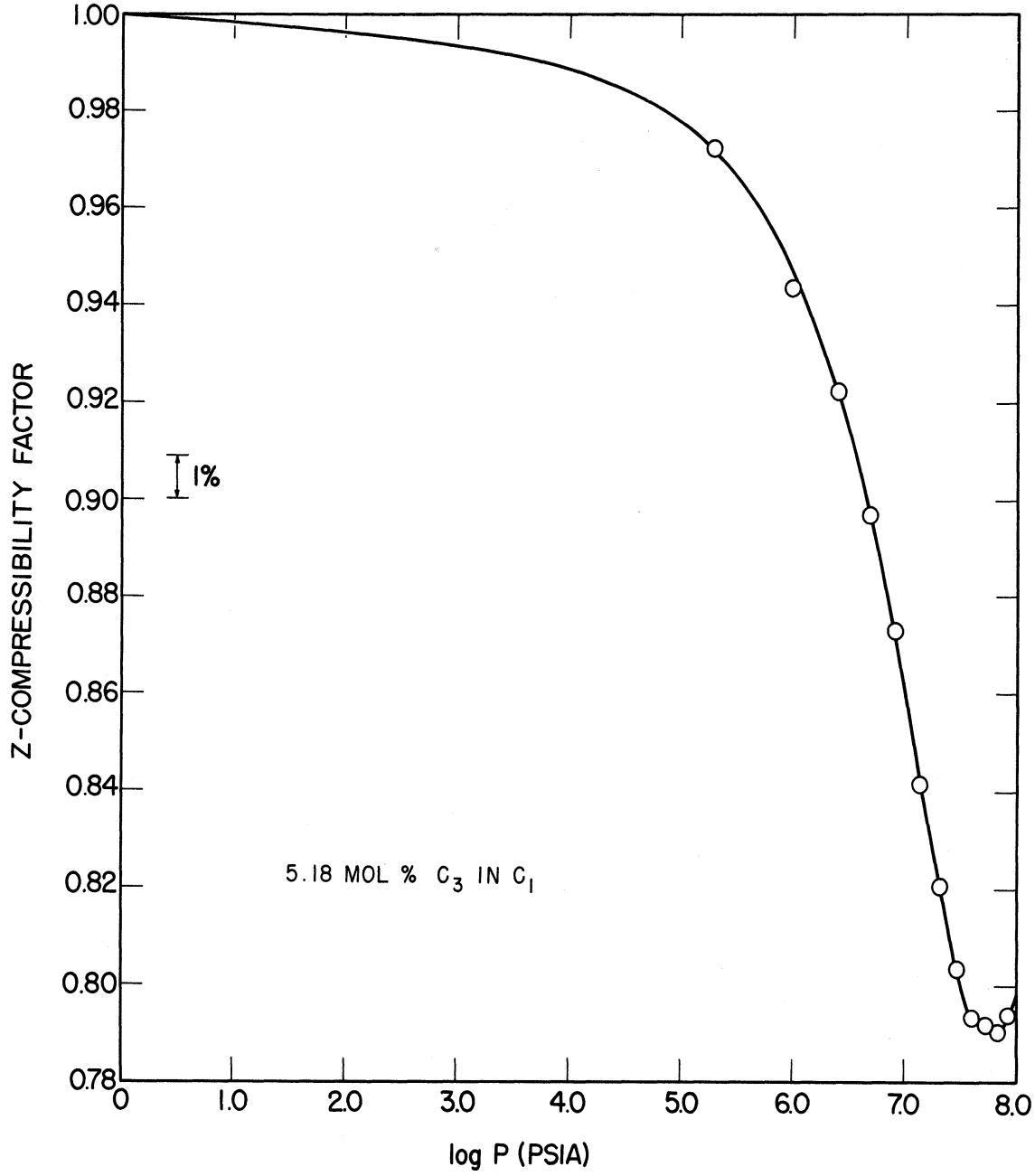

Figure AVI.1 Typical Plot of Compressibility Factor, Z, vs lnP at 91.6°F as Used to Evaluate $\int Z d\ln P$.

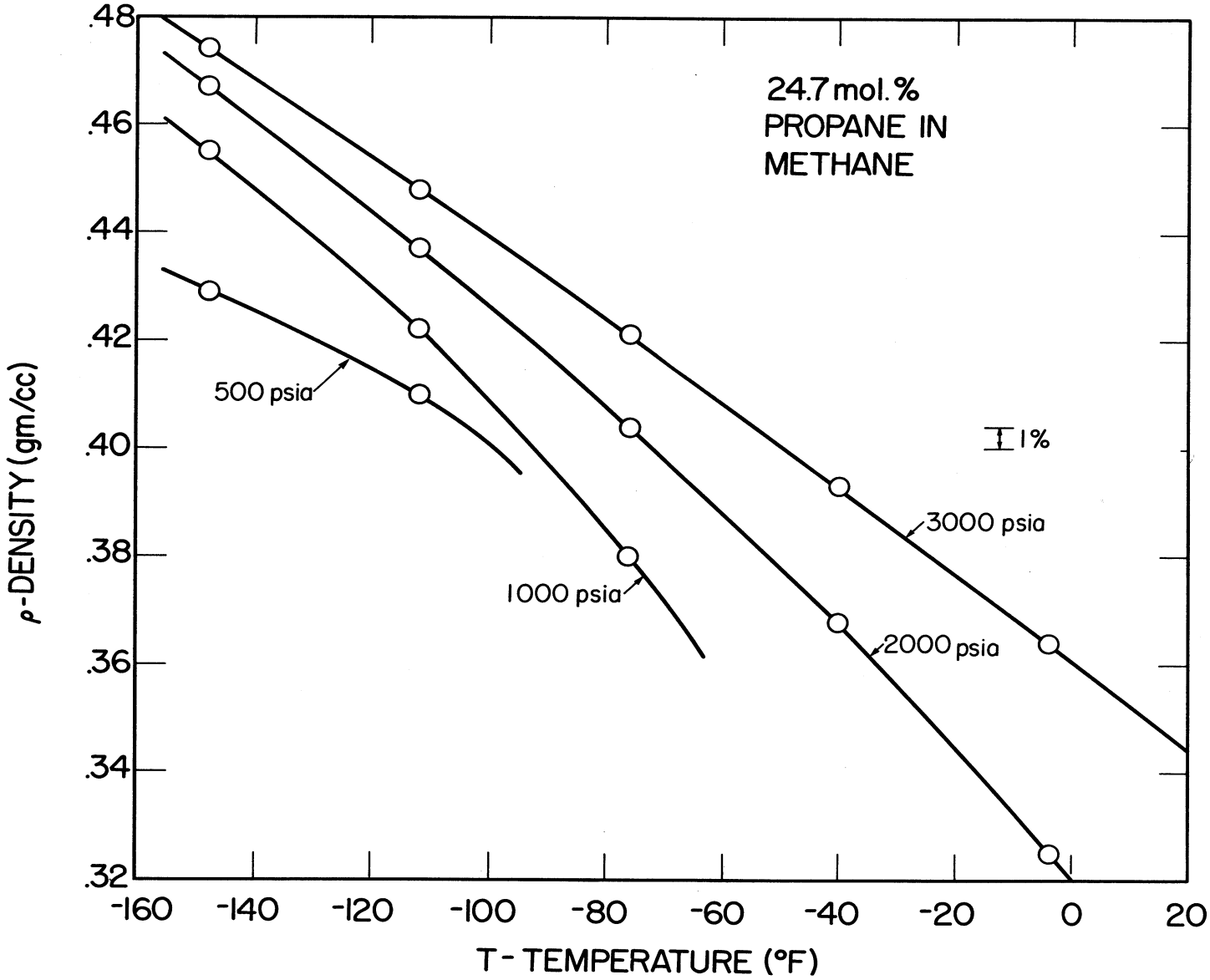

Figure AVI.2 Typical Plot of Isobaric Density, ρ, for Liquid Methane-Propane Mixture for Interpolation to Temperatures of Isothermal Calorimetric Data.

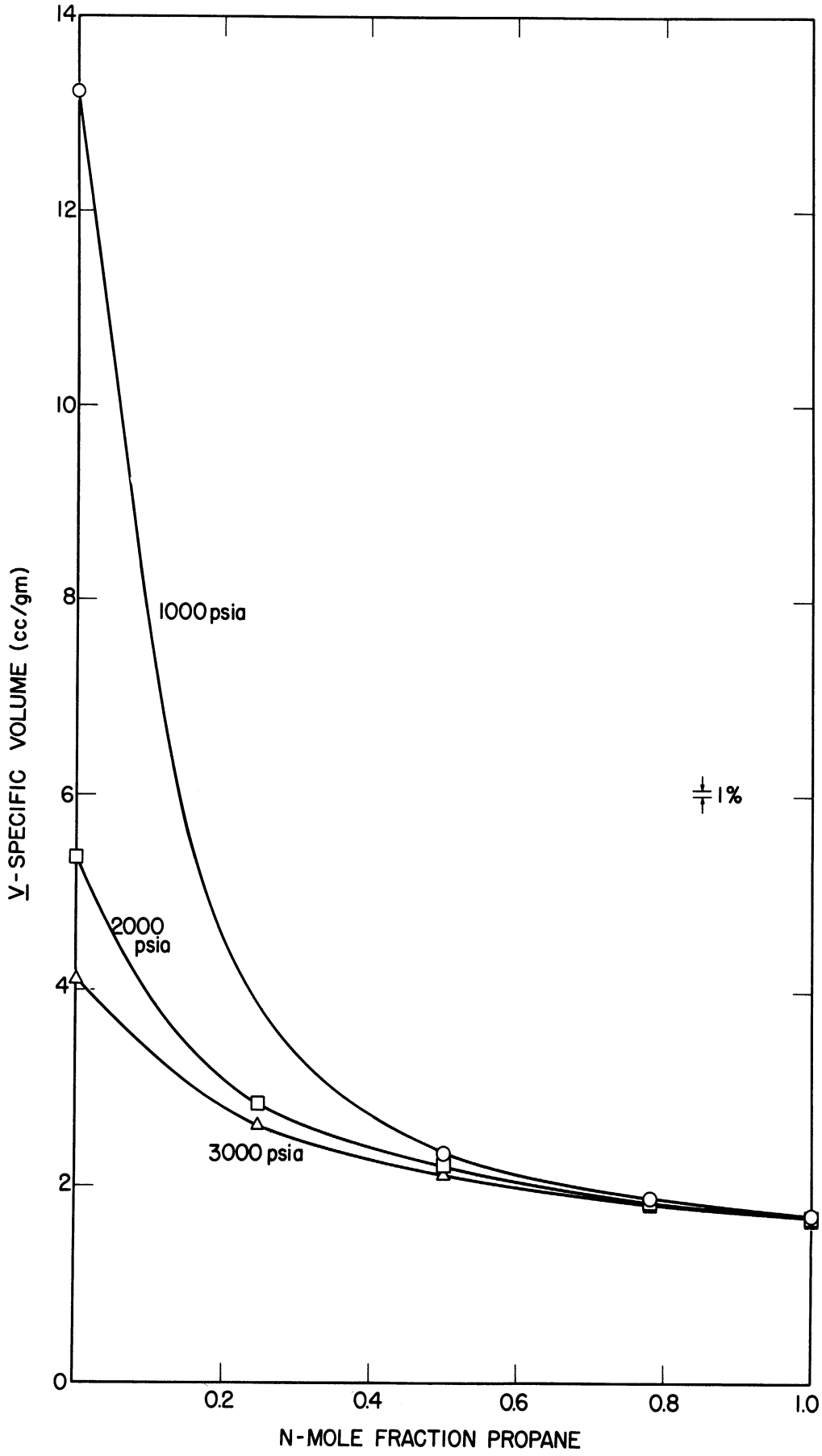

Figure AVI.3 Typical Plot of Specific, $\underline{V} = 1/\rho$ of Liquid Methane-Propane Mixture of Interpolation to Composition of Mixture.

As illustrated on this plot, density is a strong function of composition at high concentrations of methane. Thus the interpolation to 5.18% C_3 is subject to considerable variation depending on the method of placing the draftman's spline.

It was virtually impossible to estimate the volumetric behavior of the mixture at -27°F between 1000 and 1500 psia. Whereas the 5% mixture is in the single phase over the entire pressure range at this temperature, the mixtures containing 25 percent propane exists as two phases at 1000 psia.

The preliminary estimates of Z and $\underline{V}$ obtained by the interpolation procedures described in this Appendix are used to obtain first estimates of the isothermal effect of pressure on entropy as described in detail in Appendix VII. These values are checked for thermodynamic consistency as described in Appendix VIII. Adjustments are made on the estimates of Z and $\underline{V}$ in Appendix VIII to obtain values which are thermodynamically consistent with tabular values of $\underline{H}$ and $\underline{S}$. These corrected values are then used to calculate the fugacity of the mixtures at the two higher temperatures.

Appendix VII

Calculation of Entropy Differences

After the adjusted enthalpy values were obtained as described in Appendix III and preliminary interpretation of the published volumetric data was completed as described in Appendix VI, it was only necessary to utilize these results in connection with the equations of Appendix V to evaluate isobaric and isothermal differences in entropy.

Isobaric Differences in Entropy

As developed in Appendix V

$$(\underline{S}_{T_2} - \underline{S}_{T_1})_P = \frac{(\underline{H}_{T_2} - \underline{H}_{T_1})_P}{T_2} + \int_{T_1}^{T_2} \frac{(\underline{H}_T - \underline{H}_{T_1})}{T^2}\, dT \qquad (V.9)$$

The first term on the right side of the equation is readily evaluated at intervals of 10°F and at temperatures of isothermal determinations by direct substitution of correct values of $\underline{H}$ from tables. In addition to this matter of convenience, it was felt that this relation would yield values of entropy that are very consistent with the adjusted enthalpy values because normally the integral term does not contribute more than 10 percent to the value of the isobaric entropy difference.

The integral term was evaluated graphically by plotting $[(\underline{H}_T - \underline{H}_{T_1})/T^2]$ vs T as illustrated by Figure AVII.1. This particular curve is for the region of the sharp peak illustrated in

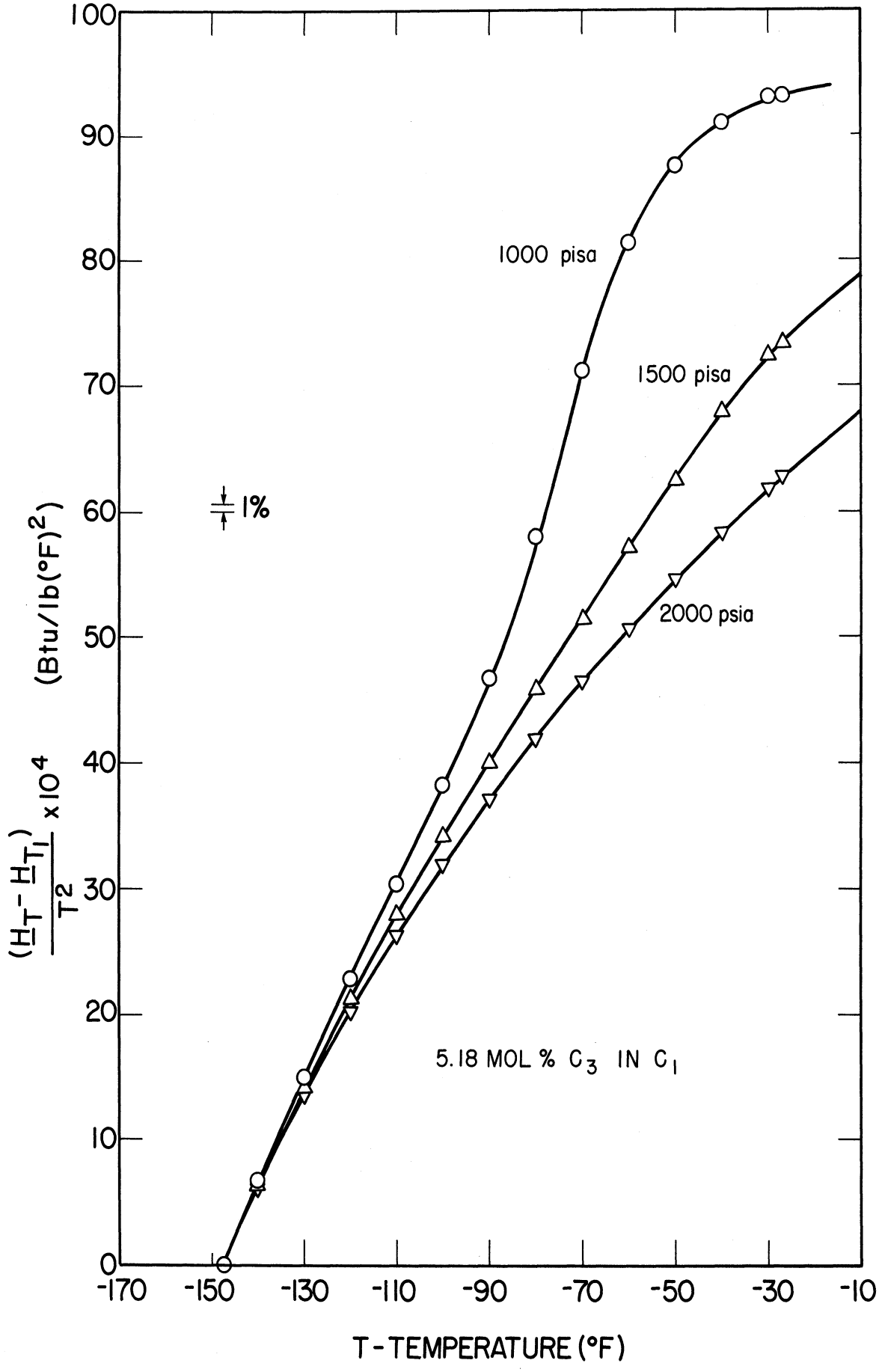

Figure AVII.1 Typical Plot Used to Evaluate Second (Residual) Term in Equation (V.9) in the Vicinity of the Peak in $C_p(T)$ at 1000 psia.

Figures AII-1 and AII-2. Note that the residual represented by the integral is a smooth function even when C_p exhibits a sharp maximum.

Note also that Equation (V.9) applies within the two-phase region of a mixture as well as in the single-phase. Therefore, the relation was applied to obtain values of $\underline{S}$ within the two-phase region. Figure AVII.2 is a plot of the residual integral across the two-phase region. Again a smooth relation is obtained.

The values thus determined were tabulated at even intervals of 10°F. In addition, differences between experimental isotherms were calculated. Two typical values are included in Figure AVII.3. They are the values presented horizontally above the isobars between the two experimental isotherms. Both values are given algebraic signs consistent with an increase in temperature. Other values are summarized on Figure 3.

Isothermal Entropy Differences

Equation (V.13) was applied directly to evaluate isothermal entropy differences at -147.4°F and at -27.0°F

$$(\underline{S}_{P_2} - \underline{S}_{P_1})_T = \frac{1}{T}\left[(\underline{H}_{P_2} - \underline{H}_{P_1})_T - \frac{1}{T}\int_{P_1}^{P_2} \underline{V}dP_T \right. \qquad \text{(V.13)}$$

Values of the isothermal enthalpy difference were determined directly from values listed in the table of adjusted enthalpies (Appendix III).

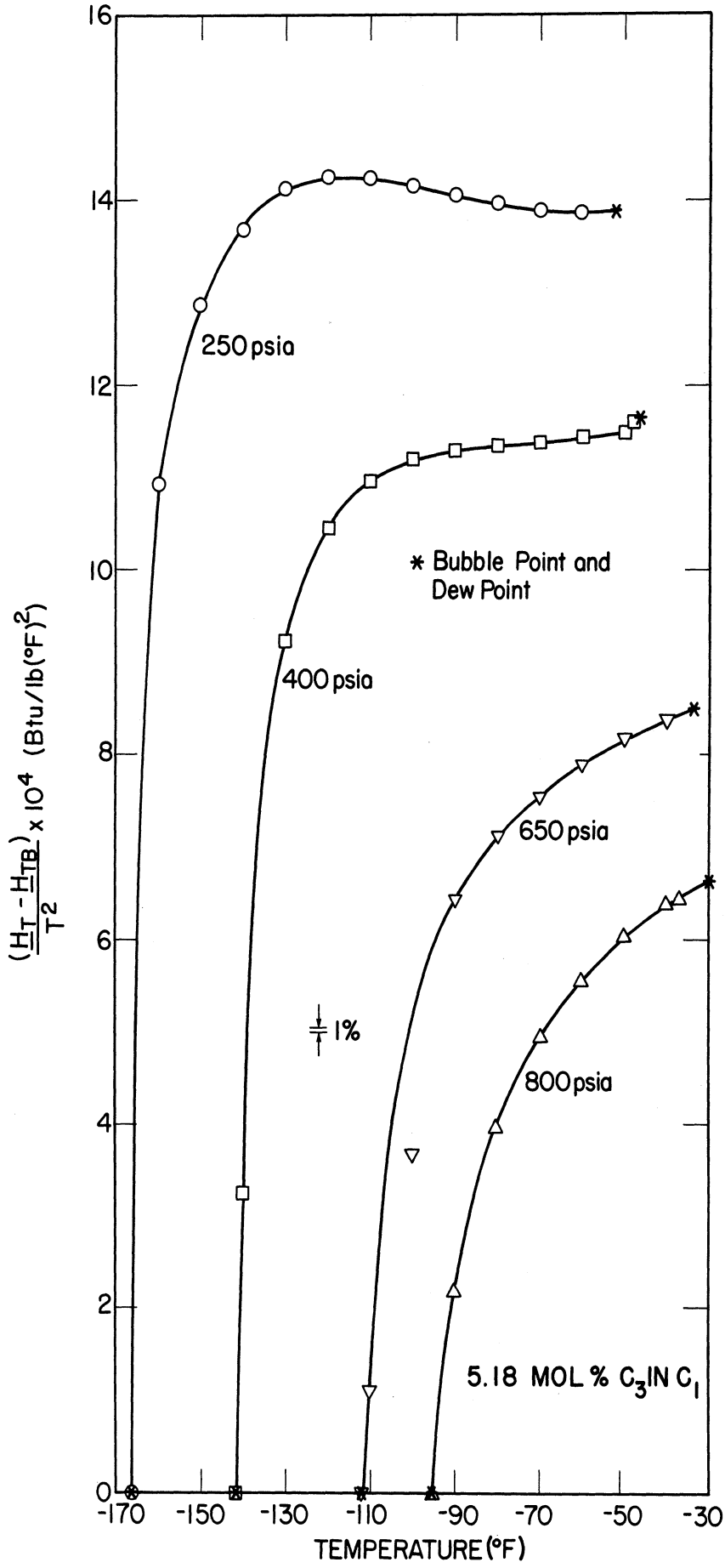

Figure AVII.2 Typical Plot Used to Evaluate Second (Residual) Term in Equation (V.9) in the Two-Phase Region.

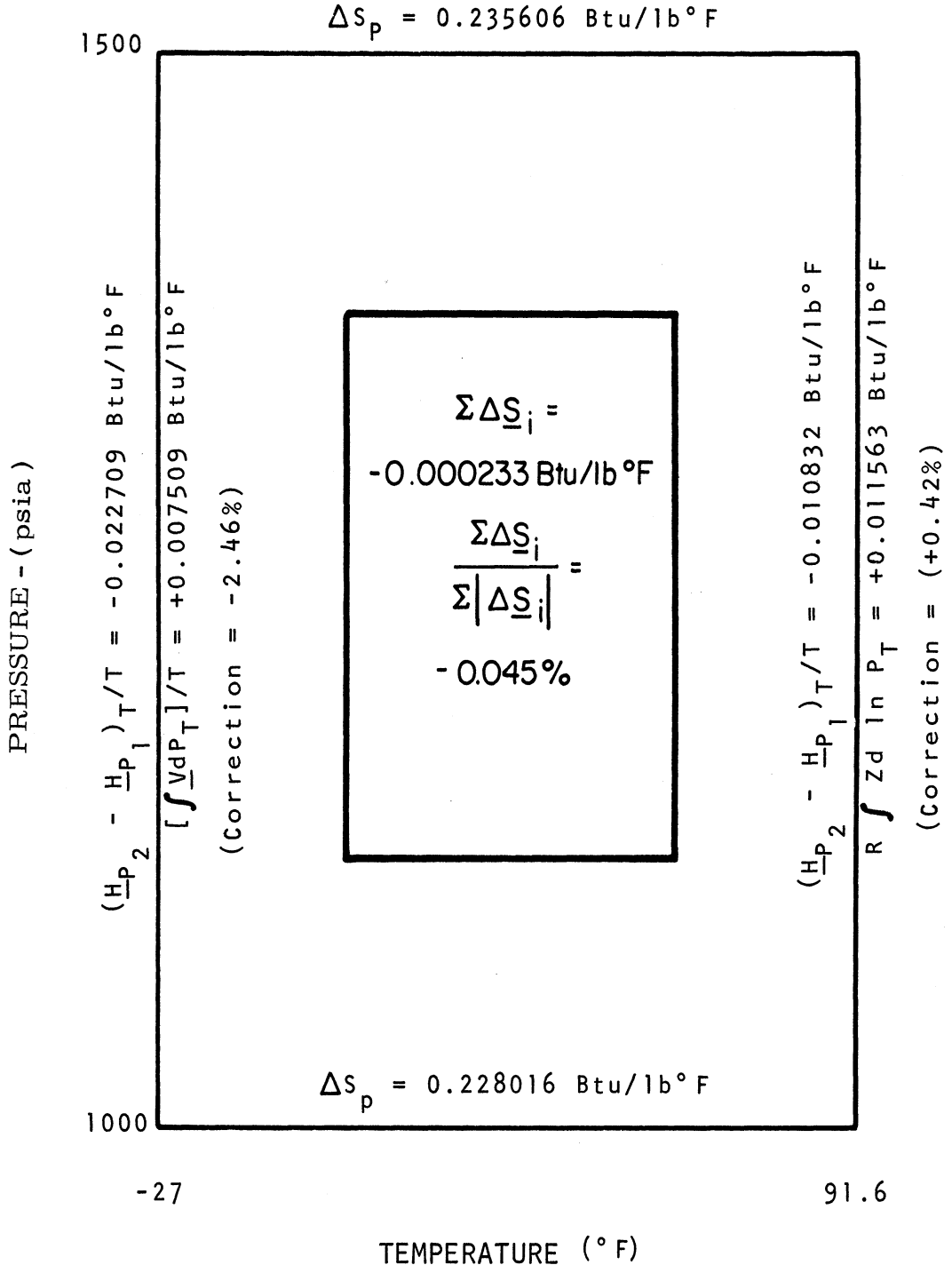

Figure AVII.3 One Complete Check of Thermodynamic Consistency of Calorimetric and Volumetric Data Used to Evaluate Entropy Differences.

Typical values of $(\underline{H}_{P_2} - \underline{H}_{P_1})/T$ are listed in Figure AVI.3. They are presented vertically to the left of the experimental isotherm. Both values are given an algebraic sign consistent with an increase in pressures. Additional values are summarized in like manner on Figure 3.

The integral term in Equation (V.12) was evaluated graphically. Plots of $\underline{V}$ vs P were made using values of $\underline{V}$ interpolated as described in Appendix VI. A typical plot is illustrated by Figure AVII.4.

One value of $(1/T)\int \underline{V}dP_T$ is presented in Figure AVII.3. It is presented vertically to the right of the experimental isotherms at -27°C. The value is given an algebraic sign consistent with an increase in pressure. However, note that a minus sign appears before the integral in Equation (V.13). Additional values are presented vertically to the right of the isotherms at -147.4 and -27.0°F, in Figure 3.

A slightly modified form of Equation (V.13) resulting from substitution of Equation (V.14) was used to determine isothermal entropy differences at 91.6 and 200°F

$$(\underline{S}_{P_2} - \underline{S}_{P_1})_T = (\underline{H}_{P_2} - \underline{H}_{P_1})/T - R \int_{P_1}^{P_2} Z d\ln P_T \qquad \text{(VII.1)}$$

As illustrated previously, the first term on the right hand side of the equation is evaluated using adjusted values of enthalpy. The integral term is evaluated by plotting the interpolated values of Z (Appendix VI) vs lnP. A typical

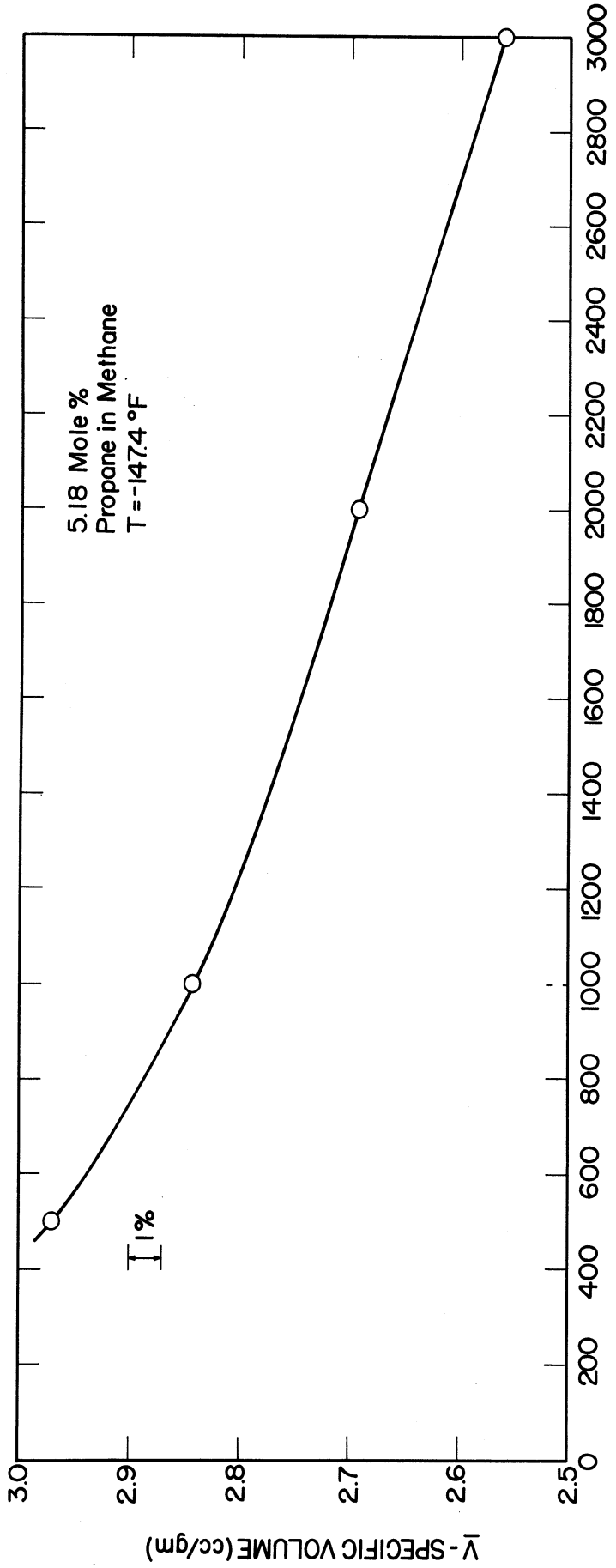

Figure AVII.4 Typical Plot Used to Evaluate $\int \bar{V} dP$ in the Compressed Liquid Region.

plot is presented as Figure AVI.1. A value is presented on Figure AVI.3 vertically to the right of the 91.6°F isotherm. The sign is associated with an increase in pressure. Note that the integral term is preceeded by a negative sign in Equation (VII.1). Additional values are summarized in like manner on Figure 3.

Appendix VIII

Thermodynamic Consistency Checks for Entropy and Adjustment of Values of Entropy, Compressibility Factor Z, and Specific Volume, V, Calculation of Fugacity.

Entropy is a thermodynamic property as is enthalpy. Therefore, checks of the thermodynamic consistency of the calculated values can be made as was done with enthalpy in Appendix III. The errors in the consistency checks can hopefully be eliminated by adjusting the volumetric values within the limits of the errors introduced experimentally and resulting from the use of interpolation procedures.

Thermodynamic Consistency Checks

The principle of the thermodynamic consistency check has been illustrated in Appendix III. The application to entropy is shown with reference to Figure AVII.3. As indicated by the first equation included in the box within the closed loop, the sum of the individual contributions to isobaric and isothermal entropy differences taken in a clockwise manner with particular attention to sign is not zero but -0.000233 Btu/lb°F or, equivalently, -0.045%. Similar summaries are included in the boxes with each closed loop of Figure 3.

Note that the maximum inconsistency introduced by integration of the residual isobaric term and the volumetric function in the isothermal legs is 0.147%. The average deviation for the 7 loops tested is 0.063%.

Corrections to Obtain Thermodynamic Consistency

It seemed highly desirable to make all corrections required to obtain thermodynamic consistency by adjusting the integral volumetric terms as long as this objective could be accomplished within the anticipated limits of accuracy of the interpolated values for Z and V.

The corrections were made by a trial and error procedure. Typical values of corrections are listed vertically within parentheses under the appropriate value in Figure AVII.3. Note that a relatively large correction (-2.45%) is required at -27°F compared with a correction of 0.42% at 91.6°F.

It seemed that such corrections were probably within the limits of accuracy of the interpolated values:

1) Huang (36,37) indicated a probable accuracy of ±1%. Interpolation could easily increase this error by a factor of two. Therefore, the correction of -2.46% seems reasonable.

2) It is difficult to assign a value for accuracy of the volumetric data at +91.6 and 200°F because of errors introduced by interpolation procedures. Corrections on the order of 0.4% appear to be justifiable.

All percentage corrections are summarized on Figure 3. The other corrections applied to Huang's data are all less than the value of -2.46% presented in Figure AVII.3. The largest correction at the elevated temperatures occurs at 200°F between 1000

and 1500°F and amounts to -0.65%. This may exceed the limits of accuracy of the interpolated volumetric data. Note that of a change of 0.008% in one of the isobaric enthalpy differences included in this loop would reduce the required correction on the volumetric term to 0.4%.

No adjustment of the enthalpy values were made. Instead the corrections listed on Figure 3 were accepted as proper and proportional adjustments in $\underline{V}$ and f were made. These values are listed for each isotherm on Tables IIa, b, c and d.

Calculation of Fugacity

As indicated in Appendix V the fugacity coefficient, f/P, is conveniently evaluated by application of the equation

$$\ln(f/P_T) = \int_0^{1\ atm} B_m dP + \int_{1\ atm}^{P} (Z_m - 1) d\ln P \qquad (V.30)$$

The second integral is readily evaluated from the plots of Z_m vs lnP. Equation (V.27) is applied together with values of the second virial coefficient for methane (35), propane (8, 38) and the interaction coefficient (8,22,38) to evaluate B_m. Values of -50.29 and 29.02 cm^3/gmole are obtained at 91.6 and 200°F respectively. The calculated values of fugacity, f, are listed at 91.6 and 200°F in Table IIb and IIa. No values are listed at -147.4 and -27°F because of the lack of values reported by Huang (36,37) at low pressures.

Appendix IX

Preparation of Mollier Diagram and Skeleton Table of Thermodynamic Properties for the Mixture.

The adjustment of volumetric data for the mixture as described in Appendix VIII yielded values of specific volume, V, fugacity, f, and isobaric and isothermal entropy differences that are thermodynamically consistent with the adjusted enthalpy values described in Appendix IV. These results were used to calculate values of absolute entropies for the mixture corresponding to experimental isobars and isotherms. A Mollier diagram was then prepared to permit interpolation of values to intermediate pressures and temperatures. The purpose of this Appendix is to describe the procedures employed in making these calculations.

Absolute Entropy of the Mixture at One Atmosphere and 91.6°F

The determination of the absolute entropy of the mixture at 25°C as a mixture of ideal gases was described in detail in Appendix V. The value obtained is 2.5876 Btu/lb°F.

The correction from an ideal gas mixture to an actual one is best made at a temperature of one of the isotherms where detailed attention is given to the estimate of enthalpy departures at low pressures. Therefore entropy of the real gas mixture was obtained at 91.6°F (closer to 25°C) and a pressure of one atmosphere. This involves two steps namely isobaric and isothermal correction to the entropy of ideal gas mixture at 25°C. Isothermal correction is made by using Equation V.26.

$$\underline{S}_{RGM,1\ atm} - \underline{S}^{\circ}_{IGM} = \frac{(\underline{H}^{\circ} - \underline{H}_{1\ atm})_{RGM}}{T} - R\int_{0}^{1} BmdP \qquad (V.26)$$

Values of enthalpy departure $(\underline{H}^{\circ} - \underline{H}_{1\ atm})$ for the real gas mixture was read off from the larger P-T-H plot, (Figure 4a and 5b) and found to be 0.5 Btu/lb. This amounts to a contribution of -0.000926 Btu/lb°F to the entropy difference. Second virial coefficient for the mixture was calculated using Equation V.27 and found to be 62.63 cm^3/gmole. Volumetric contribution in the Equation V.26 amounted to -0.0002901 Btu/lb°V. These two corrections to the ideal mixture entropy, 2.5876 Btu/lb°F yield a value of 2,586964 Btu/lb°F for the entropy of real gas mixture at 25°C and one atmosphere. Isobaric correction was made using Equation V.9 between temperatures of 77°F and 91.6°F

$$(\underline{S}_{T_2} - \underline{S}_{T_1})_P = \frac{\underline{H}_{T_2} - \underline{H}_{T_1}}{T_2} + \int_{T_1}^{T_2} \frac{\underline{H}_T - \underline{H}_{T_1}}{T^2}\, dT \qquad (V.9)$$

Isobaric enthalpy difference between temperatures of 77°F and 91.6°F was read off from the P-T-H plot and found to be 7.573 Btu/lb. Isobaric entropy differences according to Equation V.9 was found to be 0.013991 Btu/lb°F. After making both isothermal and isobaric correction value for real gas mixture entropy at 91.6°F and one atmosphere was obtained as 2.60688 Btu/lb°F.

Tables and Diagram of Thermodynamic Properties for the Mixture

Adjusted values of isothermal entropy differences at intervals 50 psia at 91.6°F as determined from calorimetric and

and volumetric data as described in Appendix VIII were used to calculate entropy values at similar pressure intervals between 14.7 and 2000 psia. These values are listed in Table IIb.

Adjusted values of isobaric entropy differences at 250, 500, 1000, 1500 and 2000 psia were utilized to determine entropy values at these pressures between -280 and +300°F. These values are listed in Table IIIa and IIIb. The values of absolute entropy at the intersection of each experimental isobar and isotherm were thus determined and were thermodynamically consistent as guaranteed by the precautions taken in Appendix VIII. The values along each isotherm are listed in Tables IIa, IIb, IIc and IId. The adjusted isobaric enthalpy values at 1700, 1200 and 1100 psia in the single-phase region and at 800, 650 and 400 psia through the two-phase region were tied into the isothermal values at -27°F to provide intermediate values. These values are likewise listed in Tables IIIa and IIIb.

It can be considered that the values listed in Tables at conditions of experimental measurements are smoothed experimental values. As such it is recommended that these values be utilized primarily in testing methods of prediction entropies of mixtures.

Two large scale (20 in. by 35 in.) plots of the skeleton entropy-enthalpy values were made. Curves were drawn through the points on the experimental isobars and isotherms in what appeared to be a self-consistent manner. Curves were drawn both in the single- and two-phase regions. Reduced copies of these plots are presented as Figures 5a and 5b.

Appendix X

Simpson's Rule

Many problems in engineering involve graphical integration. There are many procedures which are employed to facilitate such computations. Normally the interval of integration is divided into many parts and areas for each interval under the curve is found. Let us visualize one such a curve given in Figure AX.1.

Area Under Given Curve

One can divide the area to be found out into many trapezoids. If the interval of integration $x_3 - x_1$ is divided into n equal increments and the (n+1) corresponding ordinates are y_0, y_1, --- y_n then the area is given by

$$\int_{x_1}^{x_2} ydx = \left(\frac{x_3 - x_1}{n}\right) \frac{y_o}{2} + y_1 + y_2 + ----y_{n-1} + \frac{y_n}{2} \qquad (1)$$

This method is known as the "trapezoidal rule". A better method for engineers is Simpson's rule. According to this rule, assumption is made that the curve can be represented by a cubic. Sometimes it is said that Simpson's rule amounts to replacing the actual curve by a second degree parabola over the interval under consideration. Even though it is true, it can be shown as below that the integral is precisely accurate if the curve can be represented by a cubic over the interval of integration. The proof that follows is taken directly from class notes distributed by Professor R.L. Curl (19).

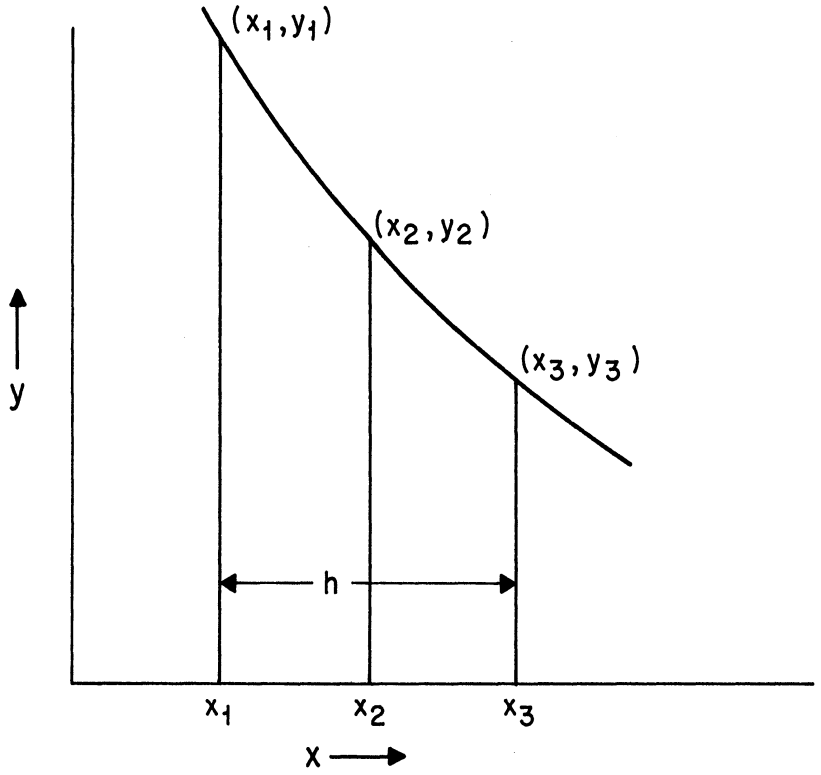

Figure AX.1 Area Under a Curve Using Trepezoidal Rule

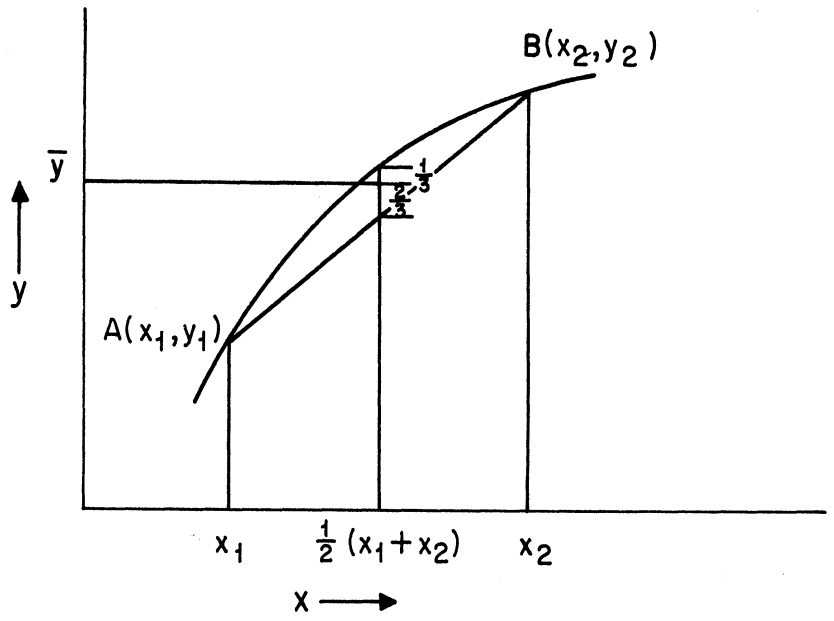

Figure AX.2 Area Under a Curve Using Simpson's Rule

Numerical Integration To Obtain Area Under A Curve

Consider a function $y(x)$ which is represented by a series of value pairs (y_i, x_i). We wish to find the area under this function between x_1 and x_2. If the values (y_i, x_i) are plotted, we may implement the numerical integration technique known as Simpson's Rule by a simple graphical method. Figure AX.2 illustrates the following steps.

Plot y_i vs x_i and draw a smooth curve through the points.

2. Locate (x_1, y_1) and (x_2, y_2) on the curve and draw a straight line AB between these points.

3. At $x = \frac{1}{2}(x_1 + x_2)$-the midpoint of the interval-sketch a vertical line from AB to the curve.

4. Locate a point at $x = \frac{1}{2}(x_1 + x_2)$ which lies 2/3 of the way from line AB to the curve. This $(\bar{y})$ is the mean value in the interval (x_1, x_2). Then:

$$\int_{x_1}^{x_2} y\,dx \doteq (x_2 - x_1)\,\bar{y}$$

Note 1. For accuracy, the distance from AB to the curve, on the graph paper, should usually be less than 10% of the distance between x_1 and x_2 on the graph paper. Use several intervals to accomplish this.

Note 2. Method is the same for curves concave upward - rule is still 2/3 of the way from the straight line.

Proof and Comments on Simpson's Rule

Represent y(n) by a polynomial expansion about x_1.

$$y(x) \quad \sum_{n=0} a_n (x-x_1)^n \tag{X.1}$$

Then

$$A = \int_{x_1}^{x_2} y\,dx = \sum_{n=0} \frac{a_n}{n+1} (x_2 - x_1)^{n+1} \tag{X.2}$$

For our approximation

$$A \doteq (x_2 - x_1) \left[\frac{y(x_1) + y(x_2)}{2} + \frac{2}{3} \; y\left(\frac{x_1+x_2}{2}\right) - \frac{y(x_1)+ y(x_2)}{2} \right] \tag{X.3}$$

$$= \frac{1}{6} (x_2 - x_1) \left[y(x_1) + y(x_2) + 4y \left(\frac{x_1 + x_2}{2}\right) \right] \tag{X.4}$$

(NOTE: This is Simpson's rule)

But from (X.1)

$$y(x_1) = a_o$$

$$y(x_2) = \sum_{n=0} a_n (x_2 - x_1)^n$$

$$y\left(\frac{x_1 + x_2}{2}\right) = \sum_{n=0} a_n \left(\frac{x_2 - x_1}{2}\right)^n$$

Hence

$$A = \frac{1}{6} \left[a_o(x_2-x_1) + \sum_{n=0} a_o(x_2-x_1)^{n+1} + 4 \sum_{n=0} \frac{a_n}{2^n} (x_2-x_1)^{n+1} \right]$$

$$= \frac{1}{6}\left[6a_o + \sum_{n=1} \left(\frac{4}{2^n} + 1\right) a_n(x_2-x_1)^{n+1}\right]$$

$$= a_o + \sum_{n=1} \frac{1}{6}\left(\frac{4}{2^n} + 1\right) a_n(x_2-x_1)^{n+1}$$

Now compare coefficients

TABLE AX.1

COMPARISON OF COEFFICIENTS OF THE SERIES GIVING AREA UNDER A CURVE USING SIMPSON'S APPROXIMATION

	Exact	Approximation
General Term	$\frac{a_n}{n+1}$	$\frac{1}{6}\left(\frac{4}{2^n} + 1\right) a_n$, $n \neq 0$
n		
0	a_o	a_o
1	$\frac{1}{2} a_1$	$\frac{1}{2} a_1$
2	$\frac{1}{3} a_2$	$\frac{1}{3} a_2$
3	$\frac{1}{4} a_3$	$\frac{1}{4} a_3$
4	$\frac{1}{5} a_4$	$\frac{1}{5} a_4$
5	$\frac{1}{6} a_5$	$\frac{1}{6} a_5$
6	$\frac{1}{7} a_6$	$\frac{1}{7} a_6$
		etc.

This approximation is therefore, exact for a third-order polynomial function. For a pure fourth-order curve (x^4), the error is $(\frac{5}{24} - \frac{1}{5}) = \frac{1}{24}$, or about 4%, or about 4% of the fourth-order term for an arbitrary fourth-order polynomial.

Procedure for Curve Fitting Using Simpson's Rule

This rule of graphical integration can be used in reverse for curve-fitting. Suppose in Figure A-VII-3, we are given a data point as we encounter in the calculations and desire to find a curve the area under which in the interval x_1-x_2 is same as that of ABCD. Following procedure may be adopted. Generally, the nature of the curve is known in terms of whether it is concave upward or convex upward. We also assume that it can be represented by a cubic. Let EFG represent the first guess for the curve. Then one can draw a straight line EIG. At $x = \frac{x_1 + x_2}{2}$ we must then have, according to Simpson's rule HI = 2 HF. This criterion can be satisfied by adjusting the position of E, F and/or G permitting one to satisfy a number of such requirements simultaneously. By a few trials, considerable experience and patience, a curve can be drawn that yields excellent agreement with all precise experimental values. Thus the criterian of equal area can be satisfied accurately with comparitive ease.

In the curve fitting work involved in this study, this procedure of curve fitting was followed wherever applicable. Otherwise areas were made equal by counting. Accurate graphical integration is facilitated greatly by application of these procedures.

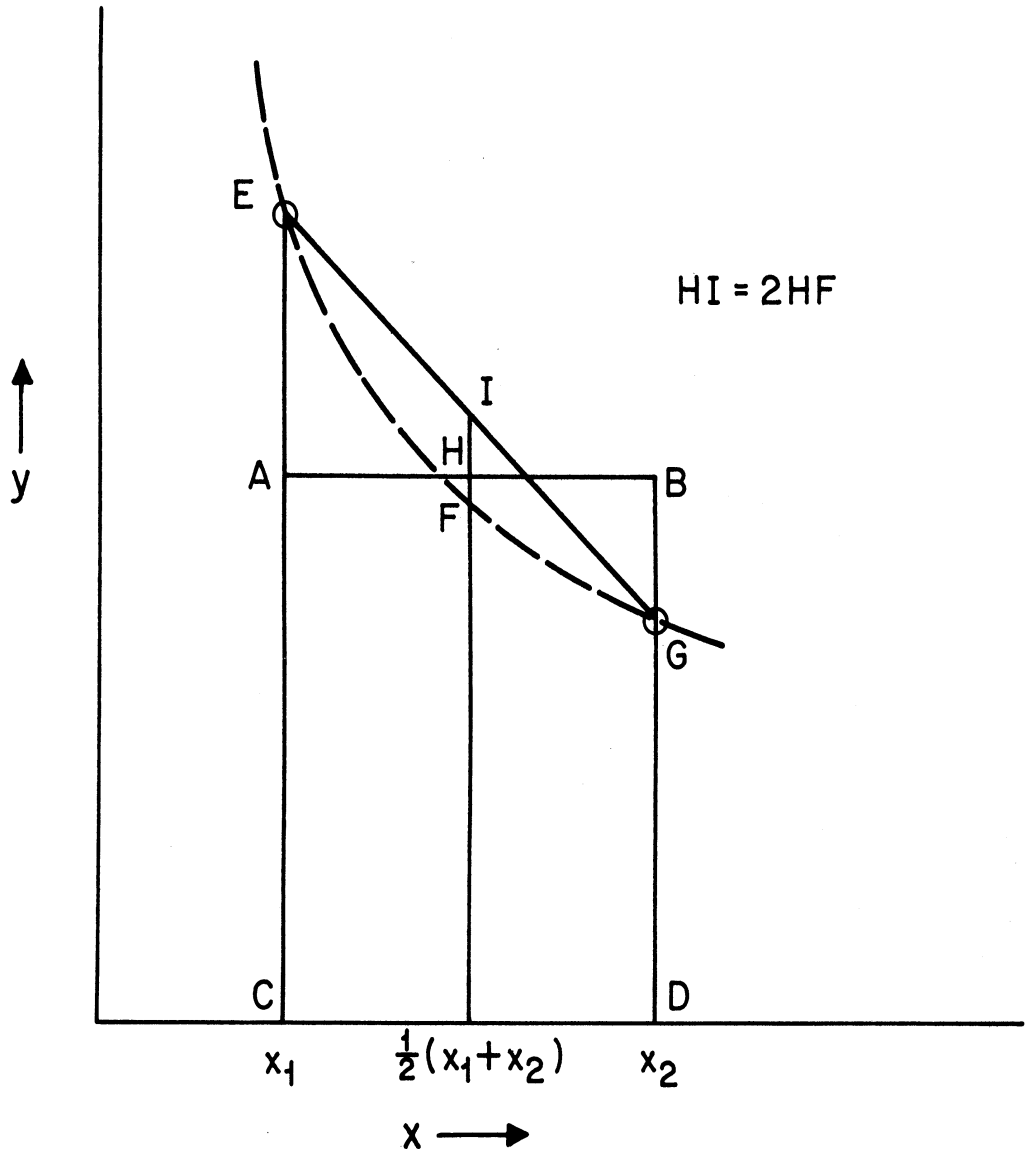

Figure AX.3 Simpson's Rule Used for Curve Fitting.

THE UNIVERSITY OF MICHIGAN

DATE DUE

9-15 9:43	